INVESTIGATION OF PROTECTION DEVICE FOR BONDED SHEATH CABLE SYSTEM

A Thesis for the degree of

MASTER OF PHILOSOPHY

Submitted to the

UNIVERSITY OF SOUTHAMPTON

By

Azedine Kebbab

1987

UNIVERSITY OF SOUTHAMPTON

ABSTRACT

FACULTY OF ENGINEERING AND APPLIED SCIENCE

ELECTRICAL ENGINEERING

Master of Philosophy

INVESTIGATION OF PROTECTION DEVICE FOR BONDED SHEATH CABLE SYSTEM

By Azedine Kebbab

Various bonded sheath cable systems are investigated with the inclusion of the protective device. Development of equivalent electrical circuit models are presented.

A selection of results is presented on the response of the protective device on different systems and for various load currents.

The results indicate that the model provides a reasonable representation of the device.

The cable system transient response using travelling-wave method is considered.

Modal analysis and Z-transform technique are thus adapted in the cross-bonded cable system transient analysis.

ACKNOWLEDGMENTS

The author would like to thank his project supervisor, Dr. A. E. DAVIES, for his helpful suggestion and encouragement during the course of this investigation.
The author would like also to thank Mr. GEOFF YATES, from Pirelli General for his kind discussion.
Acknowledgment are also offered to my wife, for her support throughout the course, and thanks to all my collegues in the Electrical Engineering Department.

SYMBOLS

The following symbols have been used throughout the thesis:

V, I	Voltage and current variables
M	Mutual inductance
i_L	Current in the non-linear inductance
V_L	Voltage accross the non-linear inductance
E_s	The induced EMF in the sheath
R_s, L_s	resistance and inductance of the sheath
L	non-linear inductance of the device
L'	differential inductance
λ	flux linkage (chapter 2 and 3)
L_c	inductance of the conductor
R_E	resistance of the ground path
t	identifies time step
Δt	step interval
w	angular frequency
r	radius
ρ	resistivity
ϵ	permittivity
μ	permeability
s	spacing between conductors
B	magnetic flux density
H	magnetic field intensity
J	current density
v, i	vectors of voltage and current variables
C_1, C_2	modal transformation matrices
Z	surge impedance matrix

λ matrix of propagation coeffients

F matrix of forward impulse responses

C connection matrix in the sheath earthing

G conductance matrix in the sheath earthing

R_e sheath earthing resistance

z Z-transform parameter

m ratio of wave transit time to step interval

Y shunt-admittance

T rotation matrix

subscripts

l,m,k,j identify node sets at the sheath discontinuities

e identifies earth-return path

1,2,3,s identify variables in the sheaths

a,b,c identify variables in a,b,c phases

superscripts

c,s identify core and sheath variables

p identifies phase-variable vectors and matrices

CONTENTS page

CHAPTER ONE

INTRODUCTION

As more underground cables are employed for transmission and distribution purposes, cable systems require that consideration is given to transienst overvoltages caused by lighting, switching surges and faults.

In cables systems, the mutual coupling between the cables create sheath losses which limit the loading capacity of the system. These losses are generated by the flow of currents in the cable sheaths caused by the induced voltages. As the sheaths have an insulation over them, for corrossive protection, arrangements have to be made to earth the sheath at various points along its length. Several methods of bonding have been used over the past years. For short cable circuits, the three sheaths may be bonded and earthed at only one point along the cable route [1]. Variations of this method were used where the cable is earthed at the terminations and at one point along its length, usually the centre. The voltages induced in the cable sheath with normal operating conditions are not dangerous for the cable plastic jacket, because it is designed to withstand these voltages. However when overvoltages due to lighting impulses and switching surges are propagated along the cable, it may be punctured [1] and [2].

Arround 1960, cross-bonding of the sheaths was introduced to

reduce the sheath losses [2] and [3]. However, cross-bonding introduces discontiniuties along the sheaths. While the arrangement elimitates the circulating currents and losses under balanced conditions, it does not prevent relatively large potentials from being present across the insulating joints. The method requires the use ofan insulator to isolate the sheaths from each other at the joints. The overvoltages which can arise across this insulation can result in a flashover of the insulation. Because of the magnitude of the overvoltages applied to the joints, it is recommended that cross-bonded systems should be protected with sheath voltage limiters. Problems can arise in providing satisfactory insulating joints, bonding apparatus and bonding connections. Under unsymmetrical conditions high sheath voltages can occur in the absence of special protective devices. These sheath voltage limiters are normally non-linear resistors installed at the bonding points which operate in the high resistance region under normal conditions thus limit the sheath currents and in the low resistance region under abnormal conditions. Thus overvoltages are limited on the cable metallic sheath to value lower than the jacket dielectric strength.

These devices must fulfill the following requirements:

(i) Withstand without thermal instability the voltage induced in the sheath by the conductor nominal current.

(ii) Withstand the power frequency voltage induced on the sheath by short circuit current in the cable conductor due to faults. This voltage depends mainly on the short circuit current value and the cable lengths.

(iii) Limit the induced voltages between sheath and ground in case of overvoltages in the system in order to avoid the puncture of the jacket.
(iv) Withstand switching surges superposed onto a power frequency voltage induced on the sheath when a fault occur on the overhead line near the cable termination. The switching surge is due to the interaction between cable capacitance and the inductance of short overhead line.

Problems with the metal oxide type of device have been experienced which have frequently tended them inoperable. If the energy absorbed exceeds its normal operating rating, the device is liable to be damaged (the temperature rises to a point where thermal runaway takes place).

This work is concerned with investigating a possible alternative device which consists of a high permeability hollow tube placed around the bonding lead. Such a device would have the same effect under normal and fault conditions as the metal oxide device. That is high impedance under normal conditions and low impedance under fault conditions, but has the advantage that under surge conditions would have zero impedance (except for the small capacitance between hollow tube and the bonding lead). In addition the problems associated with the dissipation of energy under fault conditions would be eliminated.

Overvoltages in transmission and distribution systems cannot be avoided. A detailed knowledge of this subject is

necessary for economic design of equipment in the system and for safe system operation. Overvoltages can be limited by special measures which should take into consideration the fact that they depend also on the characteristics of the equipment used, the system configuration and the manner of operation of the system.

In addition to steady state studies, transient voltages in cable systems have already been the subject of considerable investigation. Besides the use of simple equivalent circuit [1] and [21], to preduct these overvoltages, the application of symmetrical component techniques by Rhodes and Wright [4], Fourier transform techniques [5] and [7], together with field measurements [9] have been used. In all these techniques the method of solution is often tedious and requires excessive computing time.

Suitable models for representing the non-linear inductance of the device for inclusion in bonded sheath cable network are developed in chapter two. Computer simulation of voltage and current waveforms for various cable schemes are presented under full and fault load currents.

Chapter three concentrates on the non-linear volt/ampere characteristics of protection units. These protection units are made up of tubes of ferreous materials as described before. Their function is to reduce to safe values the surge voltages. Chapter three also includes the finite element field analysis of the non-linear iron tube arrangement to

determine for various load currents the resulting induced emfs.

Computed results obtained from the analysis of chapter two are presented in chapter four. To confirm the validity of the computed results, tests were conducted on cables fitted with the device (iron hollow tube). A comparison of computed and experimental results shows reasonable agreement.

Chapter five concerns the evaluation of the parameters of the cable system and the cable system transient response using travelling-wave methods in which the effects of frequency dependent parameters are taken into account. Cable system behaviour is modelled in terms of forward and backward response functions. Relatively simple formula are derived so that both response may be included in a general purpose computer program without difficulty.

Model analysis and Z-transform techniques are thus developed in chapter five. This technique was initially reported by Humpage [9]. The method is frequency dependent and is very accurate. The developement of electromagnetic transient analysis methods will bring together the frequency domain and the time domain non-linearities. The parameters of the cables are not constant, but vary with frequency, hence the frequency dependence of cable parameters has significant effects on both the wave shape and the peak voltages of some switching surges. Therefore the use of frequency domain formulation methods for the analysis of cable systems is the

best approach. Moreover it facilitates non-linear elements. The aim of chapter five is to illustrate how the Z-transform technique is applied to provide the base for a faster accurate computer method in electromagnetic transient analysis. It is mainly concerned with the transformation of the characteristics from the frequency domain to the time domain via the intermediate step using Z-transform.

Chapter six is devoted to the application of the Z-transform technique developed in chapter five, to a practical cable network, consisting of one cross-bonded section. The transient dependence of the parameters of the system, together with the non-linear operation of the protective device are both included in the application. The results obtained from the above analysis are presented and discussed in chapter seven.

CHAPTER TWO

ANALYSIS OF BONDED SYSTEMS

It is necessary to simulate the time dependent relationship of current and voltage for the core, sheath and the device (iron tube), for different cable systems as described in the preceeding sections. The system is first examined on a single-phase basis in order to determine the system conditions and configurations which lead to the most severe conditions being produced. The results obtained then provide a basis for studying the three-phase representation. The complete systems, are rather complex, and so, the investigation of the device performance is carried out by using a much simplified representation of the systems.

2.1 Single conductor in a metallic pipe.

Lead or aluminium sheath are commonly used for single-conductor cables. These pipes are situated in the magnetic field of the conductor currents and therefore, voltages will be induced in the sheaths which will give rise to the flow of induced currents. In this example it is assumed that the conductor current I(t) is returned to the generator by the ground loop or by a second conductor so far removed from the sheath that its magnetic field may be ignored. When the cable sheath is grounded at both terminations as in fig.2.1, the induced emf E_s then drives a circulating current $i_s(t)$ along the sheath, which returned through the ground circuit. The longitudinally induced emf

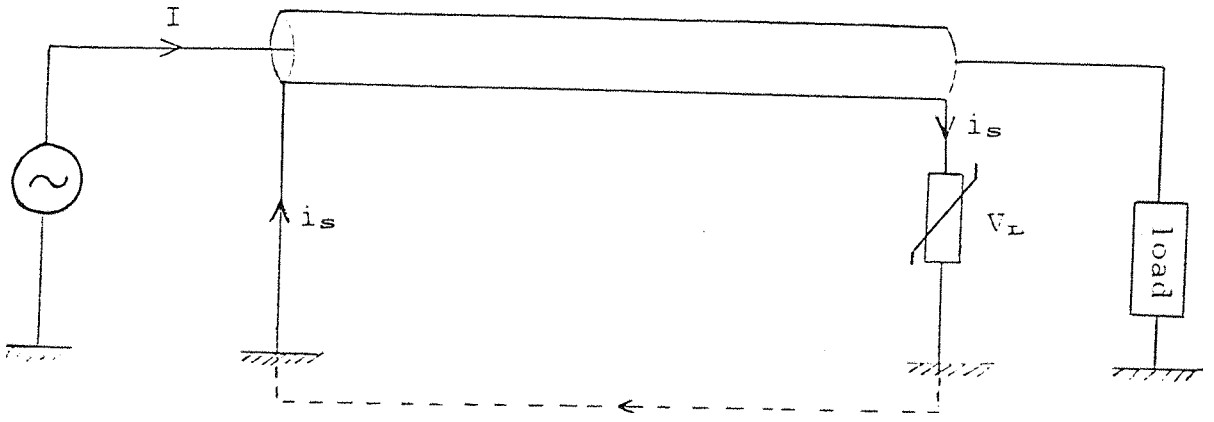

Fig.2.1 Single conductor in a metallic pipe.

in the sheath is given by:

$$E_s = M \frac{dI(t)}{dt}$$

M is the mutual inductance between the conductor and the sheath which is given by:

$$M = 2l(-1 + \ln 2l - \ln((r_o + r_i)/2))$$

where

l is the length of the cable

r_o and r_i are the inner and outer sheath radius respectively.

It is possible to deduce a simple expression to determine $i_s(t)$ resulting from full-load current in the conductor as follows:

$$0 = R_s\, i_s(t) + (L + L_s)\frac{di_s(t)}{dt} + M\frac{dI(t)}{dt} \qquad 2.1$$

L is the non-linear inductance of the device (iron tube).

R_s is the resistance of the sheath.
L_s is the the self-inductance of the sheath, on the assumption of uniform current distribution, L_s is equal to the mutual inductance between the conductor and the sheath.

2.1.1 Numerical solution.

As the B/H characteristic for the device is non-linear, the differrential inductance require a numerical solution. The backward difference method of numerical integration was adopted. By solving equation 2.1, the current flowing through the sheath is:

$$i_s(t) = \frac{-M[I(t)-I(t-\Delta t)] + (L + L_s)\, i_s(t-\Delta t)}{R_s\, \Delta t + L + L_s} \qquad 2.2$$

and the voltage drop across the iron tube is given by:

$$V_L = \frac{L}{\Delta t}\,[\, i_s(t) - i_s(t - \Delta t)] \qquad 2.3$$

2.1.2 Fault condition.

Considering a fault occuring at the far end of the cable, the system of Fig.2.1 may be represented by a simple equivalent circuit model as shown in Fig.2.2.

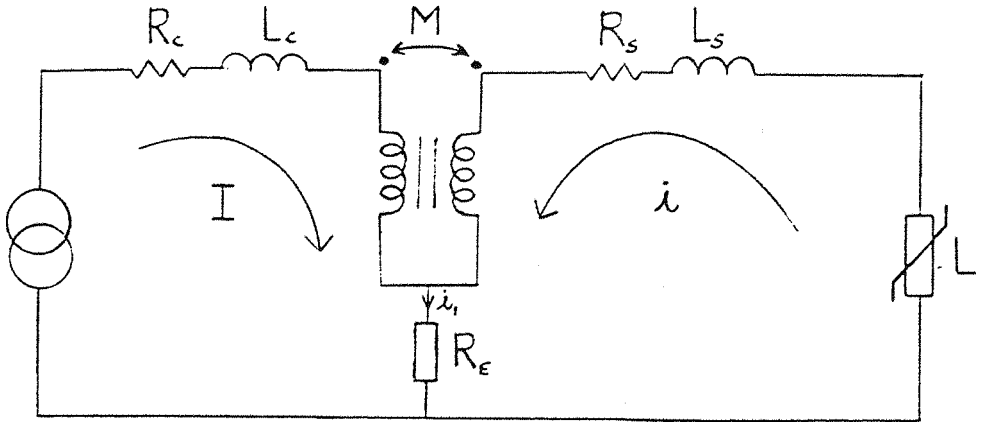

Fig.2.2 Equivalent circuit of the system.

The phase-to-earth fault is assumed to occur at the remote end of the cable near the load, and it is simulated by injecting a 50Hz current wave of high value in the core. The cable data used in the study is given in section 2.1.3.

The equation for the circuit of Fig.2.2 is:

$$R_s\, i_s(t) + (L + L_s)\frac{di_s(t)}{dt} + M\frac{dI(t)}{dt} + R_E i(t) = 0 \qquad 2.4$$

where $i(t) = i_s(t) + I(t)$

and R_E is the resistance of the ground loop.

The numerical solution for current which flows in the sheath is:

$$i_s(t) = \frac{-M[I(t)-I(t-\Delta t)] + (L + L_s)\, i_s(t-\Delta t) - R_E I(t)}{(R_s + R_E)\Delta t + L + L_s}$$

The waveforms of voltage and current of the device for normal and fault conditons are shown in Fig.4.4 and 4.5.

2.1.3 System data.

The system data considered for this chapter consisted of:

- A source current of 1600 Amps for normal load and 5 KA for a fault.
- R_{sh}= 37.3 μΩ/m
- r = 35.15 mm conductor radius
- r_o = 57.1 mm under sheath radius
- r_i = 64.45 mm over sheath radius
- d = 0.5 m spacing between cables

2.2 Single-phase system.

The first step in the calculation is to obtain an expression for the voltage-drop along the sheath. This voltage-drop will be made up of two parts, one due to the simple d.c resistance of the sheath, and the other due to the combined inductive effects of the core and sheath currents. This combined inductive effect is made up of the self-inductance of the sheath considered and three mutual inductance effects due to the two core currents and the remaining sheath current. The coefficients of self and mutual induction depend only on the dimensions of the cables and their configuration and can readly be calculated. Thus an expression for the voltage-drop along the sheath can be deduced in terms of the sheath and core currents, the dimension of the cables and geometry of their arrangement.The system studied of single-phase form as shown in Fig.2.3.

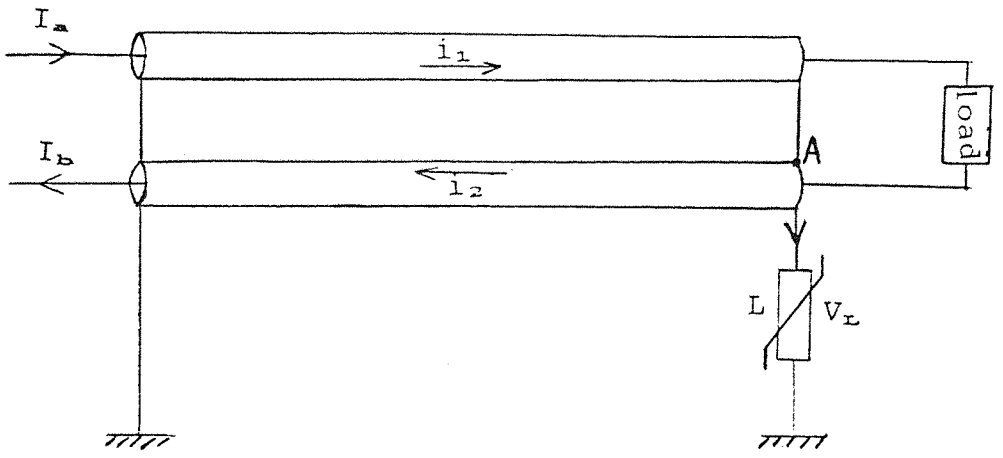

Fig.2.3 Single-phase cable system.

The voltage-drop in the sheaths are as the following expressions indicate for sheaths noted 1 and 2 respectively:

$$\Delta V_1 = R_s i_1(t) + L_{s1}\frac{di_1}{dt}(t) + M_{21}\frac{di_2}{dt}(t) + M_{a1}\frac{dI_a}{dt}(t) + M_{b1}\frac{dI_b}{dt}(t) \qquad 2.6$$

$$\Delta V_2 = R_s i_2(t) + L_{s2}\frac{di_2}{dt}(t) + M_{12}\frac{di_1}{dt}(t) + M_{b2}\frac{dI_b}{dt}(t) + M_{a2}\frac{dI_a}{dt}(t) \qquad 2.7$$

However the sheaths are earthed at both ends, so $\Delta V_1 = \Delta V_2 = 0$

and we have: $I_a(t) = -I_b(t)$

and also: $i_1(t) = -i_2(t)$

So equations 2.6 and 2.7 reduce to:

$$0 = R_s\, i_1(t) + (L_s - M_{21})\frac{di_1}{dt}(t) + (M_{a1} - M_{b1})\frac{dI_a}{dt}(t) \qquad 2.8$$

2.2.1 Numerical solution.

Using the backward difference method of the numerical integration we obtain an expression for the current in the sheath as follows:

$$i_1(t) = \frac{-(M_{a1} - M_{b1})[I(t)-I(t-\Delta t)] + (L_s - M_{21})\, i_1(t-\Delta t)}{R_s\, \Delta t + L_s - M_{21}} \qquad 2.9$$

with

$$i_2(t) = -i_1(t)$$

If we consider the sum of the current at the bonding and earthing point on Fig 2.3 ,point A ,it will be:

$$i_1(t) + i_2(t) + i_L(t) = 0 \qquad 2.10$$

it yields to $i_L(t) = 0$, which means that no current flows through the non-linear inductance L to earth.

2.2.2 Fault condition.

A single-phase-to-earth fault is considered at the end of the cable. The returning fault current will divide so as to return partly as a current through the sheath and partly as an earth current, so that the system of Fig.2.3 may be represented by the equivalent circuit as shown in Fig.2.4.

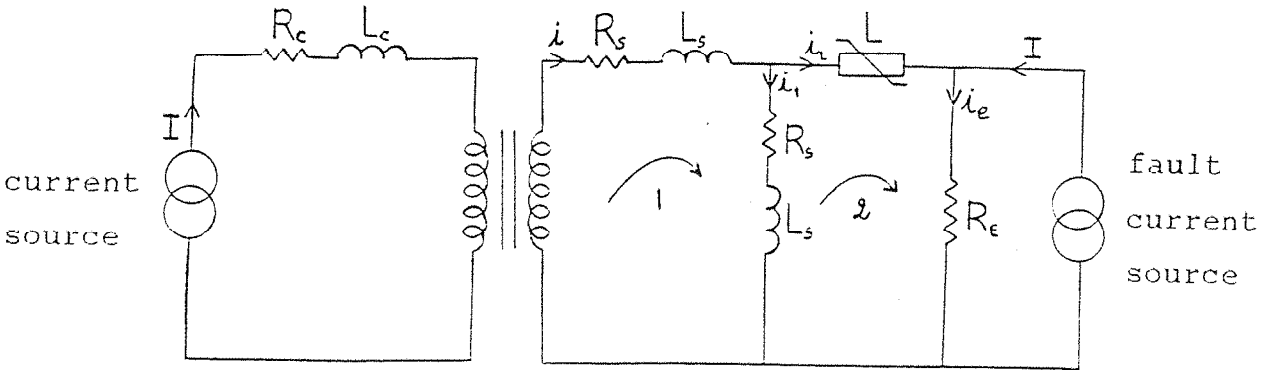

Fig.2.4 Electrical equivalent circuit for phase to ground fault.

From the equivalent electric circuit of Fig.2.4, the equations for loops number one and two are given by:

$$R_s(2.i(t)- i_L(t))+ L_s\left(2.\frac{di}{dt}(t) - \frac{di_L}{dt}(t)\right) + M_{a1}\frac{dI}{dt}(t) = 0 \qquad 2.11$$

$$-R_s i(t)+(R_s+ R_E)i_L(t) + R_E I(t) -L_s\frac{di}{dt}(t) +(L + L_s)\frac{di_L}{dt}(t)= 0 \qquad 2.12$$

with $i(t) = i_1(t) + i_L(t)$

and $i_e(t) = I(t) + i_L(t)$

If we multiply equation 2.12 by 2 and add it to equation 2.11 and rearrange it, we obtain:

$$i_L(t) = \frac{-M[I(t)-I(t-\Delta t)] + (2L + L_s)\, i_L(t-\Delta t)-2REI(t)\Delta t}{(R_s + 2R_E)\Delta t + 2L + L_s} \qquad 2.13$$

Equation 2.13 defines the current in the non-linear inductance in terms of current of the source and past histories of the elements of the system.

The voltages across the device can be written as a function of the current thus:

$$V_L(t) = \frac{L}{\Delta t}\left[i_L(t) - i_L(t - \Delta t)\right] \qquad 2.14$$

Equation 2.13 and 2.14 define the current and voltage of the iron tube in the event of a fault condition (i.e phase-to-earth). Their waveforms are shown in Fig.4.13 to Fig.4.15.

2.3 Three-phase system.

The extension of the single phase results presented above to the case of 3-phase system is not easily accomplished analytically. In order to determine how applicable the results are, the 3-phase system shown in Fig.2.5 is chosen for the simulation. Since the sheaths are bonded at both ends, and it is assumed that the sheath bonds are at the same potential. we obtain the general solution.

$$\Delta V_1 = \Delta V_2 = \Delta V_3 = 0$$

$$i_1 + i_2 + i_3 = 0$$

$$I_a + I_b + I_c = 0$$

$$0 = R_s i_1 + L_s \frac{di_1}{dt} + L \frac{di_L}{dt} + M_{21} \frac{di_2}{dt} + M_{31} \frac{di_3}{dt} + M_{a1} \frac{dI_a}{dt} + M_{b1} \frac{dI_b}{dt} + M_{c1} \frac{dI_c}{dt} \quad 2.15$$

$$0 = R_s i_2 + L_s \frac{di_2}{dt} + L \frac{di_L}{dt} + M_{12} \frac{di_1}{dt} + M_{32} \frac{di_3}{dt} + M_{a2} \frac{dI_a}{dt} + M_{b2} \frac{dI_b}{dt} + M_{c2} \frac{dI_c}{dt} \quad 2.16$$

$$0 = R_s i_3 + L_s \frac{di_3}{dt} + L \frac{di_L}{dt} + M_{23} \frac{di_2}{dt} + M_{13} \frac{di_1}{dt} + M_{a3} \frac{dI_a}{dt} + M_{b3} \frac{dI_b}{dt} + M_{c3} \frac{dI_c}{dt} \quad 2.17$$

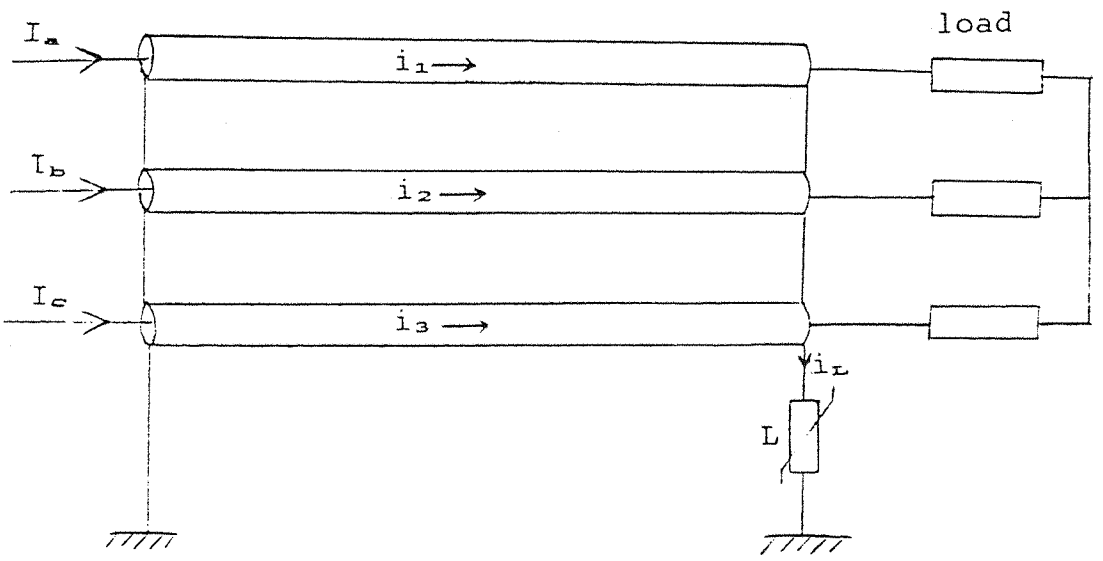

Fig.2.5 3-phase system.

From equation 2.16, replacing $I_a + I_c$ by $-I_b$ and since $i_1 + i_2 + i_3 = 0$, hence $i_L = 0$ which means that no current is leaving the sheath, giving:

$$0 = R_s i_2 + L_s.\rho i_2 + M_{12}.\rho(i_1 + i_3) + (M_{b2} + M_{a2}).\rho I_b \quad 2.18$$

where $\rho = \frac{d}{dt}$

rearranging and replacing $i_1 + i_3$ by $-i_2$ gives:

$$0 = R_s i_2 + (L_s - M_{12}).\rho i_2 + (M_{b2} - M_{a2}).\rho I_b \quad 2.19$$

$$i_2(t) = \frac{-(M_{b2} - M_{a2})[I(t)-I(t-\Delta t)] + (L_s - M_{12})\, i_2(t-\Delta t)}{R_s \Delta t + L_s - M_{12}} \quad 2.20$$

Adding equations 2.15 and 2.16 together gives:

$$R_s(i_1 + i_2) + L_s.\rho(i_1 + i_2) + M_{21}.\rho(i_1 + i_2) + (M_{31} + M_{32}).\rho i_3 + (M_{a1} + M_{a2}).\rho I_a + (M_{b1} + M_{b2}).\rho I_b + (M_{c1} + M_{c2}).\rho I_c = 0 \quad 2.21$$

replacing $i_1 + i_2$ by $-i_3$ and $I_a + I_b$ by $-I_c$ gives:

$$i_3(t) = \frac{-(M_{a1} - M_{c1})[I(t)-I(t-\Delta t)] + (L_s - M_{31})\, i_3(t-\Delta t)}{R_s \Delta t + L_s - M_{31}} \quad 2.22$$

and

$$i_1 = -(i_2 + i_3) \quad 2.23$$

The values of the inductance coeffients required in the above calculations can be obtained in terms of the geometry of the spacing as follows:

$L_c = (1/2 + 2.\ln(l/b).10^{-7}$ H/m

$L_s = [2.\ln l/d + \frac{1}{2}\frac{d^2 - 3c^2}{d^2 - c^2} + \frac{2c^4}{d^2 - c^2}.\ln d).10^{-7}$ H/m

$M_{b1} = M_{12} = M_{21} = M_{a2} = M_{2a} = M_{1b} = (2.\ln(l/S_{12}).10^{-7}$ H/m

$M_{c2} = M_{32} = M_{23} = M_{b3} = M_{2c} = M_{3b} = (2.\ln(l/S_{23}).10^{-7}$ H/m

$M_{a3} = M_{3a} = M_{c1} = M_{1c} = M_{13} = M_{31} = (2.\ln(l/(S_{12} + S_{23})).10^{-7}$ H/m

$M_{a1} = M_{1a} = M_{2b} = M_{b2} = M_{3c} = M_{3c} = (2.\ln(l/d + 1 - \frac{2c^2}{d^2 - c^2}.\ln d/c).10^{-7}$ H/m

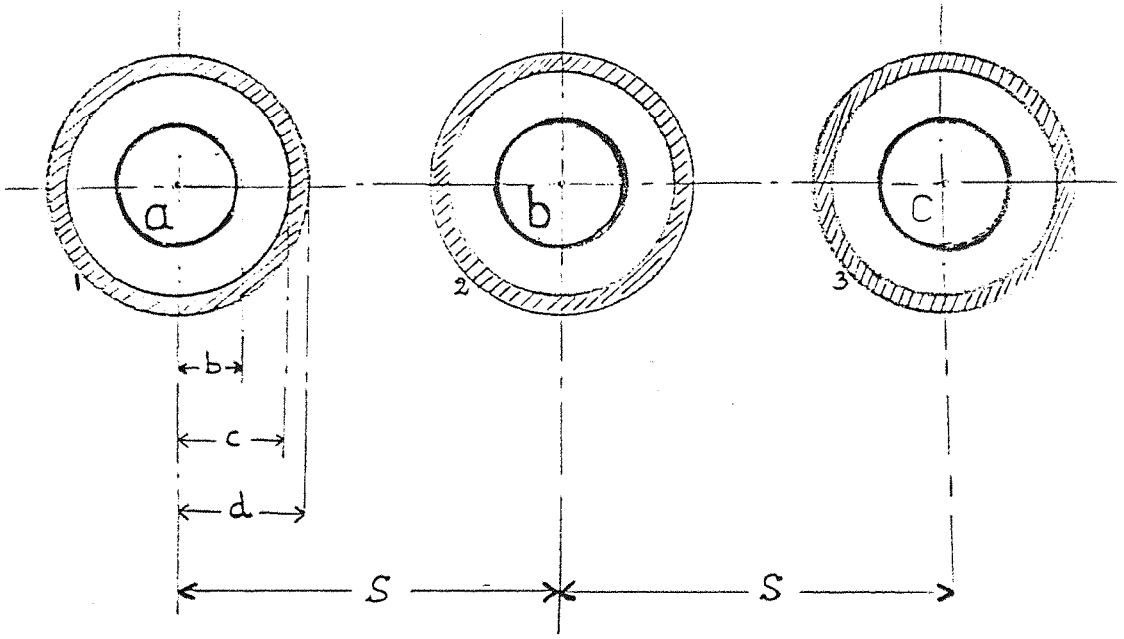

Fig.2.6 Arrangement of cables in flat spacing.

l is the distance of cores a, b and c from the neutral wire. The neutral is taken as a fictitious conductor which completes the circuit of each phase, so that we have three closed circuits for the cores and three for the sheaths. When the current are balanced the magnetic effect of the conductor is zero, since there is then no residual current.

2.3.1 Fault condition.

Under a fault condition the system of Fig.2.5 will be represented by the simple equivalent circuit as shown in fig.2.7. The fault is occuring at the end of the cable between phase "a" and the ground. The same as for the single phase system, the fault current will return partly in the sheath and partly in the earth.

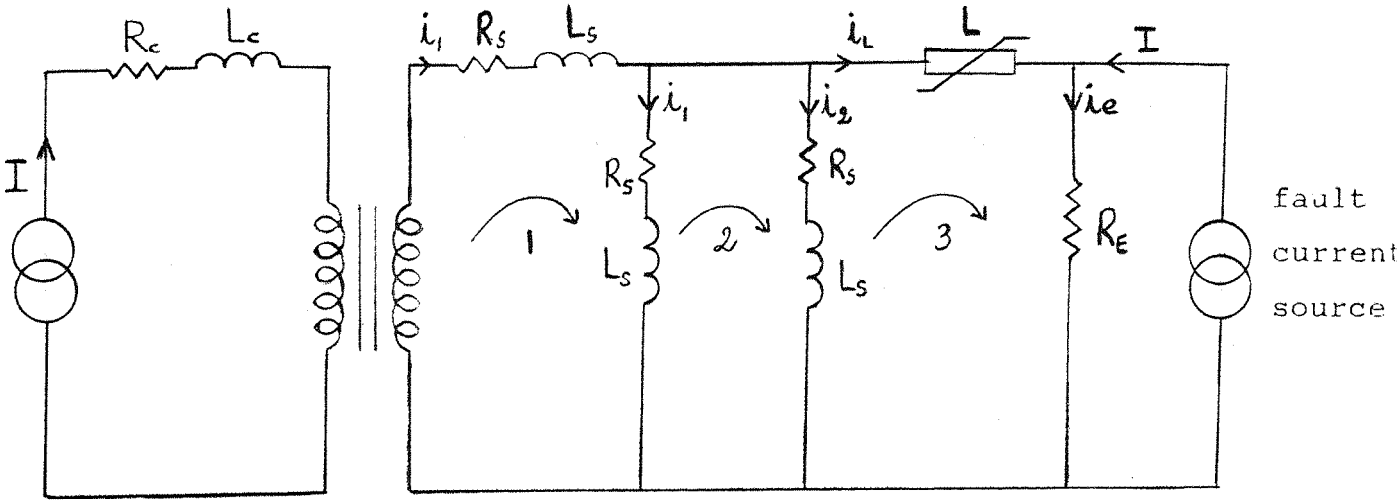

Fig.2.7 Equivalent circuit of 3-phase system under fault condition

The equations for the loops number 1,2 and 3 are:

$$R_s(i + i_1) + L_s.\rho(i + i_1) + M.\rho I = 0 \qquad 2.24$$

$$R_s(i_2 - i_1) + L_s.\rho(i_2 - i_1) = 0 \qquad 2.25$$

$$R_E i_e - R_s i_2 - L_s.\rho i_2 + L.\rho i_L = 0 \qquad 2.26$$

replacing i_1 by $i - i_2 - i_L$ in equation 2.24 and 2.25 gives:

$$R_s(2.i - i_2 - i_L) + L_s.\rho(2.i - i_2 - i_L) + M.\rho I = 0 \qquad 2.27$$

$$R_s(-i + 2.i_2 - i_L) + L_s.\rho(-i + 2.i_2 - i_L) = 0 \qquad 2.28$$

Adding equation 2.27 to 2 times equation 2.28 gives:

$$R_s(3.i_2 + i_L) + L_s.\rho(3.i_2 + i_L) + M.\rho I = 0 \qquad 2.29$$

Adding equaton 2.29 and 2.26 gives:

$$(R_s + 3.R_E)i_L + 3.R_E I + (L_s + 3.L).\rho i_L + M.\rho I = 0 \qquad 2.30$$

or

$$i_L(t) = \frac{-M[I(t)-I(t-\Delta t)] + (3L + L_s)\, i_L(t-\Delta t) - 3REI(t)\Delta t}{(R_s + 3R_E)\Delta t + 3L + L_s} \qquad 2.31$$

Equation 2.31 defines the current which flows through the device during the fault. From this the voltage across it is obtained and their waveforms are shown in Fig.4.16 and Fig.17.

2.4 Effect of the computation step length of time.

The choice of the number of steps per cycle for a step-by-step solution is of great significance and the choice of an adequate step length in the numerical solution is very important. An inadequate step will produce errors and difficulties in achieving the steady state solution. The $\frac{1}{2}$°degree/step, or 720 steps/cycle was considered adequate in both accuracy and computer time.

2.5 Comparison check of λ/i curve.

A comparison check was made to ensure that the computer program does not run into numerical instability with the function describing the λ/i curve when working up and down the curve. This check consisted of comparing two distinct methods of determining the flux for a given value of current.

From the equation:

$$V = \frac{d\lambda}{dt} = \frac{d\lambda}{di}.\frac{di}{dt} = L.\frac{di}{dt} \qquad 2.32$$

the flux at a given instant is equal to the initial flux plus a incremental flux value.

$$\lambda(t) = \lambda(0) + \Delta\lambda = \lambda(0) + L.\Delta i \qquad 2.33$$

where $L = \frac{d\lambda}{di}$ is the incremental inductance

also from equation

$$\lambda = A_1 i + A_2 \mathrm{Tanh}(A_3 i) \qquad 2.34$$

A comparison between equation 2.33 and 2.34 was made for given value of current and because of the small time step used the computer program indicated that it was within a specified tolerance (e.g. 10%).

2.6 Initial conditions.

the initial conditions must be set before the calculation process can be started. The conditions are:

It was assumed that the system had not been energized

before. Therefore, the past histories of the voltage and current are set to zero.

2.7 Computer programs.

All the programs developed in this investigation were written in Fortran 77 language for the IBM 3090 computer at the University of Southampton.

Two different programs were developed for each system.

(i) - The main program, which calculates the voltage and current on the protective device. The program starts reading all the data and setting all the initial conditions. To compute the differential inductance, a check on current is made via λ/i relationship using forward predictor method. Subsequently, the inductance is computed and the circuit equations are solved. Finally, the present value of current is stored for the next run and the loop is repeated for the next time interval until the number of steps required is reached.

(ii) - Plot program, which plots the transient and steady state of currents and voltages. This program makes use of the Gino-F Library available at the computer centre of Southampton University.

2.8 Summary.

In this chapter, a model system to study the transient and steady state conditions of the different cable systems including the non-linear inductance of the device (iron tube) has been presented. The different systems were represented by simple equivalent circuit model. The forward

predictor method was utilized to estimate a value of current at each time step of the numerical solution. A comparison check of λ/i curve on the methods of determining the flux was made. The backward difference method was adopted to solve the non-linear differential equations.

CHAPTER THREE

SIMULATION OF CABLE-SHEATH-PROTECTION UNIT

In a study of the effects of induced voltages on sheath cables, a literature search revealed that there is not a good device which would limit all overvoltages without spark gaps, unless a device has a steep front V-I non-linear characteristic (metal oxid arrester). One device which gave this non-linear effect was a sphere gap with resistor in series.

An alternative device was chosen to give a similar characteristic which consisted of: a tube in iron with a conductor inside it (bonding lead), separated by a small air gap.

To show the field behavior, a detailed field analysis on the two-dimensional core and tube is performed. The analysis adopts the existing finite-element Newton-Raphson numerical techniques, but takes into full account the field dependent non-linear characteristic of soft iron.

3.1 The study model.

Fig.3.1 shows the two-dimensional, core-air-tube, used in this study. The copper core carries the various load currents and has a relative permeability of 1. The magnetic property of the iron-tube is assumed to be isotropic.

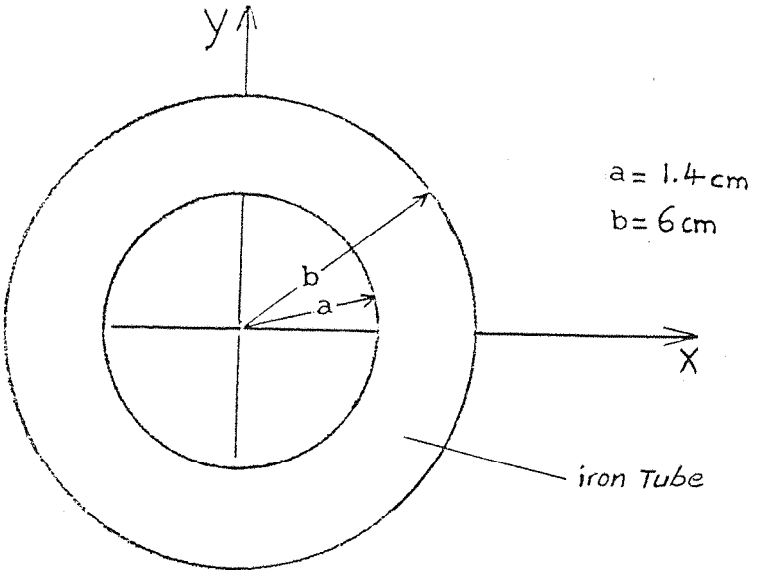

Fig.3.1 The two-dimensional model.

Furthermore, its B-H characteristic is single-valued and is shown in Fig.3.2.

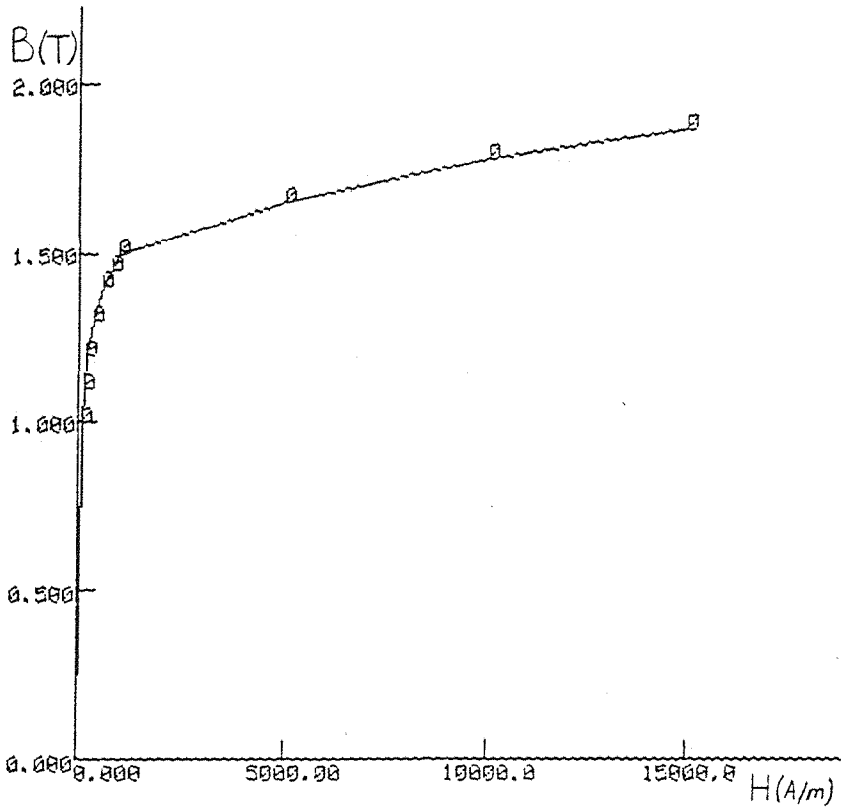

Fig.3.2 The B-H characteristic of the iron tube.

3.2 Field solutions and results.

The mathematical details of the finite-element Newton-Raphson method for determining the field will not be discussed here because they are standard and in our study we have used a package available in the department.

Fig.3.3 shows the region of interest, subdiveded into 576 elements.

Fig.3.4 shows how B in the iron tube varies as a function of the position X along the axis. And Fig.3.5 shows that H increases in the copper conductor and then decreases to approximatly zero at the out surface of the iron tube. And it was noticed also that B increases with increasing J.

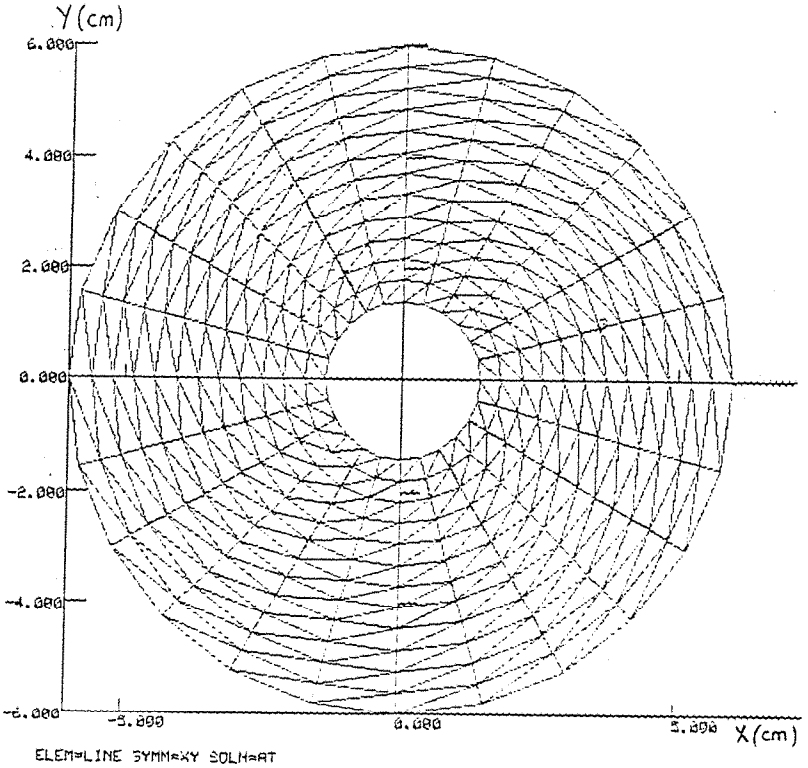

Fig.3.3 Two-dimensional finite element mesh.

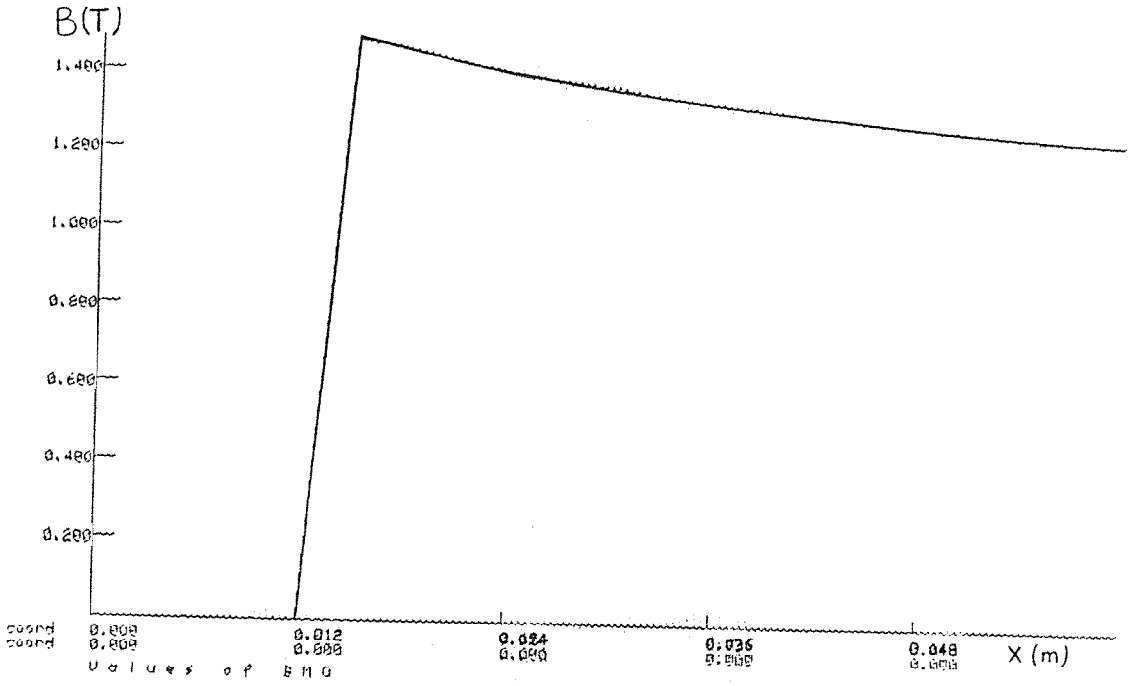

Fig.3.4 B versus x in the iron.

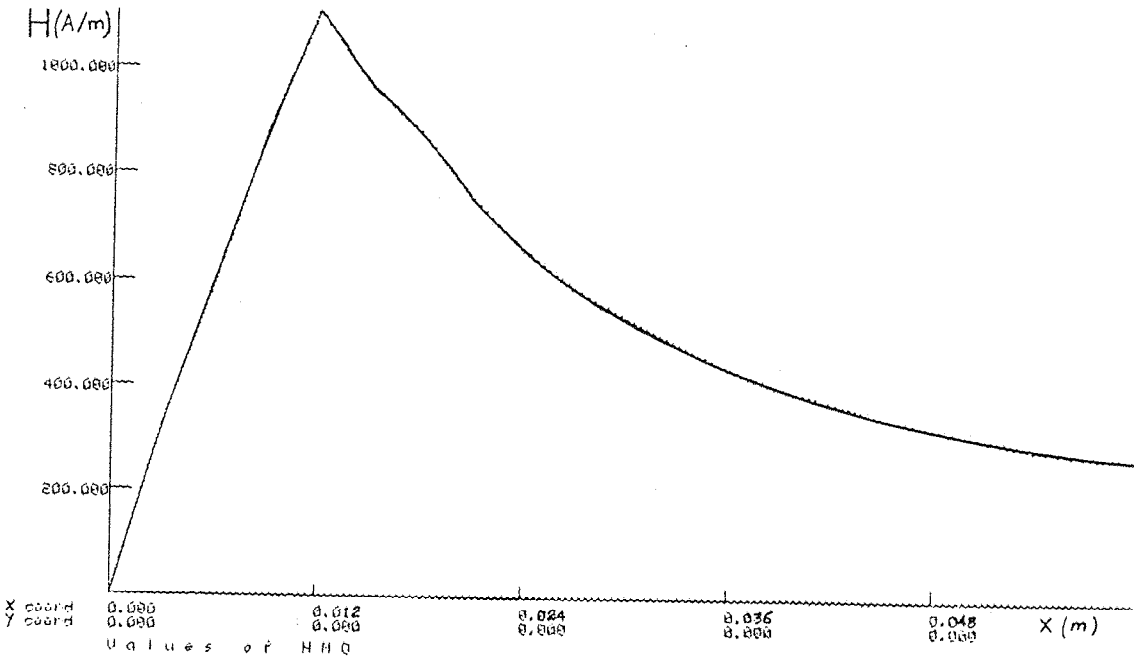

Fig.3.5 H versus x in the iron.

The magnitude of the current density, J is assumed to be uniformly distributed in the the conductor and is set at 19.735 A/m² in one case. This is equivalent to 100 Amps flowing in the conductor. Our objective here is to examine how B, vary as a function of J in the iron tube. This is done for various J, which means various load currents and various thickness of the iron tube, to determine a suitable device with a reasonable diameter.

Table 3.1 a load current of 100 A through a conductor of 2" diameter.

Size of the iron tube outer diameter in cm	voltage drop across the iron tube
12	19 V/m
13	22 V/m
20	40.5 V/m
30	65 V/m
40	88.6 V/m
46	102 V/m

Table 3.2 a load current of 100 A through a conductor of (1/2)" diameter.

Size of the iron tube	voltage drop across the iron tube
10 cm	26.2V/m

Table 3.3 a load current of 100 A through various size of conductors. The diameter of the iron tube is 12 cm.

conductor size in inch	voltage drop across the iron tube
2"	19 V/m
1"	27.5 V/m
(1/2)"	31.76 V/m

Table 3.4 a load current 1000 A through a conductor of 2" diameter.

Size of the iron tube	voltage drop across the iron tube
12 cm	23.5 V/m

These tables show the variations of the voltage drops across the iron tube as a function of its thickness. For a conductor diameter of 2" and a tube size of 12 cm diameter, with load currents of 100 A and 1000 A, Table 3.1 and 3.4 show that the voltage drop increases slightly from 19 V/m to 23.5 V/m. This indicates that the tube is operating in the saturation region. The voltage drop of 100 V can be achieved by a tube of 46 cm of diameter and a length of 1 m or by a tube of 20 cm of diameter and a length of 2.5 m. A big size of tube is not very practical so we have choosen the tube of 12 cm diameter and a length of approximatly 5 m which can

drop 100 V and can be put easly between the cable cross-bonding point and the link box.

3.3 λ/i curve.

Given the magnetic curve B = f(H) of a particular material, it is possible to calculate λ/i curve knowing particular dimensions of the equipment.

The magnetic flux density can be expressed as:

$$B = \frac{\lambda}{N.a} \qquad 3.1$$

Where λ is the instantaneous flux linkage, N is the number of turns and a is the sectional area of core. Alternatively, the magnetic field intensity H can be written as a function of current as follows.

$$H = \frac{N.i}{l} \qquad 3.2$$

Where N is the numbers of turns, i is the current and l is the length of the magnetic path.

From equation 3.1, 3.2 and knowing the B/H relationship, it is possible to write.

$$\lambda = N.a.f\left(\frac{N.i}{l}\right) \qquad 3.3$$

Equation 3.3 defines the λ/i curve in the terms of equipment dimensions.

3.4 B/H Relationship.

When working with ferromagnetic materials, the

relation between the magnetic flux density B and the magnetic field H is of considerable importance. Such a relationship is non-linear and is considered in this work as a non-linear single-valued relationship. A convenient expression to describe the B/H curve is

$$B = A_1.H + A_2.\text{Tanh } A_3.H \qquad 3.4$$

where $\text{Tanh}A_3.H$ converge to 1 rapidly and the term $A_1.H$ covers the upper region of the curve. A_1, A_2, A_3 are constants for a given magnetic path of the core material. When the field intensity approaches infinity the B/H curve is a straight line and the slope of the B/H characteristic is equal to A_1. This can be shown taking the derivative of equation 3.4 with respect to the magnetic field intensity H as follows.

$$B' = \frac{dB}{dH} = A_1 + A_2.[4.A_3\text{Exp}(2.A_3.H)/(\text{Exp}(2.A_3.H) + 1)^2] \qquad 3.5$$

where

when $H \longrightarrow \infty$

$B = A_1 = \text{slope}$

This can be visualized from Fig.3.6.

When the magnetic field intensity H increases to certain values, the expression Tanh A_3H tends to one and the B/H curve is equal to:

$$B = A_1.H + A_2 \qquad 3.6$$

and the straight line equation 3.6 cuts the B axis at B equal to B_o (see Fig.3.6) and for flux density equal to B_o, the magnetic field intensity H is equal to zero. As a result

equation 3.4 can be re-written as follows:

$$B = B'.H + B_0.\text{Tanh } A_3.H \qquad 3.7$$

To determine the value of A_3, a point has to be taken on part of the curve below the knee-point. Let this point be b (see Fig.3.6), from which the ordinates are B_b and H_b. By substituting B_b and H_b into equation 3.5, the value A_3 is given by:

$$B_b = B'.H_b + B_0.\text{Tanh } A_3.H_b$$

and

$$A_3 = \frac{\text{Tanh}^{-1}(B_b - B'.H_b)/B_0}{H_b}$$

or

$$A_3 = (2.H_b)^{-1}.\ln(B_0 + B_b - B'.H_b)/(B_0 - B_b + B'.H_b)$$

3.5 v/i characteristic of the device

By varying the level of the current flowing in the sheath,a test was carried out to achieve the v/i characteristic of the device. The v/i characteristic is shown in Fig.3.7. The v/i characteristic shows that above the knee point, for slight changes in voltage there is a large change in the value of current. Therefore, the device offers some useful advantages in limiting the overvoltages.

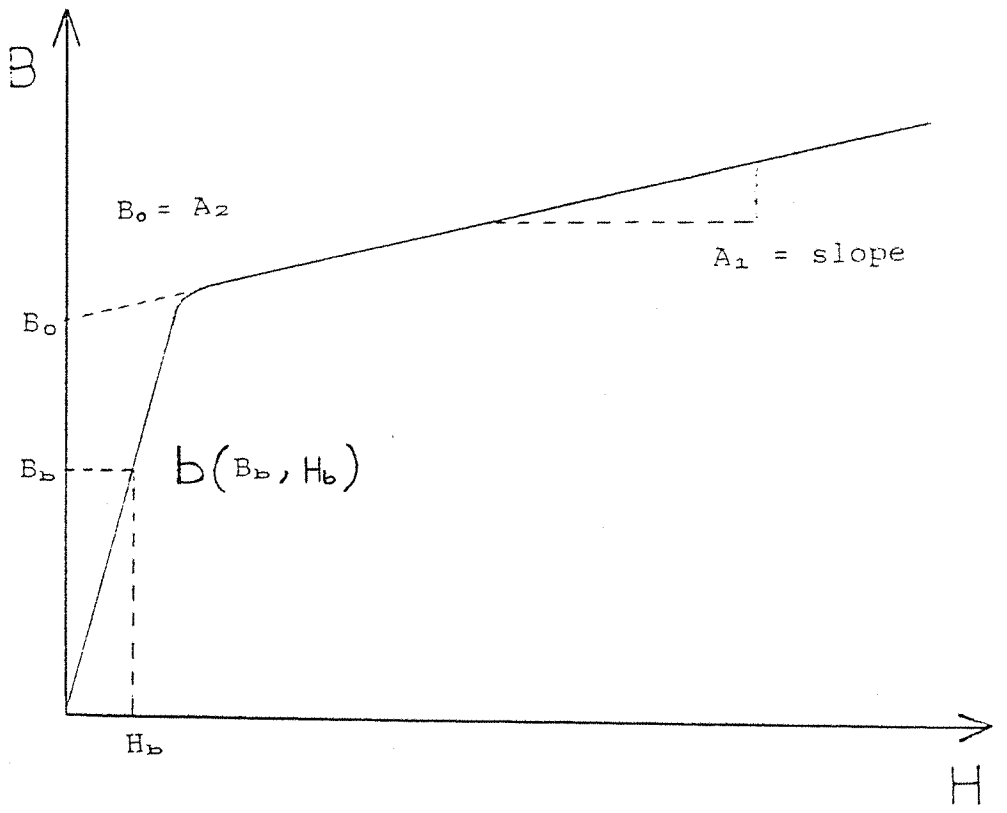

Fig.3.6 B/H Relationship.

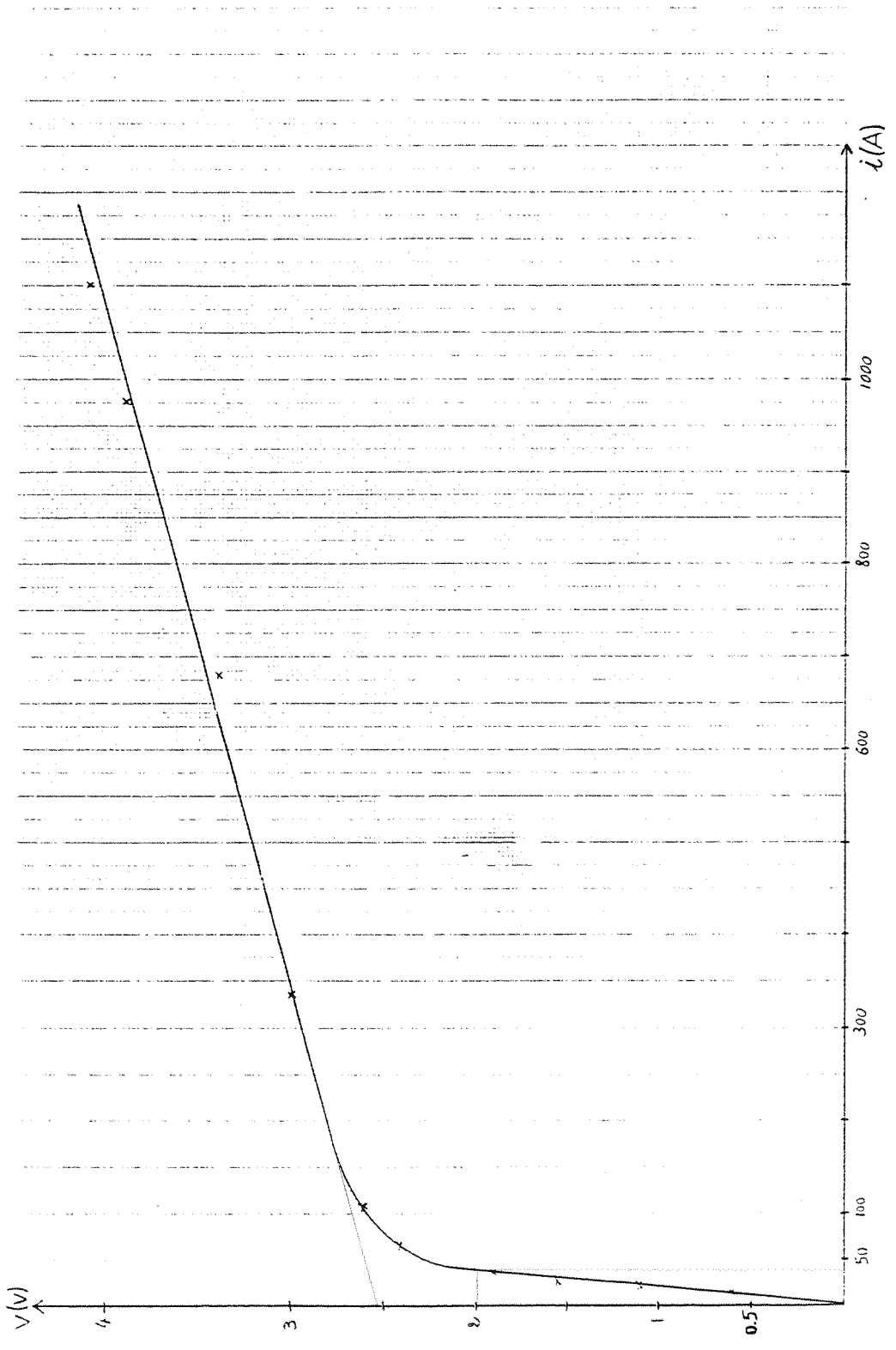

Fig.3.7 v/i characteristic of the device

3.6 Differential inductance.

As the B/H characteristic is non-linear, the differential equation 2.1 requires a numerical solution. The differential inductance is function of the current, therefore at each time step i must be solved. A λ/i relationship based on the B/H curve for the material can be derived from which the differential inductance can be obtained by a forward predictor method. From equation 3.3 and 3.4, the flux linkage can be expressed as:

$$\lambda = \frac{A_1 N^2.a}{\ell} i + A_2.N.a.\text{Tanh} \frac{A_3.N}{\ell} i \qquad 3.9$$

or

$$\lambda = A_{11}.i + A_{22}.\text{Tanh } A_{33}.i$$

where

$$A_{11} = \frac{A_1 N^2.a}{\ell} \quad , \qquad A_{22} = A_2.N.a \qquad \text{and}$$

$$A_{33} = \frac{A_3.N}{\ell}$$

Alternatively, the differential inductance can be defined as

$$L' = \frac{d\lambda}{di} \qquad 3.10$$

and equation 3.10 defines the differential inductance as a function of the B/H characteristic.

It has been shown here a way to model the magnetic non-linearity of the iron tube. An expression of the B/H characteristic was presented from which the differential inductance can be calculated for each time step of the numerical solution.

3.7 Forward predictor method.

To calculate the variable $i_s(t)$ of the previous equations, it is necessary to re-calculate at each time step the non-linear inductance L. To set the differential inductance, it is necessary to estimate the value of $i_s(t)$ for the next time step. The forward predictor method estimates the value of $i_s(t)$ at half the step interval from time at t. Considering Fig.3.7 at time equal to t and below saturation condition, the differential inductance is defined by:

$$L' = \frac{d\lambda}{di}$$

by assuming:

- at time t the component current is equal to i_b

and

- at time $t - \Delta t$ the component current is equal to i_a

the current at time $t + \Delta t$ can be defined by

$$i(t + \Delta t) = i_b + (i_b - i_a) \qquad 3.11$$

by forward predictor method equation 3.11 is given by

$$i(t + \tfrac{1}{2}\Delta t) = i_b + \tfrac{1}{2}(i_b - i_a) \qquad 3.12$$

Equation 3.12 estimates the value of i(t) at half the step interval from time at t.

After saturation, the λ/i curve is a straight line and the equation which represente the λ/i relationship impose the

following conditions:

if $i(t+\frac{1}{2}\Delta t) < I_{sat}$ then $L' = \frac{d\lambda}{di}$

if $i(t+\frac{1}{2}\Delta t) > I_{sat}$ then $L' = L_1$

Summarizing, at each time step the currents are predicted and the predicted values are utilized via λ/i curve to calculate the differential inductances.

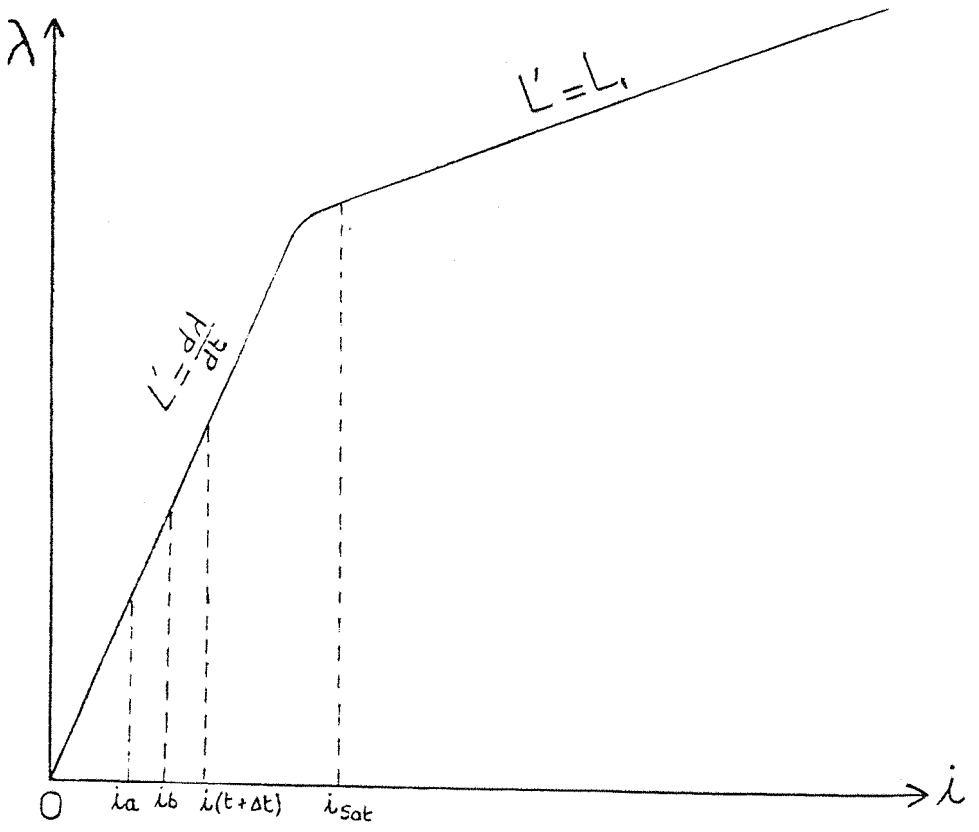

Fig.3.8 λ/i relationship.

3.8 Summary

In this chapter, the results of the finite-element method for determining the field are presented. The study model is presented as well as its B/H characteristic. The λ/i relationship is formulated as a function of the dimensions of the equipment. An expression to describe the B/H relationship from which the differential inductance can be derived is presented. The v/i experimental characteristic of the device is recorded. To estimate the value of the current for the next time step in the numerical solution the forward predictor method is presented.

CHAPTER FOUR

EXPERIMENT AND RESULTS

The computed results of the analysis of the systems described in chapter two are presented. To valid the computed results, some experiments were carried out at the laboratory on the cable system shown in Fig.4.1. Theoretical and experimental results are also presented and compared.

4.1 Single conductor in a metallic sheath.

Fig.4.2 shows the current and voltage waveforms for the system of Fig.2.1, when operating under normal load current of 1600 A. The voltage across the device is slightly distorted and is about 100 V. The current shows its typical peaky form and is nearly 200 A. The device is operating at the knee point. However, Fig.4.3 shows the current and voltage waveforms when the system is carrying a load current of 5.o KA. During the period when the device is operating in the high saturation region, the current reaches its peak value of about 3 KA and the voltage is highly distorted (50V fundamental with a superposed 280 V peak). At the instant of time when the device is out of saturation which means a small current flows in it, the instantaneous voltage is maximum of about 330 V peak. The resistance of the return path is assumed to be zero.

4.1.1 Fault condition

In the event of a fault at the far end of the cable

(fig.2.2), the fault current is assumed to return to the source by the earth which has a resistance R_e= 0.05Ω. In Fig.4.4 the current and voltage waveforms are shown, for a load current of 5.0 KA, their peaks are respectively 3.5 KA and 380 V. When the flux is below the knee point, the voltage is sinusoidal with a maximum of 60 V. When high load current is carried by the conductor(60 KA, Fig.4.5),the current is slightly distorted and reaches a peak value of 50 KA. The voltage is almost sinusoidal (60 V peak value), except for peaks which occur for a very short time.

4.2 Single-phase system

Part of the current which returns to the generator (fig.2.4), is assumed to return by a ground resistance R_e= 0.05Ω. The magnitude of the voltage depends on the impedance of the earth return path, and the size of the fault current which can be seen in Fig.4.6 to Fig.4.8. A transient current and voltage occur before they reach their steady state waveforms. For a load current of 1600 A, the voltage across the device is 80 V and the current is 100 A. For a load current of 5 KA, the voltage starts to be distorted and the current reaches a peak value of nearly 4 KA. For heavy current of 60 KA, the voltage is slightly peaky (1.5 KV) and the current reaches 50 KA. Which means that when the flux density exceeds the saturation level the inductance changes from a high value to a very low value and initiates high current to flow. This current is symmetrical but shows its typical peaks since the flux is still operating in the saturation region.

4.3 Three-phase system

The current and voltage waveforms for the three-phase system in the event of a fault condition (Fig.2.7), are shown in Fig.4.9 and Fig.4.10. It can be seen, that after reaching the steady state, the voltage across the device is 80 V and the current 100 A for a load current of 1600 A. For a load current of 5 KA the voltage across the device is nearly 230 V peak and the current is approximatly 3.7 KA, this shows that the device is well above saturation.

4.4 Description of the tests rig.

Fig.4.1 shows the arrangement adopted for all the tests. The cable core was coupled to ac transformer 240/10V and 10 KVA, by means of the variac R (240/0--270V), a variable voltage could be applied to the cable, resulting in various loading currents. The scale model cable was a low voltage cable used just to demonstrate the principle, therefore its sheath current rating was nearly equal to the load current. Bonding leads were connected to the ends of the cable sheath which go through the protective device and to earth. In this way the voltage across the device and the current through it can be read on the oscillogram connected across these ends. the variable current supplyed by ac transformer varies from 0--1000A. The length of the cable was approximatly 40m and the distance separating the cable sheaths was d=0.5m. The frequency of the alternating supply throughout the tests was 50 Hz. Tests were conducted for various currents in the main conductor, to obtain the

complete volt/ampere of the device when operating below and above saturation.

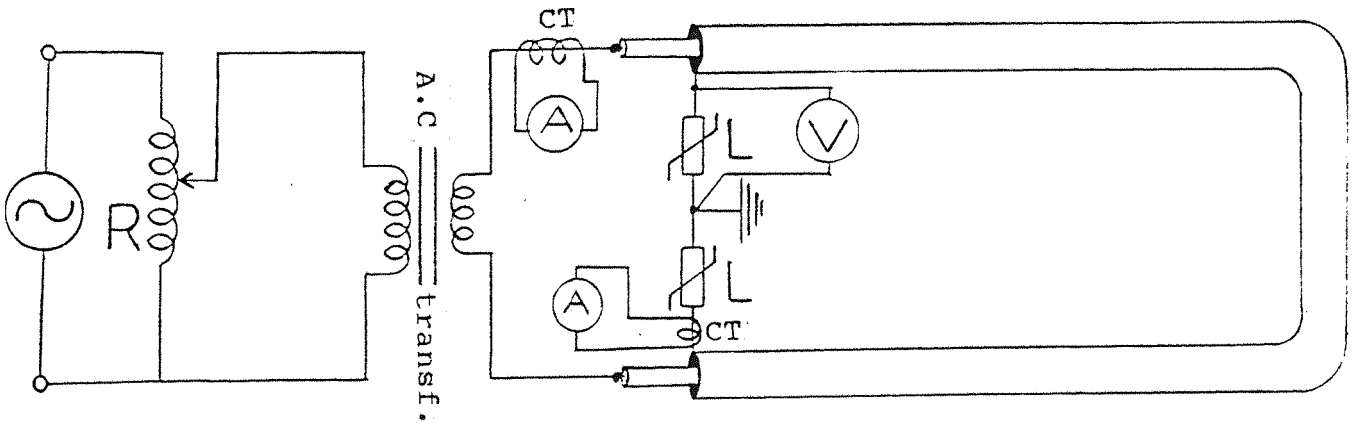

Fig.4.1 Tests rig.

4.5 Cable system data

R_c = 54.8 μΩ/m

R_{mh} = 60 μΩ/m

r = 14.0 mm conductor raduis

r_o = 16.3 mm under sheath raduis

r_i = 18.0 mm over sheath raduis

d = 0.5 m spacing between cables

overall diameter = 41.5 mm

4.6 Computed and experimental results of the test rig.

The computed results for the test rig system shown in Fig.4.1 are presented in Fig.4.11 to Fig.4.13 for various

load currents. The system has a length of about 40m, so that the induced voltage on the sheath is very small. For the load currents of 250 A, 420 A and 600 A, the voltages obtained across the device are 2.7V, 4.6V and 6.2V respectively and the current are 100 A, 250 A and 400 A. The current waveforms show their typical peaky forms and the voltages increase its distortion as the flux increases above saturation. These computed results are in good concordance with the experimental ones presented in fig.4.15 to fig.4.17 (see table 4.1). The slight difference in the waveform shapes between the experimental and computed results is due to the characteristic /i of the device which was approximated by the numerical method.

In Fig.4.14 to Fig.4.17 experimentals results of recorded signals on the oscillogram are reported, for different load current I carried by the cable system. For comparison and conclusion purposes, signals were recorded for the system with and without the device, although the figures show how the current in the sheath has been reduced with the presence of the device. The change of the current around the knee point causes a sharpening of the waveforms of the voltage accross the device.

Table 4.1 The peak values of the current and voltage on the device for various load currents.

load current	computed results		experimental results	
250A	2.7V	100A	2.6V	68A
420A	4.6V	250A	4.2V	210A
600A	6.2V	400A	5.5V	350A

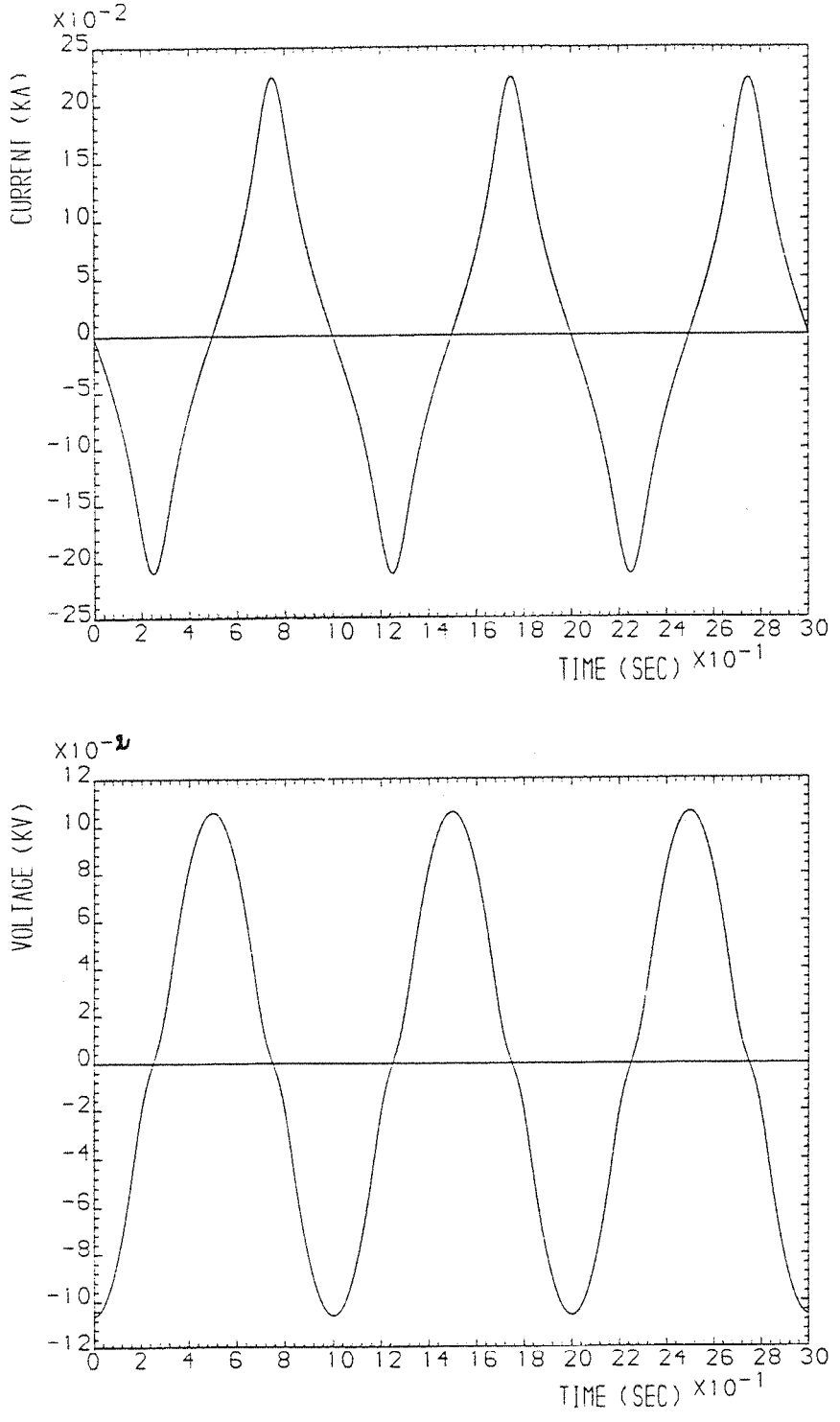

load current of 1.6 KA.

Fig.4.2 Computed current and voltage waveforms, on the device for the system of fig.2.1.

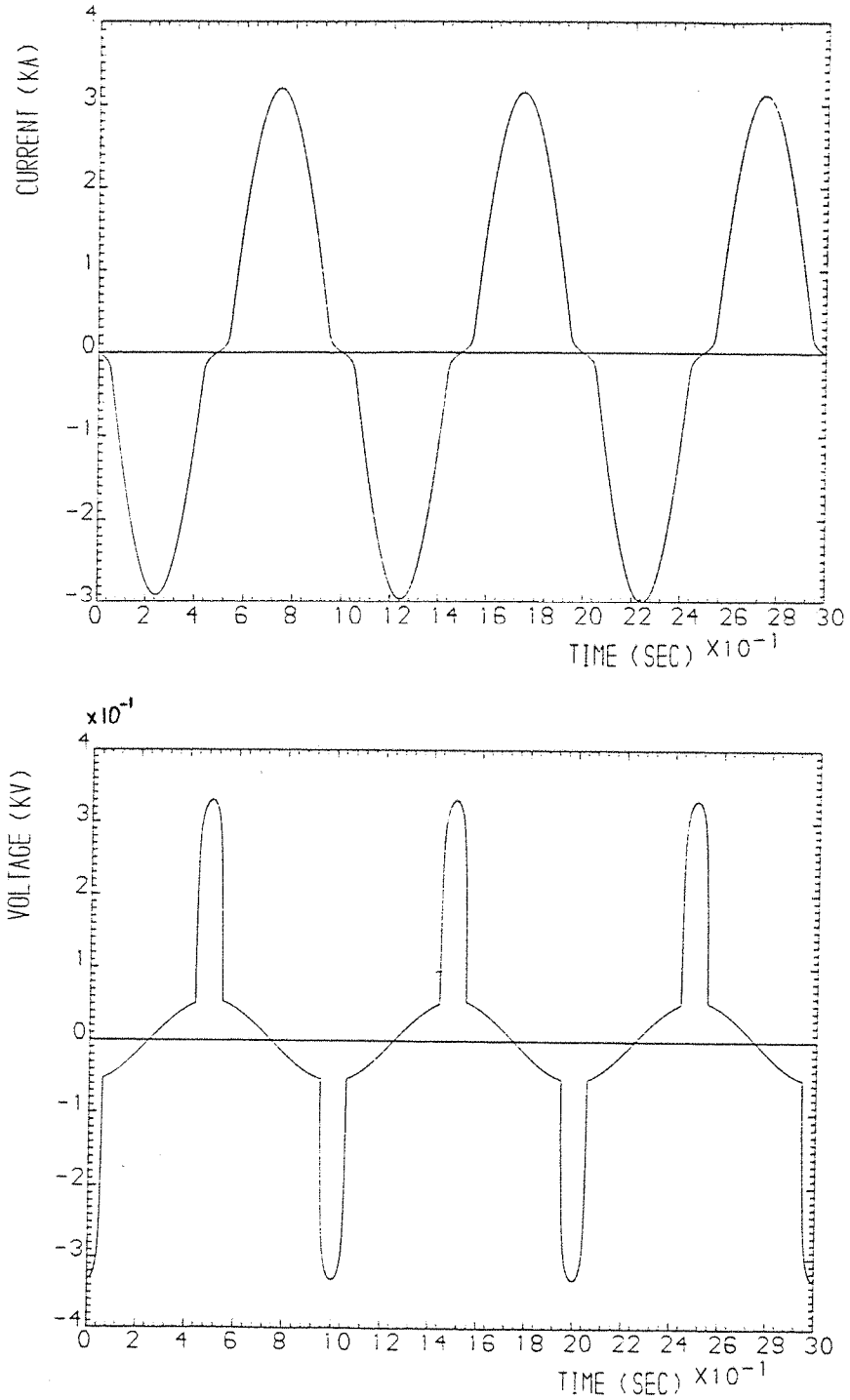

load current of 5.0 KA.

Fig.4.3 Computed current and voltage waveforms, on the device for the system of fig.2.1.

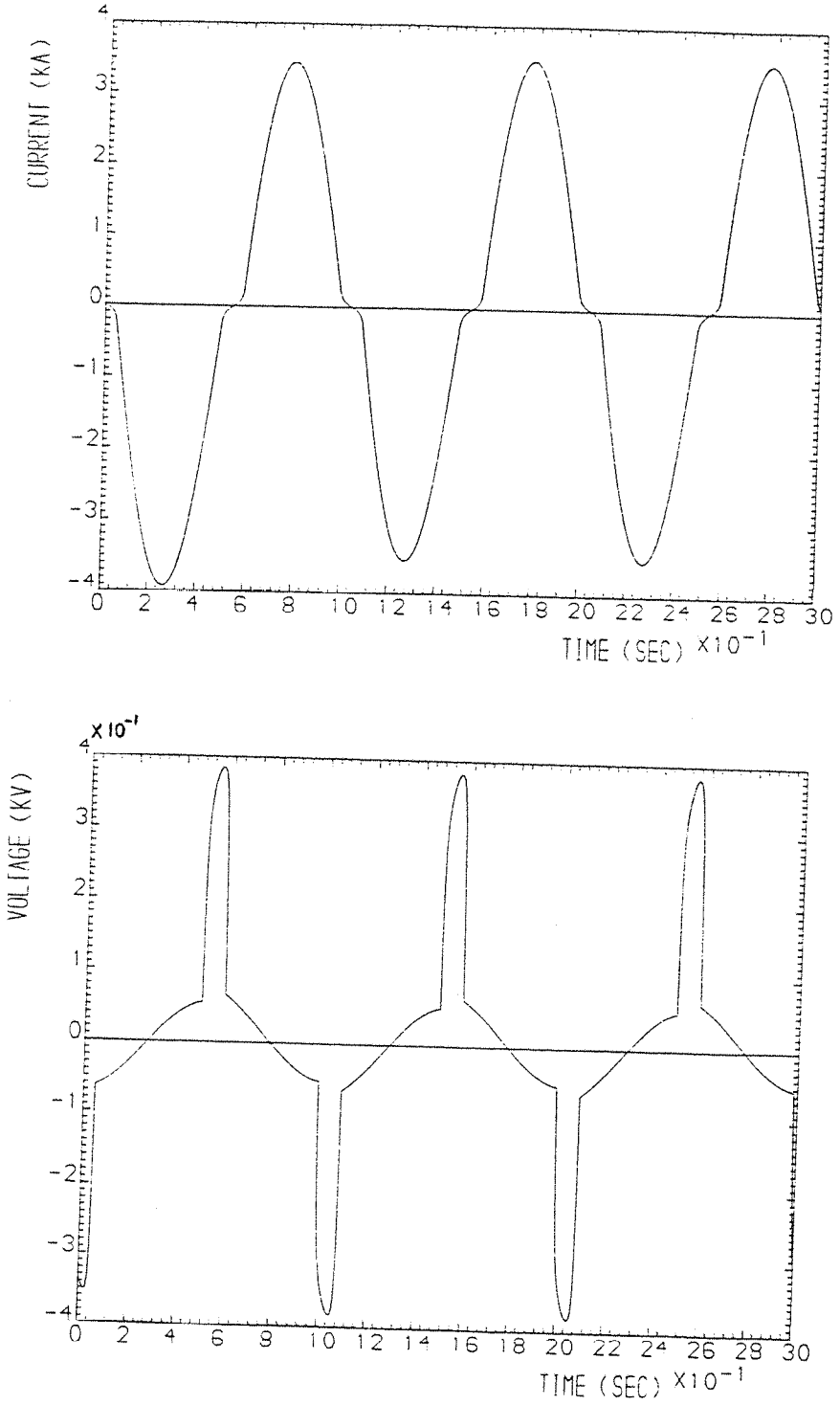

load current of 5.0 KA.

Fig.4.4 Computed current and voltage waveforms, on the device for the system of fig.2.2.

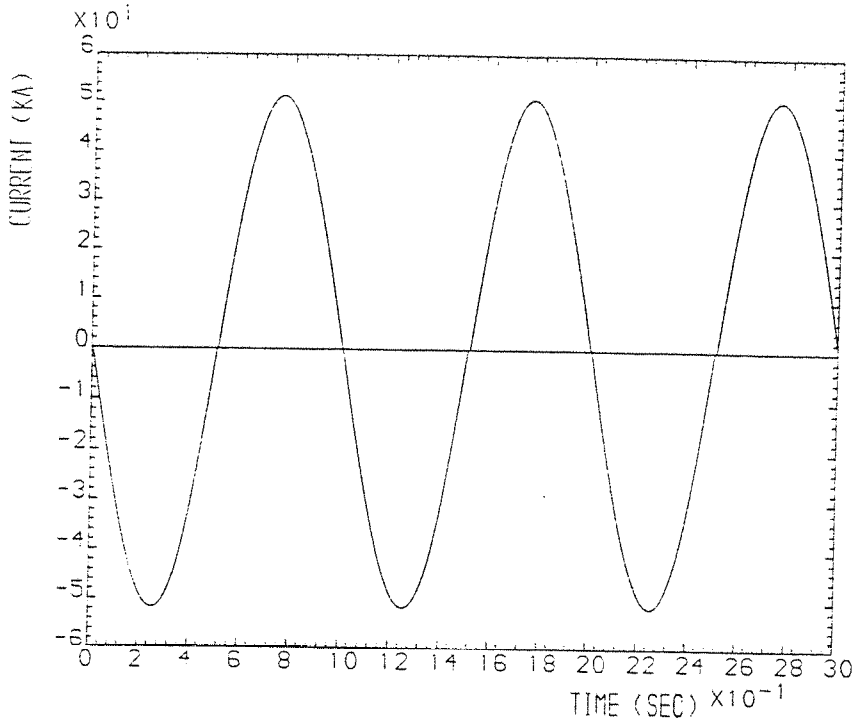

load current of 60 KA.

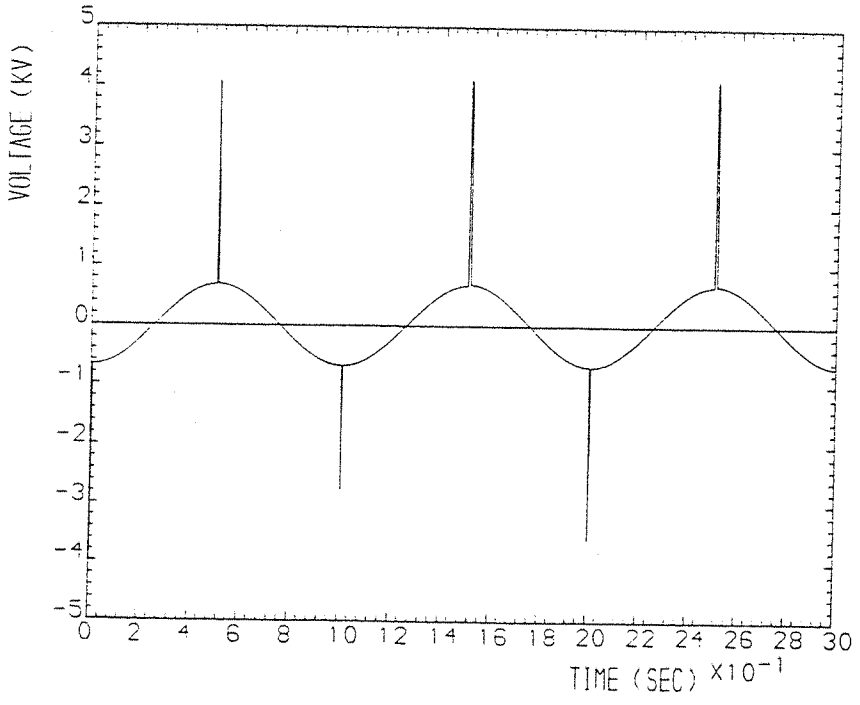

Fig.4.5 Computed current and voltage waveforms, on the device for the system of fig.2.1.

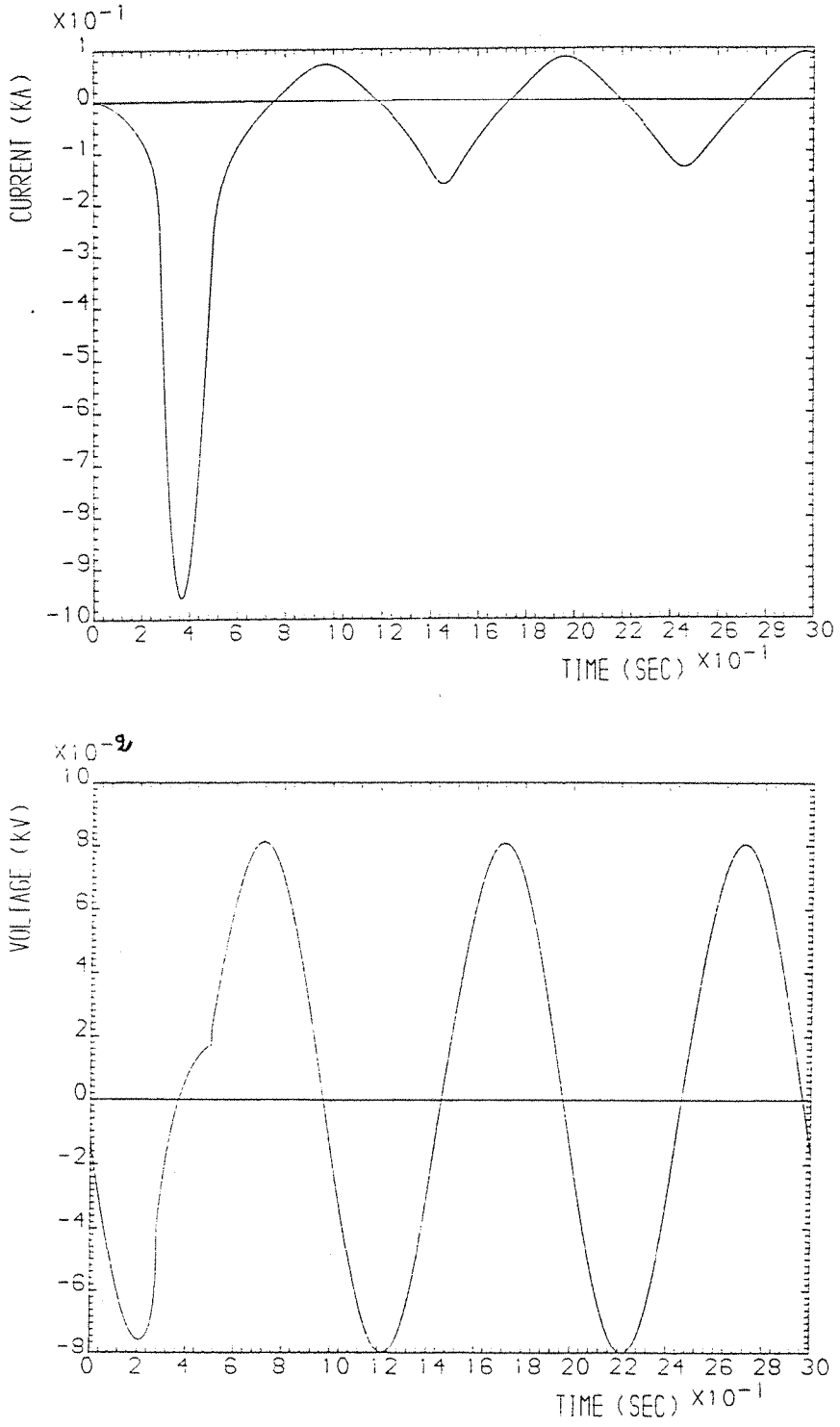

load current of 1.6 KA

Fig.4.6 Computed current and voltage waveforms, on the device for the single-phase

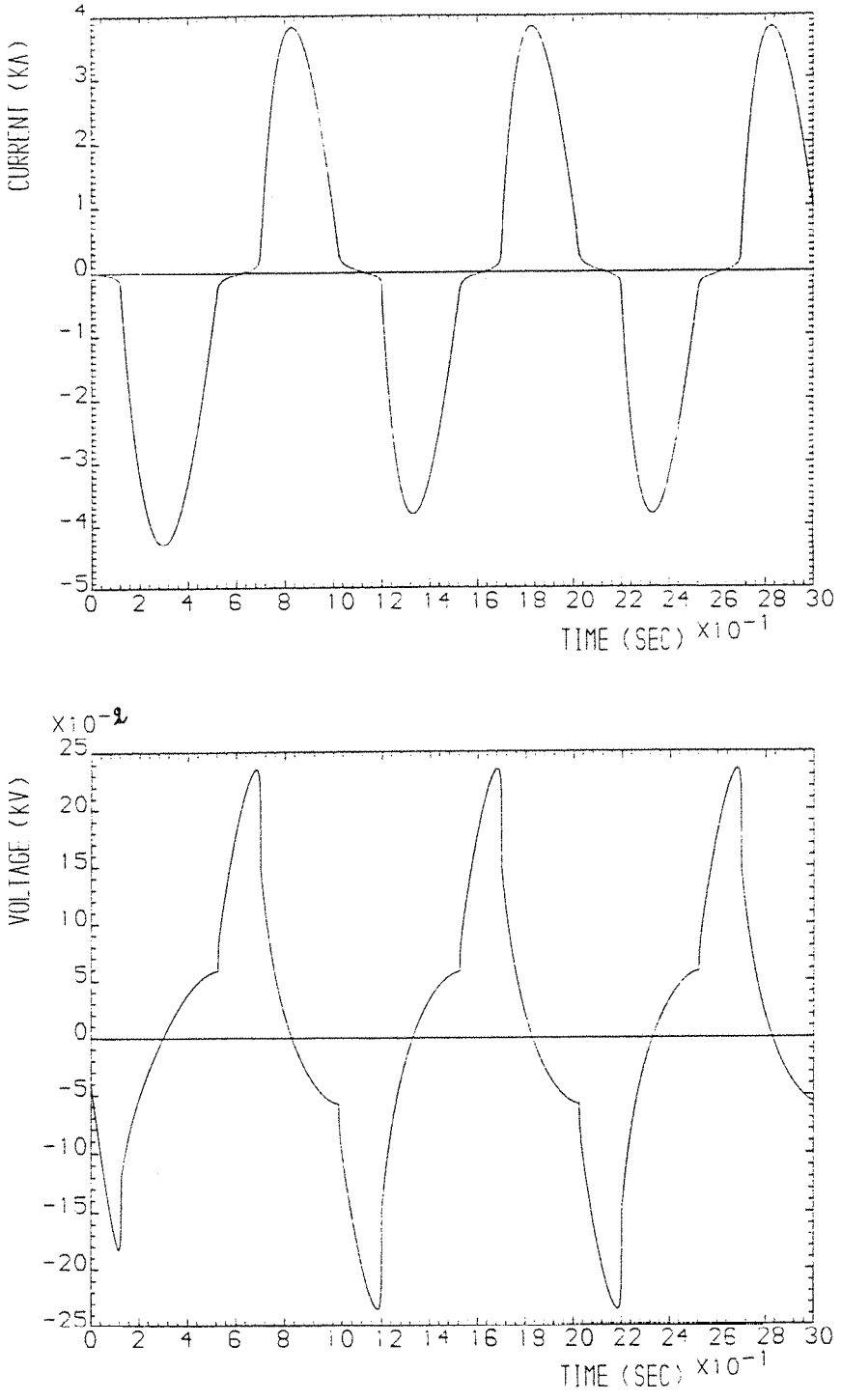

load current of 5.0 KA

Fig.4.7 Computed current and voltage waveforms, on the device for the single-phase system represented in fig.2.4.

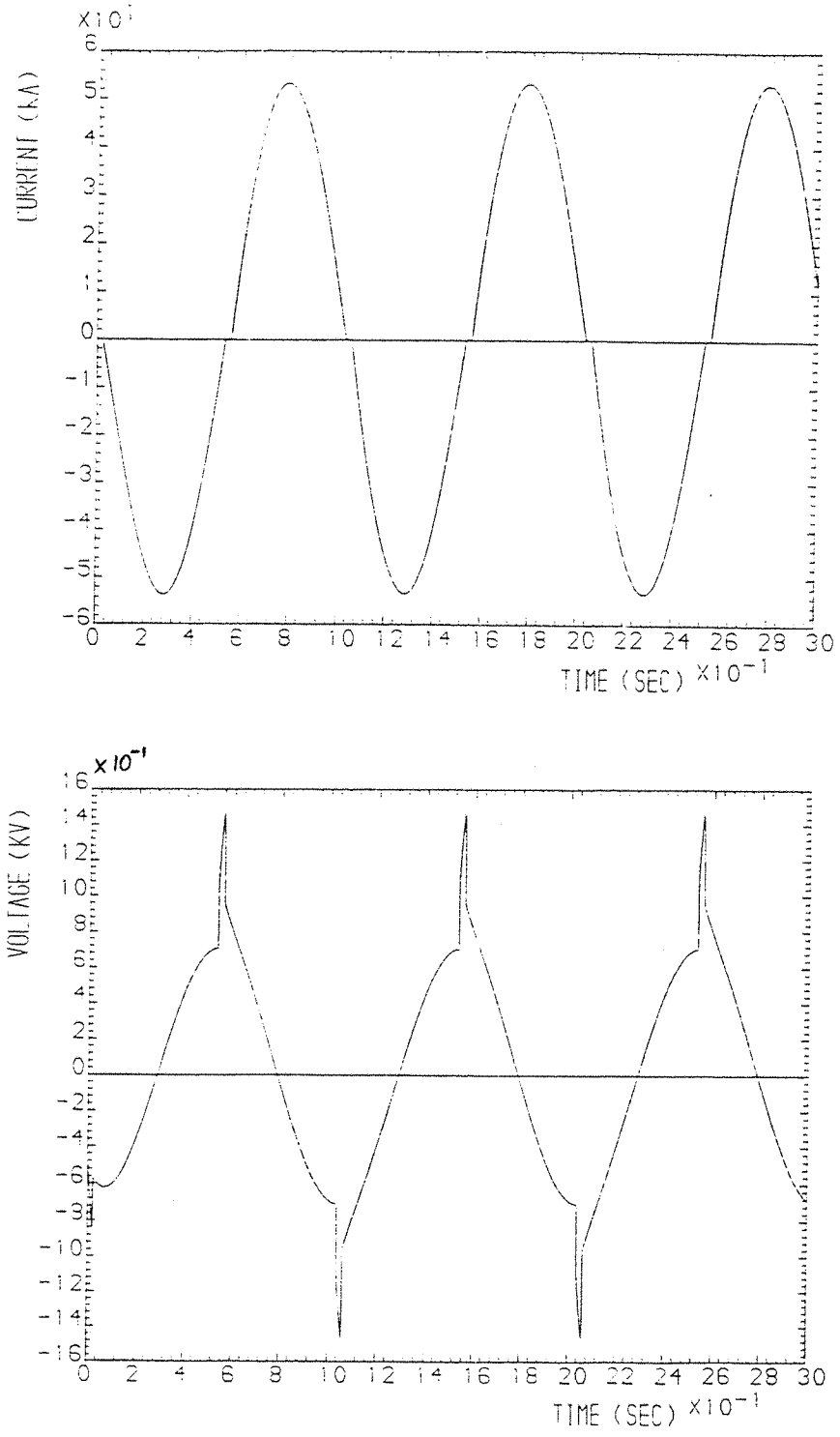

load current of 60 KA

Fig.4.8 Computed current and voltage waveforms, on the device for the single-phase system represented in fig.2.4.

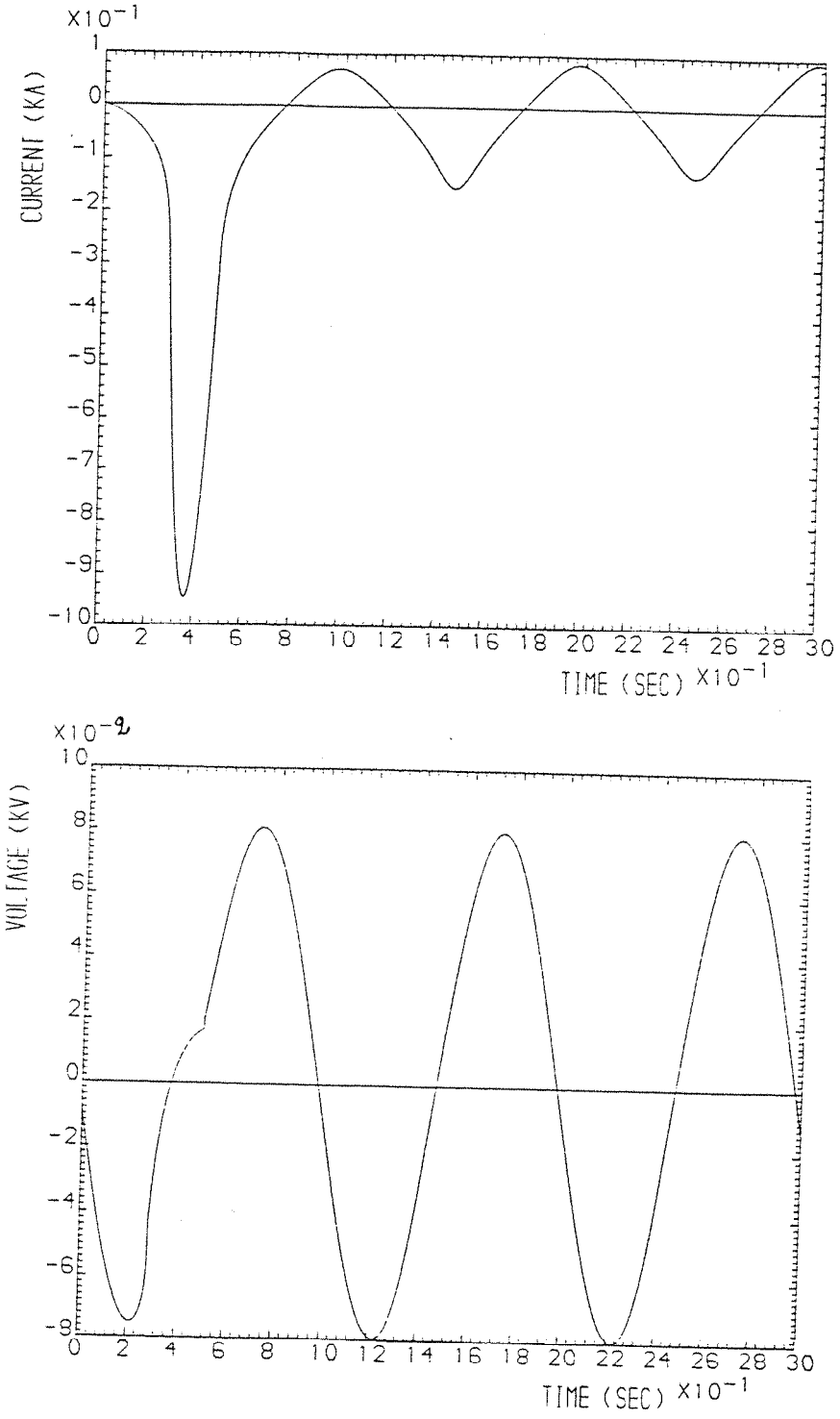

load current of 1.6 KA

Fig.4.9 Computed current and voltage waveforms, on the device for the three-phase system represented in fig.2.7.

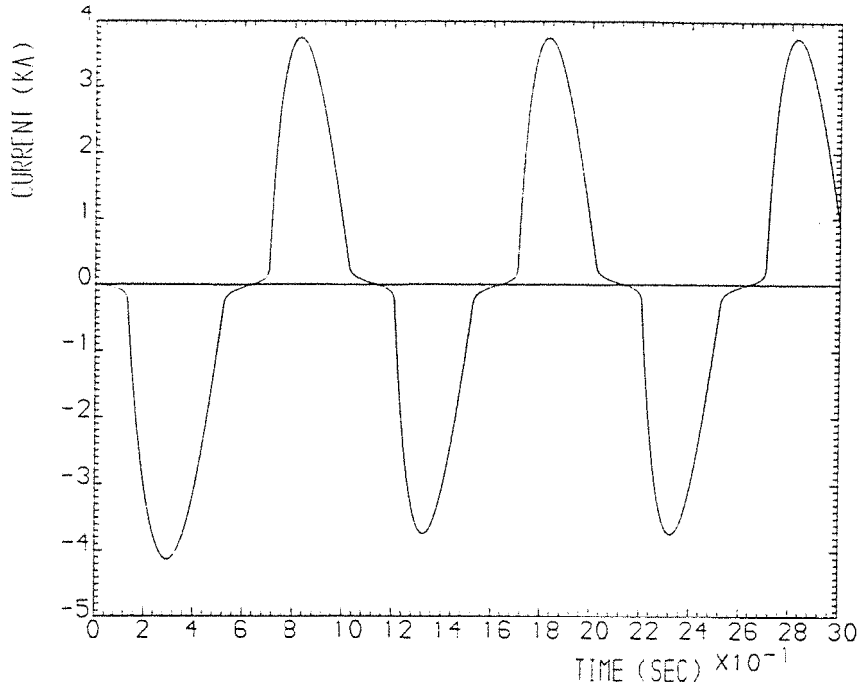

load current of 5.0 KA

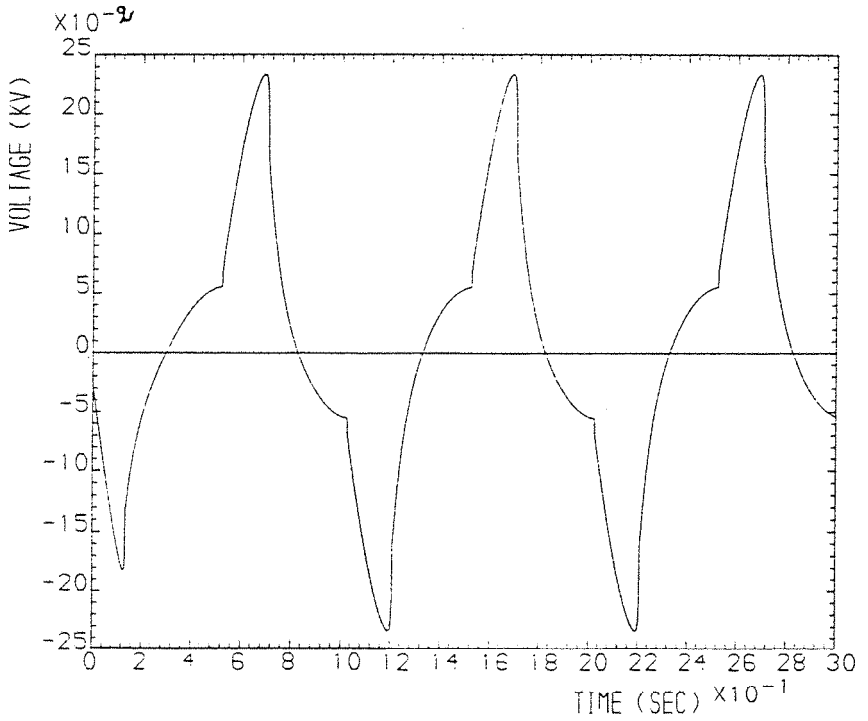

Fig.4.10 Computed current and voltage waveforms, on the device for the three-phase system represented in fig.2.7.

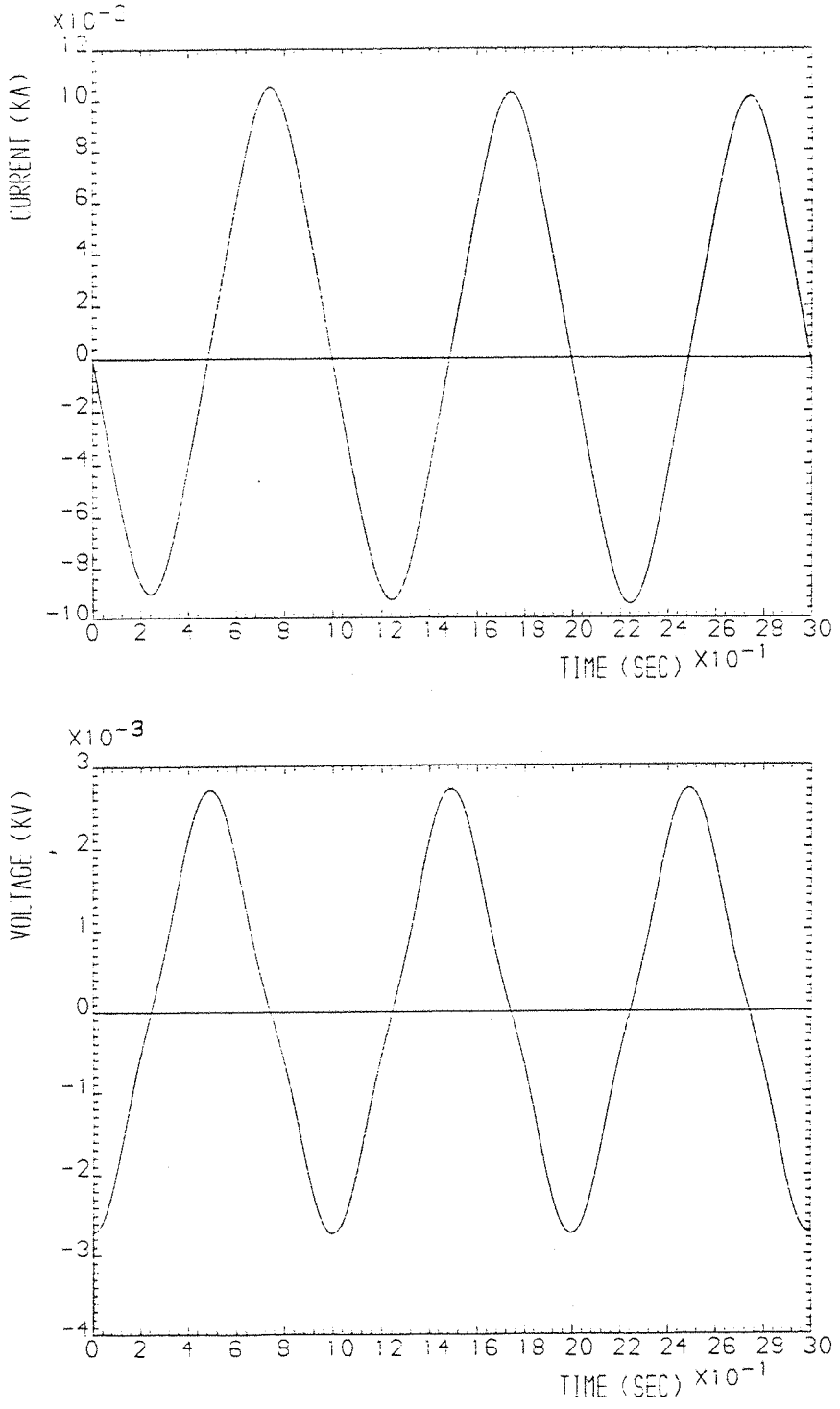

load current
of 250 A

Fig.4.11 Computed current and voltage waveforms, on the device for the system of fig.4.1.

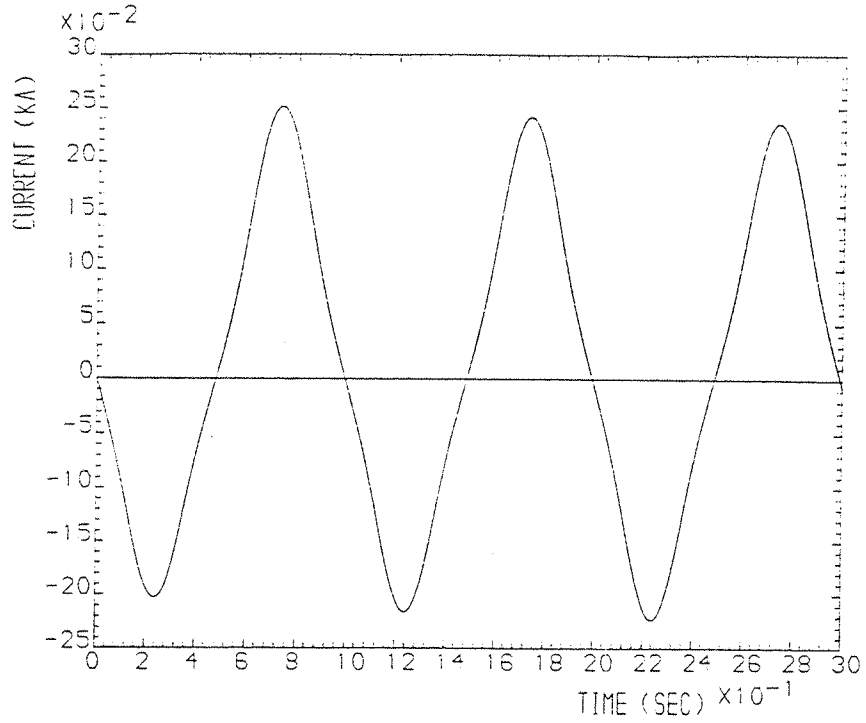

load current of 420 A

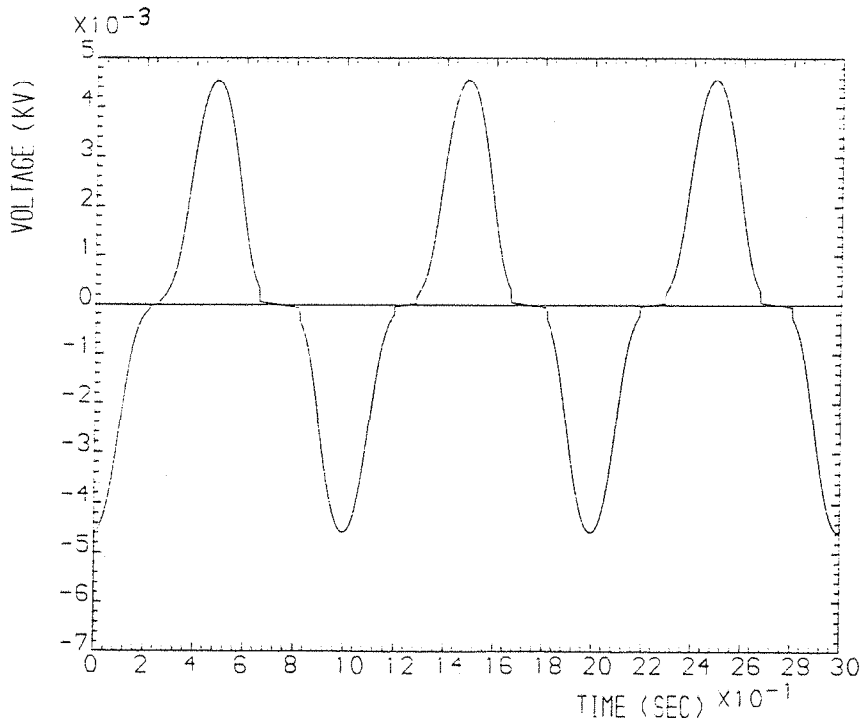

Fig.4.12 Computed current and voltage waveforms, on the device for the system of fig.4.1.

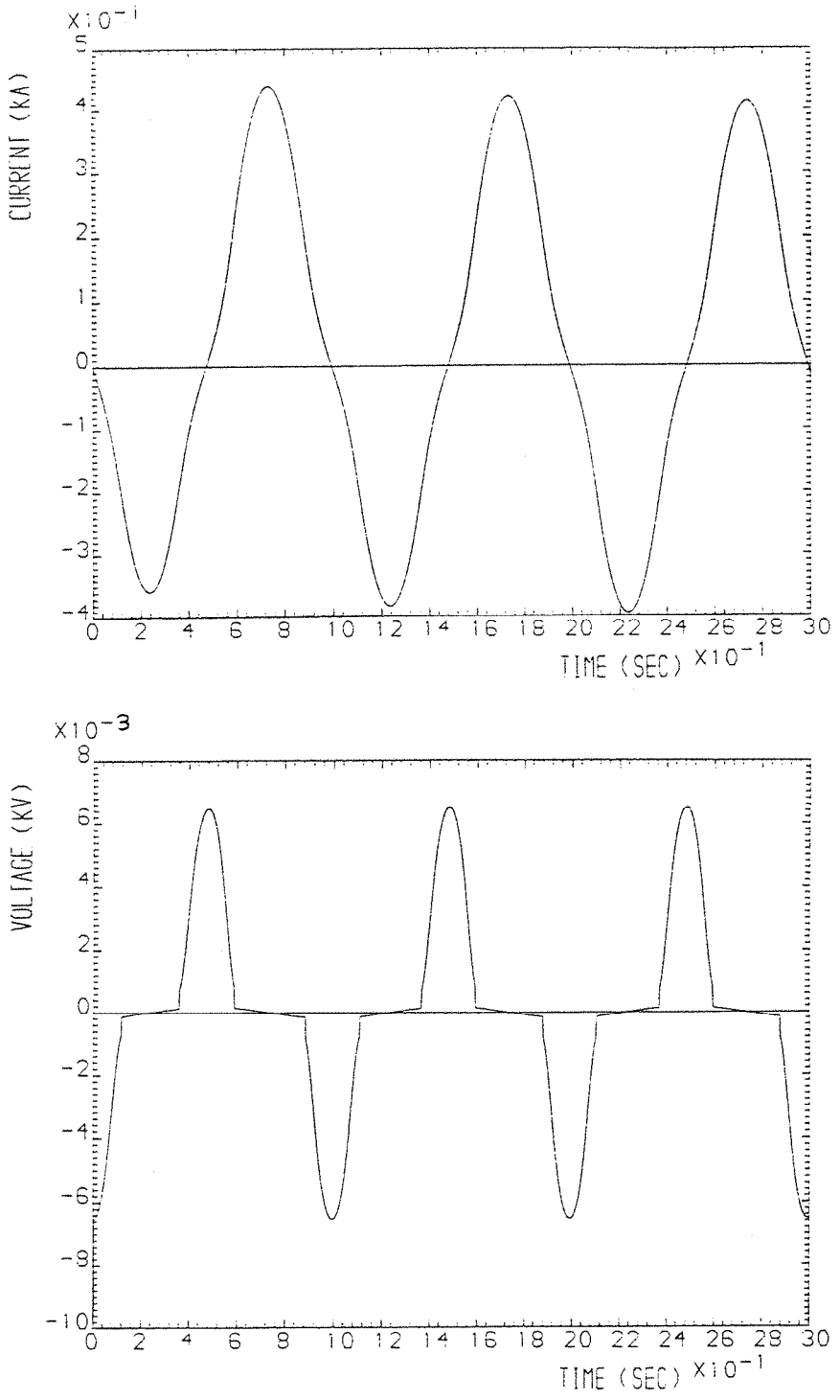

load current of 600 A

Fig.4.13 Computed current and voltage waveforms, on the device for the system of fig.4.1.

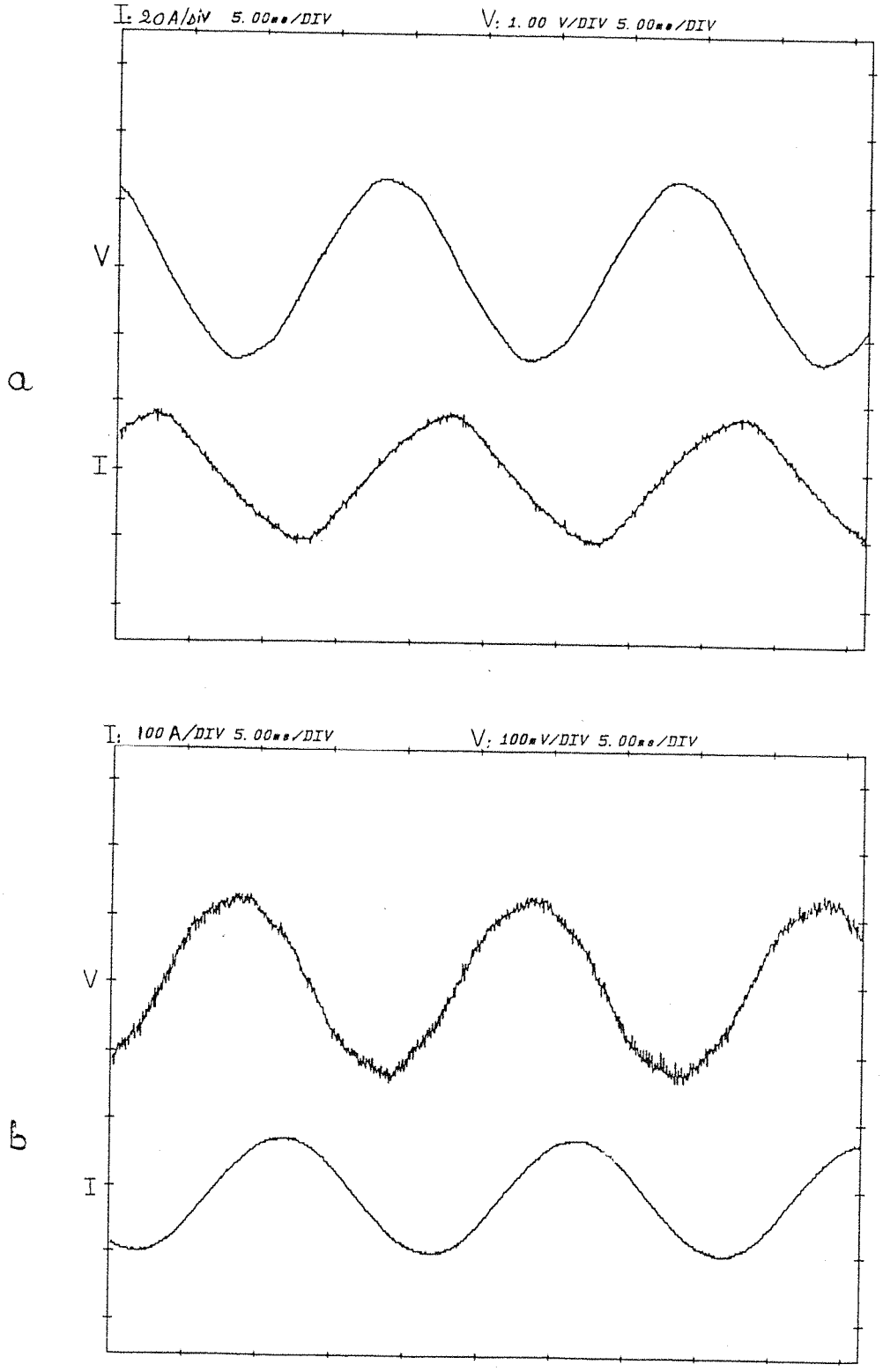

load current of 120 A

Fig.4.14 Experimental current and voltage waveforms, on the sheath for the system of fig.4.1.
a: with the device b: without device

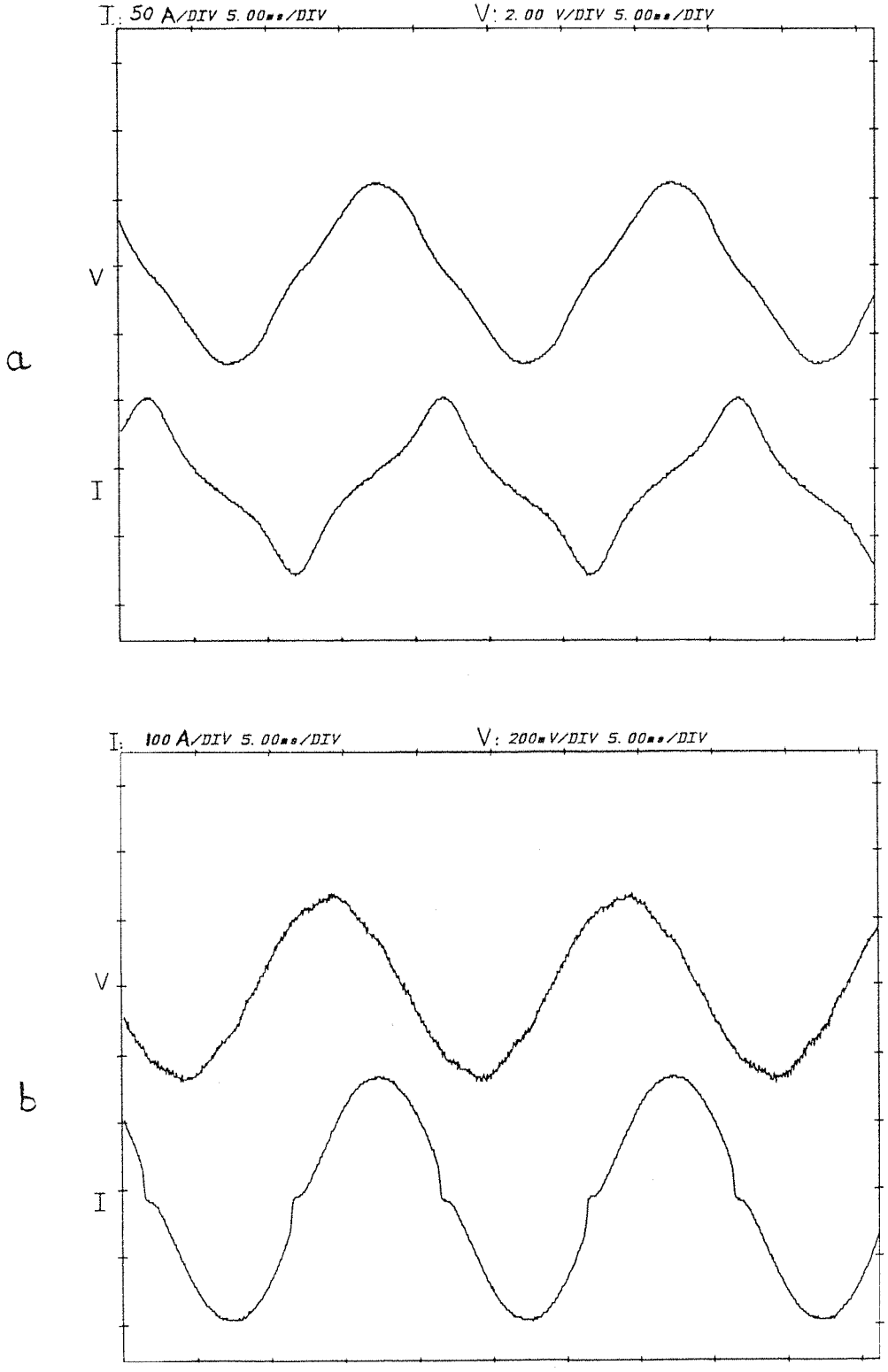

Fig.4.15 Experimental current and voltage waveforms, on the sheath for the system of fig.4.1.
a: with the device b: without device

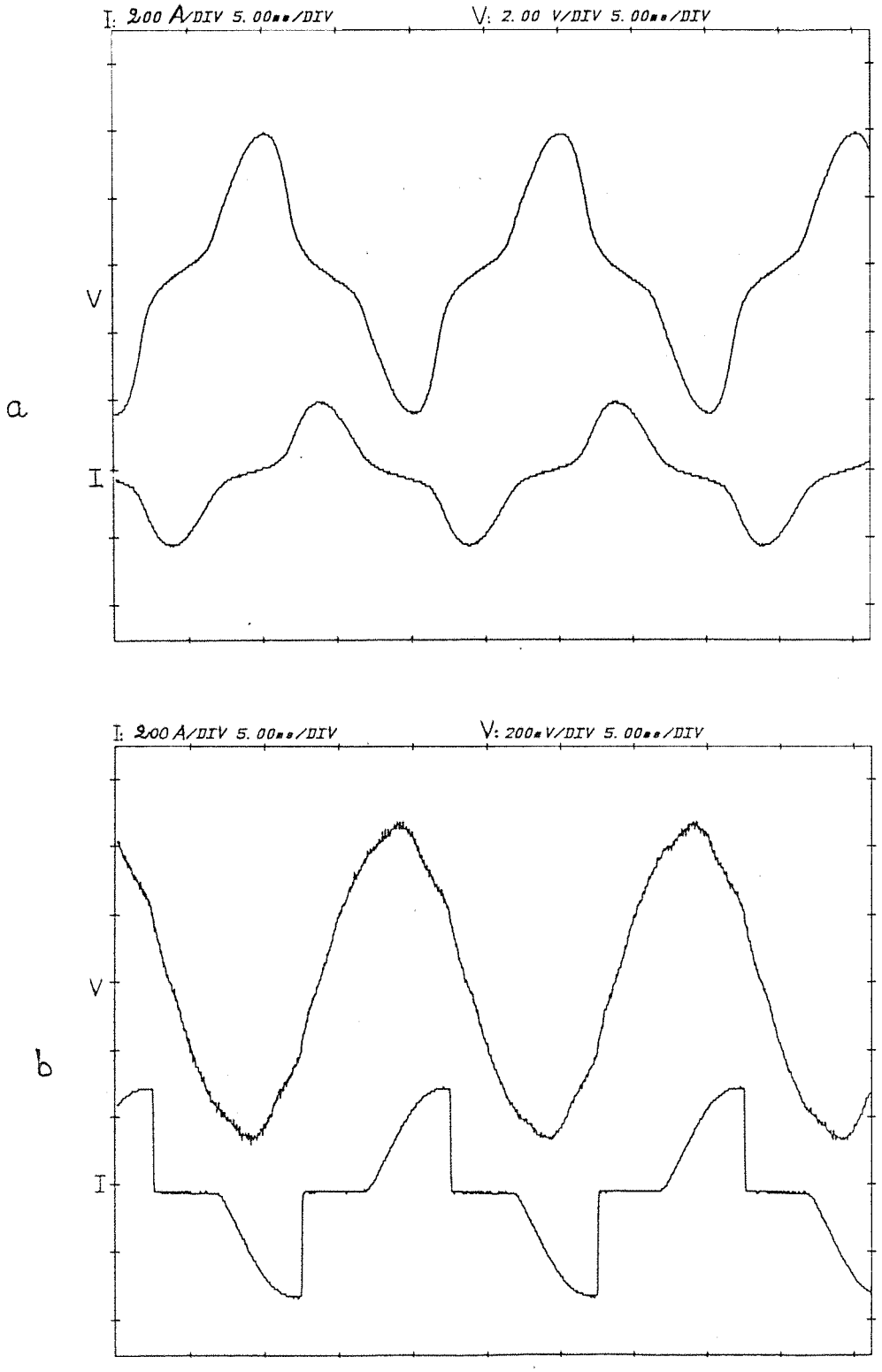

Fig.4.16 Experimental current and voltage waveforms, on the sheath for the system of fig.4.1.
a: with the device b: without device

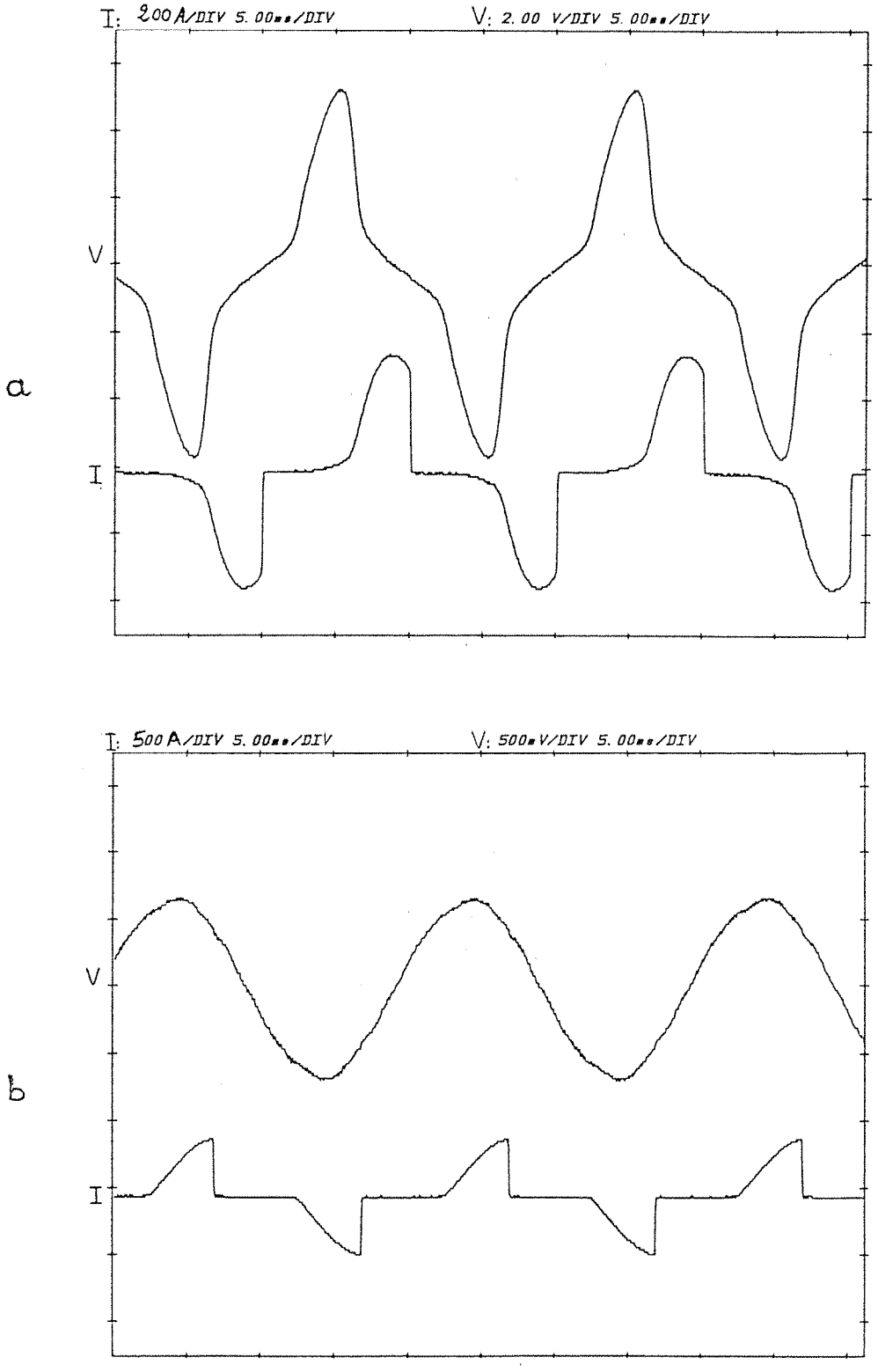

Fig.4.17 Experimental current and voltage waveforms, on the sheath for the system of fig.4.1.
a: with the device b: without device

CHAPTER FIVE

EVALUATION OF THE CABLE SYSTEM PARAMETERS

This chapter describes a general formulation of impedances and admittances of single-core coaxial cables. The method of transient analysis proposed here is based on the theory of wave propagation in multiconductor system, and therefore, takes into account all the metallic conductors in the system as well as the ground itself. The method of analysis may be interpreted in terms of natural modes of propagation. The characteristics of these modes, as a function of frequency are given for a representative cable system.

The Z-transform technique which is mainly concerned with the transformation of the cable characteristics from the frequency domain to the time domain is illustrated.

5.1 Current and voltage relations on a transmission system.

The basic equations that describe the behaviour of a multiconductor transmission system are as follows:

$$\frac{dV^p(x,t)}{dx} = -Z^p(t)\, I^p(x,t) \qquad 5.1$$

and

$$\frac{dI^p(x,t)}{dx} = -Y^p(t)\, V^p(X,t) \qquad 5.2$$

where $V^p(x,t)$ and $I^p(x,t)$ are column matrices representing the phase voltage and current at a point x at the instant t along the system, and $Z^p(t)$ and $Y^p(t)$ are square matrices representing the series impedance and shunt admittance matrices per unit length respectively.

These equations are transformed into the frequency domain as

$$\frac{dV^p}{dx}(x,w) = -Z^p(w)\, I^p(x,w) \qquad 5.3$$

and

$$\frac{dI^p}{dx}(x,w) = -Y^p(w)\, V^p(x,w) \qquad 5.4$$

or simply as

$$\frac{dV^p}{dx} = -Z^p I^p$$

and

$$\frac{dI^p}{dx} = -Y^p V^p$$

Differentiating equations 5.3 and 5.4 with respect to x and substituting one in the other give:

$$\frac{d^2V^p}{dx^2}(x,w) = Z^p(w)Y^p(w)\, V^p(x,w) = P(w)V^p(x,w)$$

and

$$\frac{d^2I^p}{dx^2}(x,w) = Y^p(w)\, Z^p(w)\, I^p(x,w) = P^t(w)\, I^p(x,w)$$

for $P(w) = Z^p(w)\, Y^p(w)$

and $P^t(w) = Y^p(w)\, Z^p(w)$

$Z^p(w)$ and $Y^p(w)$ are always symetrical, so that the product of $Z^p(w)$ $Y^p(w)$ leads to the transpose of $Y^p(w)$ $Z^p(w)$.
Modal and actual variables are related by

$$V^p(w,x) = C_1(w)\ V(w) \qquad 5.7$$

$$I^p(w,x) = C_2(w)\ I(w) \qquad 5.8$$

Using these transform relationships in equations 5.5 and 5.6 give:

$$\frac{d^2V}{dx^2}(x,w) = \lambda^2(w)\ V(x,w) \qquad 5.9$$

and

$$\frac{d^2I}{dx^2}(x,w) = \lambda_t^2(w)\ I(x,w) \qquad 5.10$$

where $\lambda^2(w) = C_1^{-1}(w)\ P(w)\ C_1(w)$

and $\lambda_t^2(w) = C_2^{-1}(w)\ P(w)\ C_2(w)$

Elements of $\lambda^2(w)$ are eigenvalues of $P(w)$ and as the eigenvalues of $P(w)$ are those of its transpose, $\lambda_t^2(w) = \lambda^2(w)$. $C_1(w)$ and $C_2(w)$ are matrices of eigenvectors of $P(w)$ and $P_t(w)$ respectively.
Solving equations 5.9 and 5.10 as ordinary differential equations in x, results in equations:

$$V(w,x) = \mathrm{Exp}(-(w,x))A(w) + \mathrm{Exp}(\ (w,x))B(w) \qquad 5.11$$

$$Z(w)i(w,x) = \mathrm{Exp}(-(w,x))A(w) - \mathrm{Exp}(\ (w,x))B(w) \qquad 5.12$$

A(w) and B(w) are to be found from the boundary conditions.

Z(w) is a matrix of modal surge impedances:

$$z(w) = C_1^{-1}(w)\ Z^{P}(w)\ C_2(w)$$

and $$Z(w) = \lambda^{-1}(w)\ z(w)$$

5.2 Cables parameters.

The electrical characteristics [10] of a cable system are defined completely by the two basic parameters shunt admittance and series impedance, both per unit length.

5.2.1 Shunt admittance.

Consider the basic cable system shown schematically in Fig.5.1. The cable system constists of an inner conductor, radius r_1 , resistivity ρ_1 , conductor dielectric with permitivity ϵ_1 , sheath inner and outer raduis r_2 and r_3 and resistivity ρ_2, sheath dielectric with permitivity ϵ_2, and outer raduis r_4, and earth-return path with resistivity ρ_3. The shunt admittance submatrix of the i^{th} cable has the dimension 2x2 and is:

$$Y_1 = \begin{bmatrix} Y_1 & -Y_1 \\ -Y_1 & Y_1+Y_2 \end{bmatrix}$$

where $$Y_1 = g_1 + jw2\pi\epsilon_1/\ln(r_2/r_1) \qquad 5.13$$

$$Y_2 = g_2 + jw2\pi\epsilon_2/\ln(r_4/r_3) \qquad 5.14$$

with g_1 and g_2 are the leakage conductances across the inner

and outer insulations (but in our study they will be neglected).

The admittance matrix Y is assembled from the N submatrices Y_i which are along the diagonal. The soil acts as an electrostatic shield between cables and hence off diagonal submatrices are zero.

$$Y = \begin{bmatrix} Y_1 & 0 & 0 \\ 0 & Y_2 & 0 \\ 0 & 0 & Y_3 \end{bmatrix} = \begin{bmatrix} Y_1 & -Y_1 & 0 & 0 & 0 & 0 \\ -Y_1 & Y_1+Y_2 & 0 & 0 & 0 & 0 \\ 0 & 0 & Y_1 & -Y_1 & 0 & 0 \\ 0 & 0 & -Y_1 & Y_1+Y_2 & 0 & 0 \\ 0 & 0 & 0 & 0 & Y_1 & -Y_1 \\ 0 & 0 & 0 & 0 & -Y_1 & Y_1+Y_2 \end{bmatrix}$$

5.2.2 Series impedance.

The submatrices Z_i are assembled along the diagonal of the Z matrix in the same order as for the shunt admittance matrix.

$$Z_i = \begin{bmatrix} Z_1 & Z_3 \\ Z_3 & Z_2 \end{bmatrix}$$

where $Z_1 = z_1 + z_2 + z_3 + z_5 + z_6 + z_7 - 2z_4$

$Z_2 = z_5 + z_6 + z_7$

$Z_3 = z_5 + z_6 + z_7 - z_4$

These expressions simplify at low frequencies, when Z sheath-inner = Z sheath-outer = $z_4 = R_{dc}$, and z_4 disappears from the expressions.

These seven component impedances for the cable shown in Fig.5.1 are obtained as described:

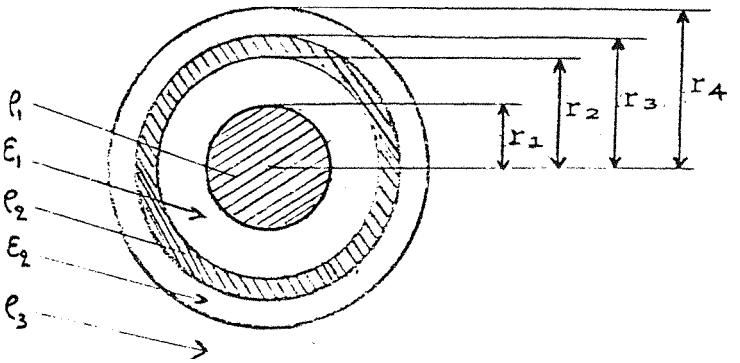

Fig.5.1 Basic configuration.

z_1, the internal impedance of the inner conductor is given by

$$z_1 = (\rho_1 m/2\pi r_1).\coth(0.777 m r_1) + 0.356\rho_1/\pi r_1 \qquad \Omega/m$$

where $m = (jw\mu/\rho_1)$

z_2, the impedance due to the time varying magnetic field in the inner insulation:

$$z_2 = (jw\mu/2\pi)\ln(r_2/r_1) \qquad \Omega/m$$

z_3, the inner sheath internal impedance. This impedance is

calculated from the voltage drop on the inner surface of the sheath per unit current which returns via the inner conductor.

$$z_3 = (\rho_2 m/2\pi r_2).\coth(m\Delta) - \rho_2/2\pi r_2(r_2 + r_3) \quad \Omega/m$$

where $\Delta = r_3 - r_2$

z_4, the sheath mutual impedance is given by

$$z_4 = (\rho_2 m/\pi(r_2 + r_3))\operatorname{cosech}(m\Delta) \quad \Omega/m$$

z_5, the outer sheath internal impedance is given by:

$$z_5 = \rho_2 m.\coth(m\Delta) + \rho_2/2nr_3(r_2+r_3) \quad \Omega/m$$

z_6, the impedance due to the time varying flux in the outer insulation.

$$z_6 = (jw\mu/2\pi).\ln(r_4/r_3) \quad \Omega/m$$

z_7, the self impedance of the earth-return path.

$$z_7 = (jw\mu/2\pi)(-\ln(\gamma m r_4/2) + 1/2 - 4mh/3) \quad \Omega/m$$

γ =1.781 Euler's constant

h=the depth

The Z matrix takes the form :

$$Z = \begin{bmatrix} Z_1 & Z_{12} & Z_{13} \\ Z_{21} & Z_2 & Z_{23} \\ Z_{31} & Z_{32} & Z_3 \end{bmatrix}$$

and $$Z_{ji} = \begin{bmatrix} Z_{ji} & Z_{ji} \\ \\ Z_{ji} & Z_{ji} \end{bmatrix}$$

The off diagonal are not zero, but take account of the mutual inductance between cables.

The impedances Z_{ji} may be calculated from Pollaczek's formulas. The mutual impedance Z_{ji} between the $i^{th}$and j^{th}cables is given by :

$$Z_{ji} = (jw\mu/2\pi)(-\ln(\gamma m S_{ji}/2) + 1/2 - 2ml/3) \quad \Omega/m.$$

where S_{ji} distance between the $i^{th}$and j^{th}cables.

l the sum of the depths of the $i^{th}$and j^{th}cables.

The developed form of Z will be :

$$Z = \begin{bmatrix} Z_1 & Z_3 & Z_{12} & Z_{12} & Z_{13} & Z_{13} \\ Z_3 & Z_2 & Z_{12} & Z_{12} & Z_{13} & Z_{13} \\ Z_{21} & Z_{21} & Z_1 & Z_3 & Z_{23} & Z_{23} \\ Z_{21} & Z_{21} & Z_3 & Z_2 & Z_{23} & Z_{23} \\ Z_{31} & Z_{31} & Z_{32} & Z_{32} & Z_1 & Z_3 \\ Z_{31} & Z_{31} & Z_{32} & Z_{32} & Z_3 & Z_2 \end{bmatrix}$$

The matrix products ZY and $(ZY)^t$ possess only three distinct eigenvalues, and therefore three distinct propagation constants :

$$\lambda_1 = \lambda_3 = \lambda_5 = \sqrt{Y_1(Z_1 - Z_2)}$$
$$\lambda_2 = \lambda_4 = \sqrt{Y_2(Z_2 - Z_3)}$$
$$\lambda_6 = \sqrt{Y_2(Z_2 + 2Z_3)}$$

So we define three distinct modes:
mode 1 is the coaxial mode
mode 2 is the inter-sheath mode
mode 0 is the zero-sequence sheath mode

To diagonalise the matrix products, the modal transformation matrices is constructed so that each column vector is an eigenvector of the corresponding eigenvalue.
The matrices that satisfy this condition are:

$$C_1 = \begin{bmatrix} 1 & 2/3 & 0 & -1/3 & 0 & 1/3 \\ 0 & 2/3 & 0 & -1/3 & 0 & 1/3 \\ 0 & -1/3 & 1 & 2/3 & 0 & 1/3 \\ 0 & -1/3 & 0 & 2/3 & 0 & 1/3 \\ 0 & -1/3 & 0 & -1/3 & 1 & 1/3 \\ 0 & -1/3 & 0 & -1/3 & 0 & 1/3 \end{bmatrix}$$

$$C_2 = (C_1^{-1})^t$$

$$C_i^{-1} = \begin{bmatrix} 1 & -1 & 0 & 0 & 0 & 0 \\ 0 & 1 & 0 & 0 & 0 & 1 \\ 0 & 0 & 1 & -1 & 0 & 0 \\ 0 & 0 & 0 & 1 & 0 & -1 \\ 0 & 0 & 0 & 0 & 1 & -1 \\ 0 & 1 & 0 & 1 & 0 & 1 \end{bmatrix}$$

The characteristic modal impedance matrix may be obtained by means of:

$$Z = \lambda^{-1} C_i^{-1} Z^{p} C_2$$

It takes the form:

$$Z = \begin{bmatrix} Z_1' & 0 & 0 & 0 & 0 & 0 \\ 0 & 2Z_2' & 0 & Z_1' & 0 & 0 \\ 0 & 0 & Z_1' & 0 & 0 & 0 \\ 0 & Z_1' & 0 & 2Z_2' & 0 & 0 \\ 0 & 0 & 0 & 0 & Z_1' & 0 \\ 0 & 0 & 0 & 0 & 0 & 3Z_0' \end{bmatrix}$$

where

$$Z_1' = \lambda_1 / Y_1, \quad Z_2' = \lambda_2 / Y_2, \quad Z_0' = \lambda_6 / Y_2$$

Z is a nondiagonal matrix because there is a mutual coupling between the intersheath modes owing to the fact that $C_2 \neq C_1$. The characteristic modal impedances are complex and frequency dependent. These impedances for minor section of length l=500m are computed for different frequencies and they are shown in fig.5.2.

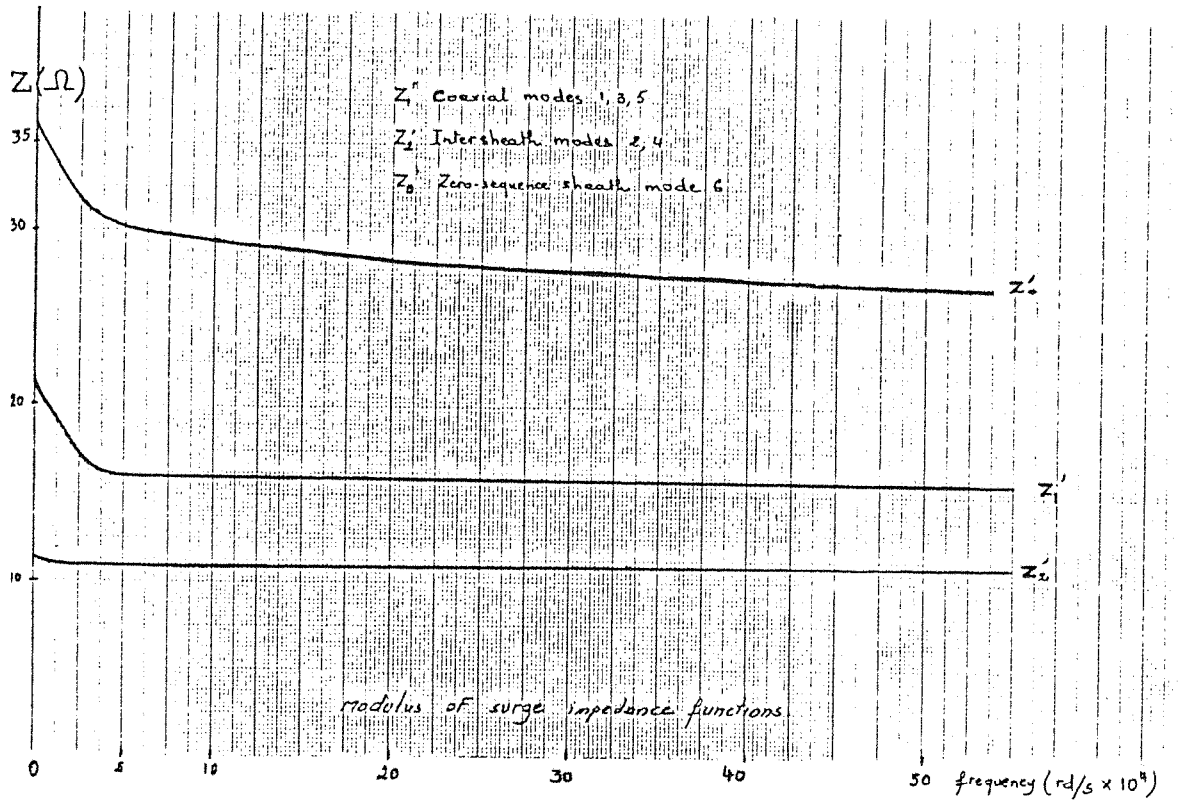

Fig.5.2 Modulus of surge impedance functions.

5.3 Forward impulse response function.

Solving the second-order modal equations leads directly to the surge impedance function and to the forward impulse response.

For a transmission system of length l , the matrix of forward impulse response is:

$$F_1(w) = \mathrm{Exp}(-\lambda(w)l)$$

The variation with frequency of the modulus of the impulse response for the cable system considered is shown in Fig.5.3.

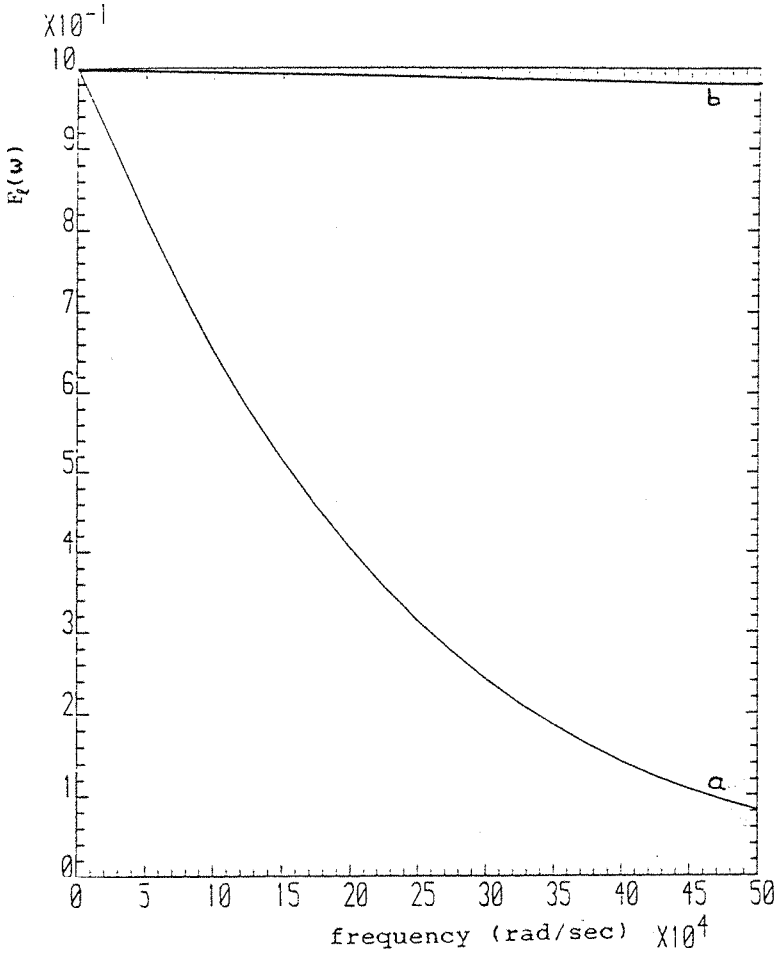

Fig.5.3 Forward impulse response.

a : sheath zero mode.

b : responses for the 3 coaxial modes and the 2 inter-sheath modes.

5.4 Wave transit times.

The matrix of propagation coefficients can be separated into real and imaginary parts:

$$\lambda(w) = \alpha(w) + j\beta(w)$$

Wave transit times are given by : $\beta(w)l/w$

The constant wave transit times for the three modes for our

cable system are given below:

T_0 = 44 μs

T_1 = 3.14 μs

T_2 = 18.84 μs

5.5 Equation systems in the frequency domain.

Combining equation 5.11 and 5.12 lead to the frequency-domain equation system. For a minor section between node set k and j we can write:

$$v_k(w) - z_{kj}(w)i_{kj}(w) = F_{kj}(w)\ (\ v_j(w) + z_{kj}(w)i_{jk}(w)\ )$$

$$v_j(w) - z_{kj}(w)i_{jk}(w) = F_{kj}(w)\ (\ v_k(w) + z_{kj}(w)i_{kj}(w)\ )$$

$z_{kj}(w)$ is the matrix of core and sheath surge impedances.
$F_{kj}(w)$ is the matrix of forward impulse responses.
The frequency-dependence of modal impulse responses are confined in the sheath zero mode while the core and sheath responses are taken constant. For the surge impedance only the sheath zero mode is frequency-dependence and the remaining modes are represented by a constant.

5.6 Equations in the Z-plane.

Expressing in the Z-plane, the cable system equations become:

$$v_k(z) - z_{kj}(z)i_{kj}(z) = F_{kj}(z)\ (\ v_j(z) + z_{kj}(z)i_{jk}(z)\ )$$

$$v_j(z) - z_{kj}(z)i_{jk}(z) = F_{kj}(z)\ (\ v_k(z) + z_{kj}(z)i_{kj}(z)\ )$$

If Δt is the sampling interval in the time-domain, the Z-transform from the F-domain to the Z-domain is defined by the expression:

$$z = \exp(jw\Delta t)$$

The form of the mode 1 forward impulse response is then:

$$F_1(w) = \exp(-jwT_1)$$

Setting $T_1 = m_1 \Delta t$ where m_1 is an integer gives:

$$F_1(z) = z^{-m_1}$$

Similar for mode 2 :

$$F_2(z) = z^{-m_2}$$

where $T_2 = m_2\Delta t$

For the sheath-zero mode forward impulse response :

$$F_o(w) = \exp(-jwT_o)\ F_{no}(w)$$

where $T_o = m_o\Delta t$, using this gives:

$$F_o(z) = z^{-m_o}F_{no}(z)$$

Δt is chosen to be:

$$\Delta t = 3.14\ \mu s$$

so that $m_1 = 1$

$m_2 = 6$

$m_o = 14$

and note that $F_{n1}(w)$ and $F_{n2}(w)$ are considered to be unity. To form $F_{no}(z)$ we use the multi-product rational-function

form:

$$F_{no}(z) = A \prod \frac{1 + a_k z^{-1} + b_k z^{-2}}{1 + c_k z^{-1} + d_k z^{-2}}$$

but we use N = 2 the simplest form with a good accuracy:

$$F_{no}(z) = \frac{x_1(1+x_2 Z^{-1}+x_3 Z^{-2})}{(1+x_4 Z^{-1}+x_5 Z^{-2})(1+x_6 Z^{-1}+x_7 Z^{-2})}$$

where $x_1, x_2, \ldots\ldots x_7$ are unknown coefficients.
Consider the least square function:

$$Q(X) = [\ |F_{no}(zi)| - |F^*_{no}(zi)|\ ]^2$$

where $X = (x_1, x_2, \ldots\ldots x7)$
$|F^*_{no}(zi)|$ is the discrete value at $Z = z_i$ obtained from the numerical points of $|F_{1o}(w)|$.
Therefore the unknown coefficients X are found to make Q(X) close to zero by the Quasi-Newton minimization procedure.
This minimization procedure can be done by calling the NAG Fortran Library Routine E04FDF available at the computer center at Southapton University.
The expression can only be stable if the pole and zero locations of the formulation lie within the unit circle in the z-plane. The stability criterion is achieved.
From the above considerations, a program is developed to formulated the Z-domain expression. It is found that:

$$F_{no}(z) = \frac{Y_1(1+Y_2Z^{-1}+Y_3Z^{-2})}{(1+Y_4Z^{-1}+Y_5Z^{-2}+Y_6Z^{-3}+Y_7Z^{-4})}$$

with:

$Y_1 = 0.0797$

$Y_2 = 0.1212$

$Y_3 = 0.8783$

$Y_4 = -2.1015$

$Y_5 = 1.5352$

$Y_6 = -0.464$

$Y_7 = 0.0497$

And the results for Z(z) are as follows:

$Z_1(z) = 15.7\ \Omega$

$Z_2(z) = 10.85\ \Omega$

$$Z_o(z) = \frac{z_o(1+x_1Z^{-1}+x_2Z^{-2})}{(1+x_3Z^{-1}+x_4Z^{-2}+x_5Z^{-3}+x_6Z^{-4})}$$

with

$z_o = 26.8\ \Omega$

$x_1 = -0.3392$

$x_2 = -0.3968$

$x_3 = -0.4351$

$x_4 = -0.3557$

$x_5 = 0.0004$

$x_6 = 0.01234$

It is helpful to simplify the equations 5.15 and 5.16 by

defining the forward characteristics as:

$$F_m(w) = V_m(w) + Z(w)i_m(w) \qquad 5.19$$

$$F_r(w) = V_r(w) + Z(w)i_r(w) \qquad 5.20$$

and the backward characteristics as:

$$B_m(w) = V_m(w) - Z(w)i_m(w) \qquad 5.21$$

$$B_r(w) = V_r(w) - Z(w)i_r(w) \qquad 5.22$$

Expressing equations 5.15 and 5.16 in terms of the above characteristics, it yields:

$$B_m(w) = F_1(w)\, F_r(w) \qquad 5.23$$

$$B_r(w) = F_1(w)\, F_m(w) \qquad 5.24$$

Equations 5.23 and 5.24 are the basic equations for later analysis.

The equations 5.19 to 5.24 can be transformed to Z-plane directly:

$$F_m(z) = V_m(z) + Z(z)i_m(z) \qquad 5.25$$

$$F_r(z) = V_r(z) + Z(z)i_r(z) \qquad 5.26$$

$$B_m(z) = V_m(z) - Z(z)i_m(z) \qquad 5.27$$

$$B_r(z) = V_r(z) - Z(z)i_r(z) \qquad 5.28$$

$$B_m(z) = F_1(z)\, F_r(z) \qquad 5.29$$

$$B_r(z) = F_1(z)\, F_m(z) \qquad 5.30$$

The cable characteristic in Z-plane is described by equations 5.25 to 5.30, they are in the form for inverse transformation.

5.7 Inversion to the time domain.

The final step of the formulation is the return from the Z-plane to the time domain by inverse Z-transform operation. Taking inverse Z-transform of equation 5.25 to 5.30, it gives the following recursive relationships:

$$F_s(n) = V_s(n) + Z(n)i_s(n) \qquad 5.31$$

$$F_r(n) = V_r(n) + Z(n)i_r(z) \qquad 5.32$$

$$B_s(n) = V_s(n) - Z(n)i_s(n) \qquad 5.33$$

$$B_r(n) = V_r(n) - Z(n)i_r(n) \qquad 5.34$$

$$B_s(n) = F_r(n-1) \qquad 5.35$$

$$B_r(n) = F_s(n-1) \qquad 5.36$$

Eliminating B_s from the sets of equations of 5.33 and 5.35 gives:

$$V_s(n) - Z_1 i_s(n) = V_{sp}(n-p) \qquad 5.37$$

where $V_{sp}(n-p)$ is the previous step-values for p equal to m_1, m_2 and m_0 for each mode respectively.

Similary for the sets equations 5.34 and 5.36 gives:

$$V_r(n) - Z_1 i_r(n) = V_{rp}(n-p) \qquad 5.38$$

CHAPTER SIX

TRANSIENT ANALYSIS OF CROSS-BONDED CABLE SYSTEMS

There is considerable literature [4 to 13] on the transient analysis of cross-bonded cable systems. It was found that computation time becomes a major problem. This chapter, is concerned with the development of a more efficient, fast and accurate method of analysing cross-bonded systems by digital computer. The Z-transform [19] is adopted in the cross-bonded cable analysis because it has the principal advantage of linking the frequency domain and the time domain. This is important because cable parameters, are frequency dependent.

6.1 Z-plane formulation for minor section of cable.

Typical sheath transpositions and connections for a part of high-voltage cable system are shown in Fig.6.1. Applying the sets of equations 5.37 and 5.38 to the minor section between node sets k and j gives:

$$V_k(n) - Z_1 i_{kj}(n) = V_{kp}(n-p) \qquad 6.1$$

$$V_j(n) - Z_1 i_{jk}(n) = V_{jp}(n-p) \qquad 6.2$$

For a minor section of the system, the boundary conditions which have to be evaluated are those of sheath transpositions, sheath earthing and sheath voltage limiters operation.

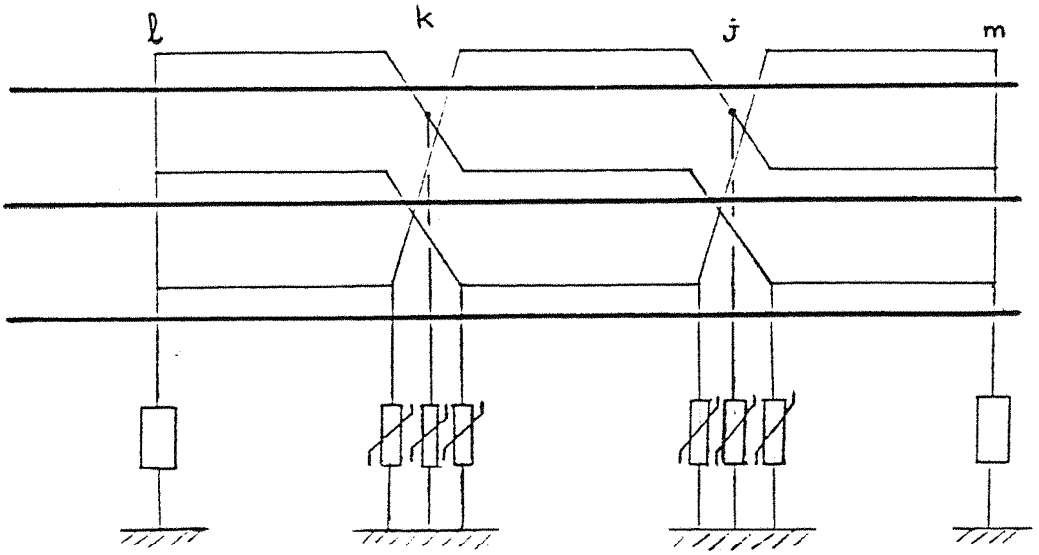

Fig.6.1 Cross-bonded cable system of three minor sections.

6.2 cable specifications.

The 1500m cross-bonding system of the Kirke-Searing type is used. The system consists of one major section, comprised of three indentical cables laid in trefoil formation below a depth of 1m and they have a separation of 0.5m. The sheaths are solidly bonded and directly earthed at both ends through 0.075 ohm ground resistances. The remaining data is summarized in table 6.1.

Table 4.1cable dimensions.

Core diameter	70.30 mm
Sheath inner diameter	114.20 mm
Sheath outer diameter	129.80 mm
Resistivity of core	1.7×10^{-8} Ωm
Resistivity of sheath	2.1×10^{-7} Ωm
Permittivity of core insulation	$3.5\times\epsilon_o$
Permittivity of sheath insulation	$4.0\times\epsilon_o$
Earth resistivity	50 Ωm

6.3 Sheath transpositions.

On either side of the transposition point k, we have the sets of equations:

$$V_{k1}(n) - Z_1 i_{k1}(n) = V_{k1p}(n-p) \qquad 6.3$$

$$V_{kj}(n) - Z_1 i_{kj}(n) = V_{kjp}(n-p) \qquad 6.4$$

Phase voltages and currents vectors are:

$$[V^p(n)]^t = V_a^c(n),\ V_a^s(n),\ V_b^c(n),\ V_b^s(n),\ V_c^c(n),\ V_c^s(n)$$

$$[i^p(n)]^t = i_a^c(n),\ i_a^s(n),\ i_b^c(n),\ i_b^s(n),\ i_c^c(n),\ i_c^s(n)$$

modal and actual variables are inter related by:

$$V^p(n) = C_1 V(n) \qquad V(n) = C_1^{-1} V^p(n)$$

$$i^p(n) = C_2 i(n) \qquad i(n) = C_2^{-1} i^p(n)$$

using equations 6.3 and 6.4 gives the phase variables sets:

$$V^p_{k1}(n) - Z_1^p i^p_{k1}(n) = V^p_{k1p}(n-p) \qquad 6.5$$

$$V^p_{kj}(n) - Z_1^p i^p_{kj}(n) = V^p_{kjp}(n-p) \qquad 6.6$$

where

$$Z_l^p = C_1 Z_1 C_2$$

$$V^p_{k1p}(n-p) = C_1 V_{k1p}(n-p)$$

$$V^p_{kjp}(n-p) = C_1 V_{kjp}(n-p)$$

The transposition matrix T is:

$$T = \begin{bmatrix} 1 & 0 & 0 & 0 & 0 & 0 \\ 0 & 0 & 0 & 1 & 0 & 0 \\ 0 & 0 & 1 & 0 & 0 & 0 \\ 0 & 0 & 0 & 0 & 0 & 1 \\ 0 & 0 & 0 & 0 & 1 & 0 \\ 0 & 1 & 0 & 0 & 0 & 0 \end{bmatrix}$$

so that:

$$V^{p}_{kl}(n) = T\, V^{p}_{kj}(n)$$

$$i^{p}_{kl}(n) = -T\, i^{p}_{kj}(n)$$

Pre-multiplying equation 6.6 by T and replacing $i^{p}_{kj}(n)$ by $-T^{-1}i^{p}_{kl}(n)$ gives:

$$V^{p}_{kl}(n) + Z_t i^{p}_{kl}(n) = TV^{p}_{kjp}(n-p) \qquad 6.7$$

where

$$Z_t = TZ^{p}_{l}T^{-1}$$

Eliminating $i^{p}_{kl}(n)$ from equations 6.5 and 6.7 gives:

$$V^{p}_{kl}(n)=[U+Z_t[Z^{p}]^{-1}]^{-1}[Z_t\,[Z^{p}]^{-1}V^{p}_{klp}(n-p)+TV^{p}_{kjp}(n-p)] \qquad 6.8$$

knowing $V^{p}_{kl}(n)$ all other variables at the cross-bonding point can be found:

$$i^{p}_{kl}(n) =[Z^{p}]^{-1}[V^{p}_{kl}(n-p) - V^{p}_{klp}(n-p)] \qquad 6.9$$

$$V^{p}_{kj}(n) = T^{-1}V^{p}_{kl}(n)$$

$$i^{p}_{kj}(n) = -T^{-1}i^{p}_{kl}(n)$$

and modal variables:

$$V_{kl}(n) = C_1^{-1}V^{p}_{kl}(n)$$

$$V_{kj}(n) = C_1^{-1}V^{p}_{kj}(n)$$

$$i_{kl}(n) = C_2^{-1}i^{p}_{kl}(n)$$

$$i_{kj}(n) = C_2^{-1}i^{p}_{kj}(n)$$

And similarly, for the second transposition point, at node set j all the variables of the first transposition point with subscripts kl and kj are changed to jk and jm respectively and equations for both transposition points are

obtained.

6.4 Sheath earthing.

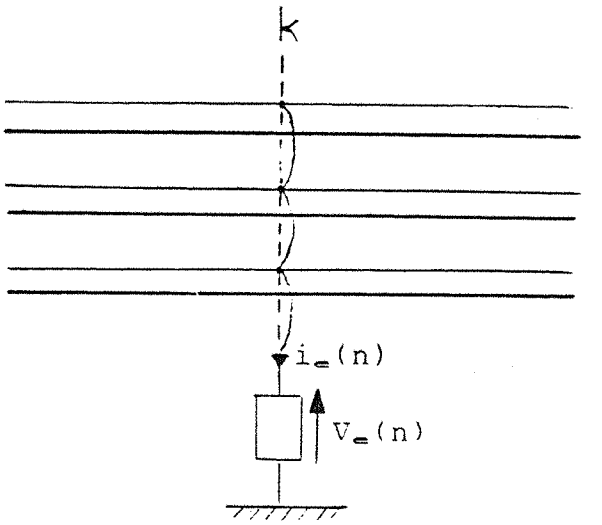

Fig.6.2 Sheath earthing at both ends

We define a connection matrix C which is:

$$C = \begin{array}{c} \\ ac \\ bc \\ cc \\ e \end{array} \begin{array}{c} \begin{array}{cccccc} ac & as & bc & bs & cc & cs \end{array} \\ \begin{bmatrix} 1 & 0 & 0 & 0 & 0 & 0 \\ 0 & 0 & 1 & 0 & 0 & 0 \\ 0 & 0 & 0 & 0 & 1 & 0 \\ 0 & 1 & 0 & 1 & 0 & 1 \end{bmatrix} \end{array}$$

these reduced the order vectors:

$$V^{p}(n) = C_t \begin{bmatrix} V^{c}(n) \\ \\ V_e(n) \end{bmatrix}$$

$$V^{pr}(n) = \begin{bmatrix} V^{c}(n) \\ \\ V_e(n) \end{bmatrix}$$

$$i^{pr}(n) = \begin{bmatrix} i^{c}(n) \\ \\ -i_{e}(n) \end{bmatrix}$$

with this notations:

$$V^{p}(n) = C_{t}V^{pr}(n)$$

$$C\ i^{p}(n) = i^{pr}(n)$$

replacing $V^{p}(n)$ and $i^{p}(n)$ by $V^{pr}(n)$ and $i^{pr}(n)$ in equation 6.9 gives:

$$i^{pr}(n) = Y_{pr}V^{pr}(n) - i_{1p}(n-p) \qquad 6.10$$

where $Y_{pr} = C[Z^{p}]^{-1}C_{t}$

and

$$i_{1p}(n-p) = C[Z^{p}]^{-1}\ V^{p}{}_{1p}(n-p)$$

For the common sheath earth return path:

$$V_{e}(n) = R_{e}i_{e}(n)$$

Defining matrix G by:

$$G = \left[\begin{array}{ccc:c} 0 & 0 & 0 & 0 \\ 0 & 0 & 0 & 0 \\ 0 & 0 & 0 & 0 \\ \hdashline 0 & 0 & 0 & 1/Re \end{array}\right]$$

which gives:

$$\begin{bmatrix} 0 \\ \cdots\cdots \\ i_{e}(n) \end{bmatrix} = G\ V^{pr}(n) \qquad 6.11$$

Adding equations 6.10 and 6.11 gives:

$$\begin{bmatrix} i^c(n) \\ \cdots\cdots \\ 0 \end{bmatrix} = [Y_{pr} + G]\, V^{pr}(n) - i_{1p}(n-p) \qquad 6.12$$

we use the partitions:

$$Y_{pr} + G = \left[\begin{array}{c|c} Y_{11} & Y_{12} \\ \hline Y_{21} & Y_{22} \end{array}\right]$$

and $$i_{1p}(n-p) = \begin{bmatrix} i^c{}_{1p}(n-p) \\ \cdots\cdots\cdots \\ i^s{}_{1p}(n-p) \end{bmatrix}$$

with these partitions equation 6.12 gives:

$$i^c(n) = Y_{11}V^c(n) + Y_{12}V_e(n) - i^c_{1p}(n-p) \qquad 6.13$$

$$0 = Y_{21}V^c(n) + Y_{22}V_e(n) - i^s_{1p}(n-p) \qquad 6.14$$

On eliminating from these equations the sheath voltage at the earth point $V_e(n)$ gives:

$$i^c(n) = Y'_{11}V^c(n) + i^c(n-p) \qquad 6.15$$

where

$$Y'_{11} = Y_{11} - Y_{12}Y_{22}^{-1}Y_{21}$$

and $$i^c(n-p) = Y_{12}Y_{22}^{-1}i^s{}_{1p}(n-p) - i^c{}_{1p}(n-p)$$

From eqation 6.14 we obtain $V_e(n)$:

$$V_e(n) = Y_{22}^{-1}[-Y_{21}V^c(n) + i^s{}_{1p}(n-p)] \qquad 6.16$$

Vector $V^{pr}(n)$ is then available from :

$$[V^{pr}(n)]^t = [V^c(n)]^t,\ V_e(n)$$

and the original vector of core and sheath:

$$V^p(n) = C_t V^{pr}(n)$$

and the vector currents $i^p(n)$ is obtained from equation 4.9.

6.5 Sheath voltage limiters.

When sheath voltage limiters at points of sheath transpositions are connected, the non-linear characteristics of devices are to be superimposed on the constraints of sheath transpositions.

Sheath voltages either side of a transposition point are related by:

$$V^p_{k1}(n) = TV^p_{kj}(n) \qquad 6.17$$

We therefore replace the previous equation relating sheath currents by:

$$i^p_{k1}(n) = Ti^p_{kr}(n) + Ni_a(n) \qquad 6.18$$

where $N = \text{diag}\ (0,1,0,1,0,1)$,

$i_a(n)$ is the vector of current flowing in the devices.

The device consists of a resistor R, a capacitor C and a non-linear inductance L in parallel as shown in Fig.6.4. The explicit form of these matrices are:

$$R = \text{diag}\ (0,R,0,R,0,R)$$

$$L = \text{diag}\ (0,L_1,0,L_2,0,L_3)$$

$$C = \text{diag}\ (0,C,0,C,0,C)$$

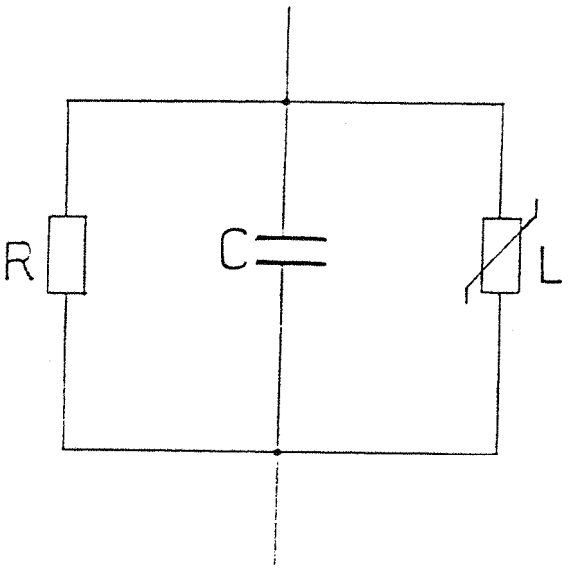

Fig.6.4 Equivalent circuit of the device (sheath voltage limiter).

therefore the vector of currents flowing in each branch of the device are defined as follows:

$$i_1(t) = V_{k1}(t)/R$$

$$i_2(t) = \frac{\Delta t}{L} V_{k1}(t) + i_2(t-\Delta t)$$

$$i_3(t) = \frac{C}{\Delta t}(V_{k1}(t) - V_{k1}(t-\Delta t))$$

So the vector $i_a(n)$ is equal to the sum of the previous vectors:

$$i_a(n) = i_1(n) + i_2(n) + i_3(n)$$

or

$$i_a(n) = (1/R + \frac{\Delta t}{L} + \frac{C}{\Delta t})V_{k1}(n) + i_2(n-1) - \frac{C}{\Delta t} V_{k1}(n-1) \quad 6.19$$

Equations 6.17 to 6.19 together with equations 6.3 and 6.4, give the complete set of equations for the connection points of the devices.

The core and sheath voltages are obtained by combining all

these equations together to give:

$$V^{p}_{k1}(n)=[U+\ Z_t[Z^p]^{-1}\ +Z_tN(1/R+\ \Delta tL^{-1}+\ \frac{1}{\Delta t}.C)N]^{-1}$$
$$[Z_t[Z^p]^{-1}V^{p}_{k1p}(n-p)+TV^{p}_{kjp}(n-p)\ -Z_tN(i_2(n-1)-\frac{1}{\Delta t}.C.N.V^{p}_{k1}(n-1))] \qquad 6.20$$

And similarly, for the second transposition point all the equations of the first were repeated.

6.6 Open and loaded circuit.

If the cable end is on open-circuit, core currents in equation 6.12 are set to zero so that:

$$V_4^{pr}(n) = [Y_{pr}+G]^{-1}i_{4p}(n-p) \qquad 6.21$$

where $V_4^{pr}(n) = \begin{bmatrix} V_4^{c}(n) \\ \\ V_{e4}(n) \end{bmatrix}$

If the cable end is loaded with resistances R_1 and R_2 as shown in Fig.6.5, equations 6.13 and 6.14 are used, together with the core voltages which are:

$$V_4^{c}(n) = [\ R_1 + R_2\ ]i_4^{c}(n) \qquad 6.22$$

The explicit form of R_1 and R_2 are:

$$R_1 = \begin{bmatrix} R & 0 & 0 \\ 0 & R & 0 \\ 0 & 0 & R \end{bmatrix} \quad \text{and} \quad R_2 = \begin{bmatrix} R & R & R \\ R & R & R \\ R & R & R \end{bmatrix}$$

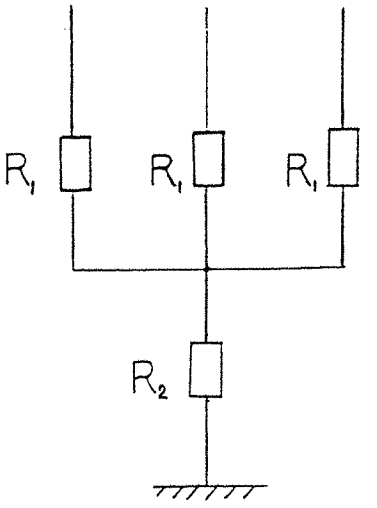

Fig.6.5 The load resistors.

Replacing the core currents in equation 6.13 by

$$i_4^c(n) = [\ R_1 + R_2\ ]V_4^c(n) \qquad 6.23$$

gives:

$$[R_1+R_2]^{-1}V_4^c(n) = Y_{11}V_4^c(n) + Y_{12}V_{e4}(n) - i_{4p}^c(n-p) \qquad 6.24$$

$$0 = Y_{21}V_4^c(n) + Y_{22}V_{e4}(n) - i_{4p}^s(n-p) \qquad 6.25$$

Substituting the value of $V_{e4}(n)$ from equation 6.25 in equation 6.24 gives the core voltages:

$$V^c(n) = [[R_1+R_2]^{-1}-Y'_{11}]^{-1}[Y_{12}Y_{22}^{-1}i_{4p}^s(n-p) - i_{4p}^c(n-p)] \qquad 6.26$$

and the sheath voltages from equation 6.25 is:

$$V_{e4}(n) = Y_{22}[-Y_{21}V_4^c(n) + i_{4p}^s(n-p)] \qquad 6.27$$

Core and sheath voltages and currents at the open-circuited or loaded end of the cable are obtained to complete the solution.

To test the system under fault condition, a short circuit was made in taking one element of the matrix R_1 and a row of R_2 equal to zero which means phase-to-earth fault. Or two elements of R equal to zero is the phase-to-phase fault.

CHAPTER SEVEN

RESULTS OF COMPUTER SIMULATION FOR CROSS BONDED SYSTEM

7.1 Introduction.

The diagram and data of the cable system considered are presented in Fig.6.1 and section 6.2 respectively of chapter six. The switching mode considered is that, only core "a" is energised in the multiconductor cable system. This asymmetry in the energising mode is one which allows the freqency dependencies in the earth mode to be tested. To examine sheath-voltage solutions three non-linear inductance are installed at both the first and second cross-bonding points. The computer program which gives the transient results of a cross-bonded system using Z-transform has been tested for many cases, but only a selection of results is presented.

7.2 Core voltages at the receiving-end.

The receiving-end voltages waveform on the energised core "a" and the unenergised core "b" and "c" are shown in Fig.7.1. There is an initial step occuring after about 9μs. This delay is determined by the travel time for the cable. The receiving-end peak voltage amplitude is approximatly 270 KV which is 1.8 time the sending-end voltage. It is the coaxial mode which is responsible for the initial receiving-end voltage. The coaxial mode, which travels faster than the two remaining modes, therefore arrives at the receiving-end first, and reflects on the two other cores

"a" and "b". This appears as negative and positive steps at the receiving-end of these two cores as seen in Fig.7.1. It shows the travelling waves during the first $6x10^{-4}$secs, which will attenuate progressively, until the steady state conditions are reached.

7.3 Sheath voltages across the devices.

Without the device in circuit surges voltages as high as about 40 KV are produced on the cable sheaths to earth (Fig.7.2). The results demonstrate also how the travelling wave phenomena is reflected in the sheaths. The transient sheath-voltage waveforms of the three cables for the first cross-bonding point, with the connection of the non-linear inductance device in circuit is shown in Fig.7.4. The travelling wave in the presence of the device damps quickly ($2x10^{-4}$secs), followed by a dynamic period and finally steady state.

7.4 Voltages across the insulating joints.

The voltages across the insulating joints at the first cross-bonding point without and with the device in circuit are presented in Fig.7.3 and Fig.7.5. These voltages are the most severe in the cable system. With the device in circuit the maximum peak value of voltage was reduced from about 80 KV to about 25 KV and the travelling period is damped very quickly. The current flowing in the devices for the first cross-point are shown in Fig.7.6. It reaches a peak value of about 7 KA, then damps rapidly to a very small value.

7.5 Sheath voltages at the second cross-bonding point.

Fig.7.7 shows the sheath voltage at the second cross-bonding point. At the second cross-bonding point the voltage profile is similar to that of the first cross-bonding point with slightly reduced peak values.

7.6 Loaded system.

Fig.7.8 shows the sheath voltages at the first cross-bonding point when the system is loaded. As the voltages induced in the sheaths are proportional to the load current in the conductor, the greater the load current is , the greater the sheath voltage is recorded on the sheath. Comparing Fig.7.8 and Fig.7.2 when the system is unloaded, we can see that the voltage peaks vary form -18 KV to 11 KV for the unloaded system and for the loaded system they vary from -28 KV to 18 KV. At the time $t=20x10^{-4}$sec the values of the voltages for the loaded and unloaded systems are 5 KV and 2 KV respectively.

7.7 Faulted system.

For the phase-to-phase fault considered, between the phases "a" and "b",the surge overvoltages tend to arise within the two faulted cables and sheaths, the remaining conductor experiences relatively lower induced sheath voltage (Fig.7.9). The fault considered is the switching of the 3-phases on a faulted system and the voltage across the insulating joints as well as the current through the devices at the first cross-bonding point are shown in Fig.7.10 and Fig.7.11. At the instant just after the switching, the

voltages across the device to earth reach a peak value of about 50 KV on phase "a" and about 40 KV on phase "b" however the current is very low. When the short circuit between the two phases persists the currents increase to high values (330 KA peak on phase "a" and 210 KA peak on phase "b"), but the voltages decrease to very small values. It shows that the device is operating in the high saturation region,a large current is flowing in the device, but the voltage across it is kept low which is the object of the device.

7.8 Sensitivity of the parameters of the device.

The parameters of the device are very sensitive. The results presented are obtained with $C=3.0\times10^{-6}$ F. Increasing the value of C it will reduce the voltage across the device until a short circuit to earth can be made. The value of the resistance R was taken equal to 1000Ω, which has a negliable effect on the system. L is the non-linear inductance of the device and its effect depends on its dimension.

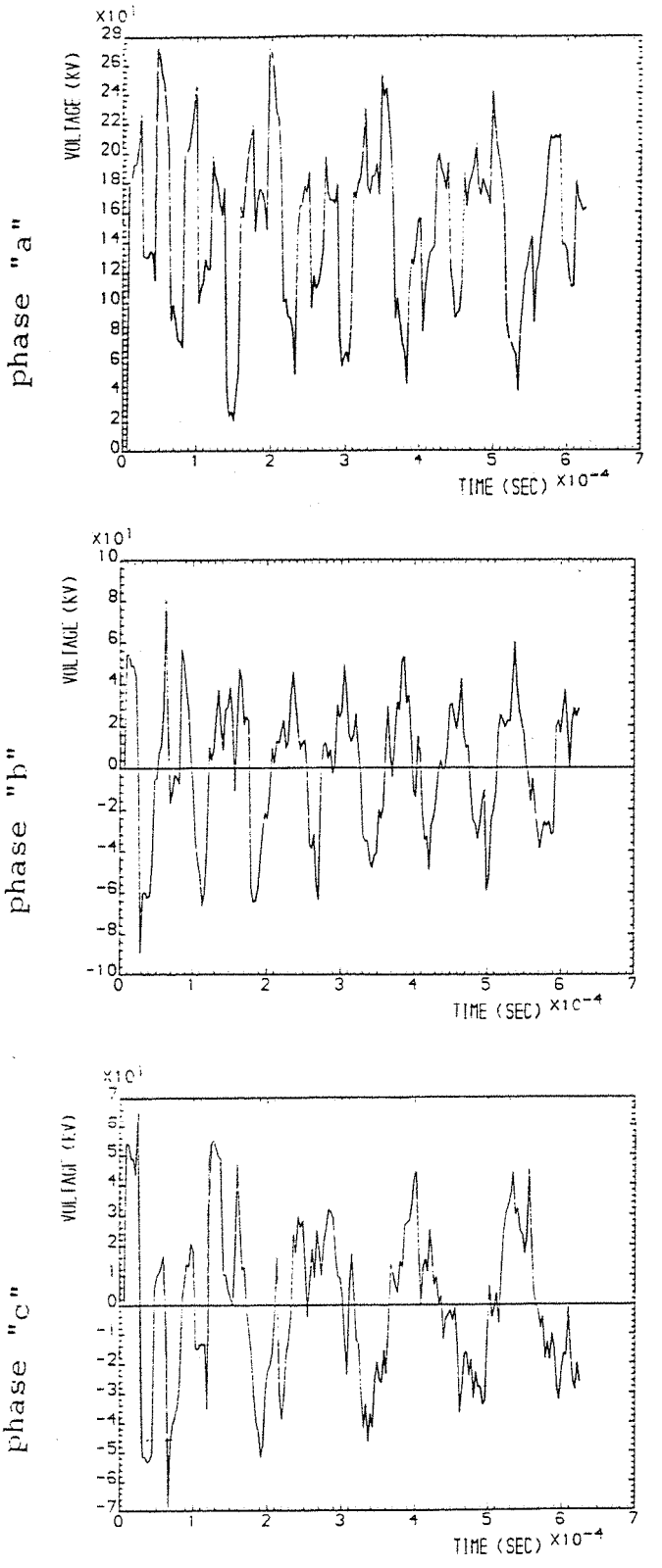

Fig.7.1 Remote end core voltage transients

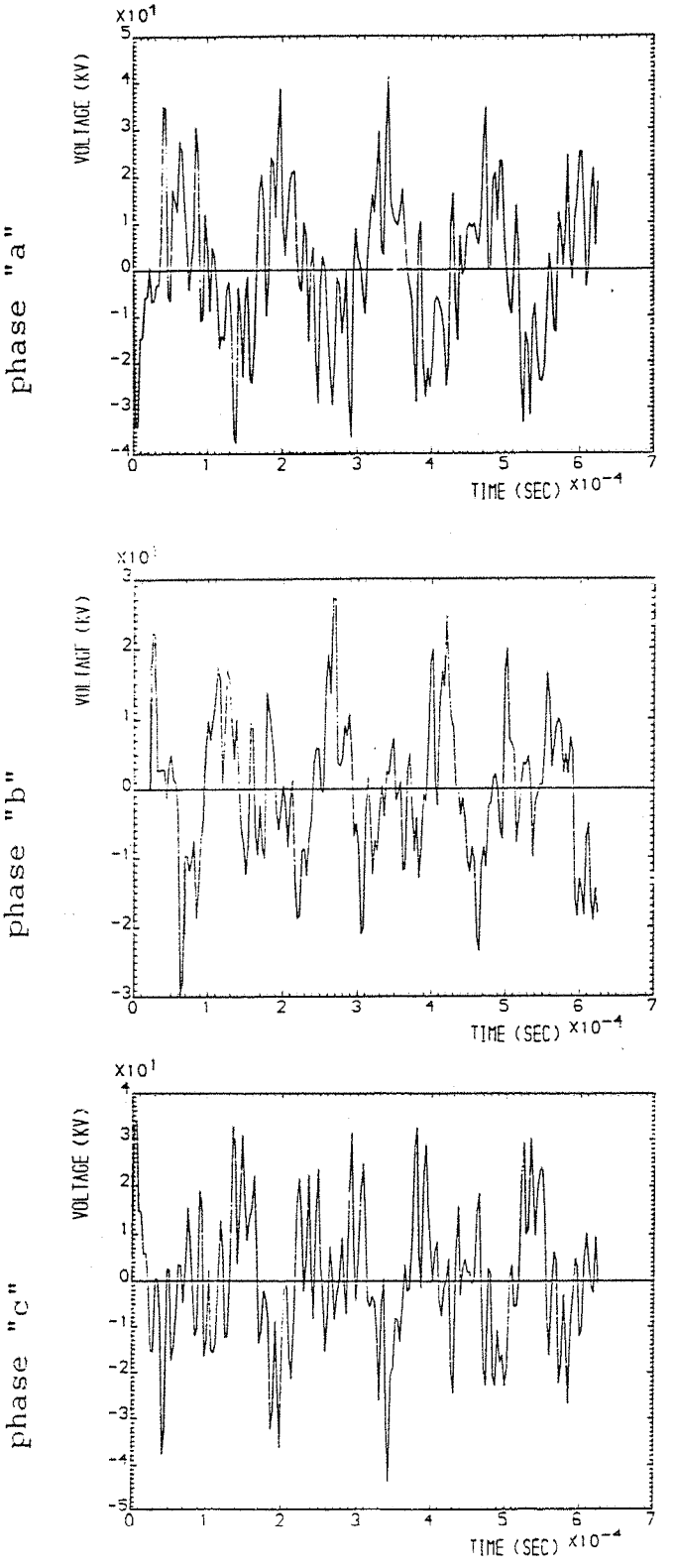

Fig.7.2 Sheath voltage transients at the first cross-bonding point, without the device.

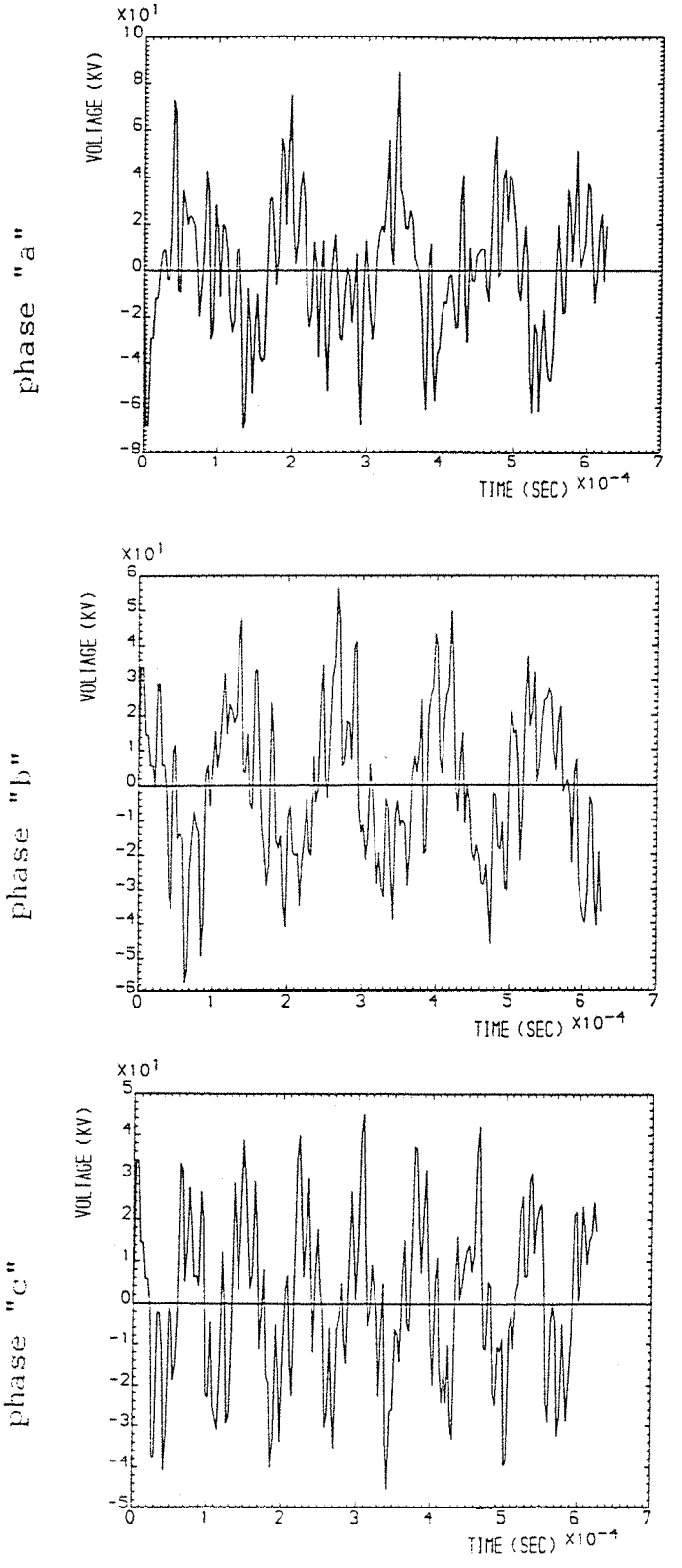

Fig.7.3 Voltages across the insulating joints at the first cros-bonding point, without the device.

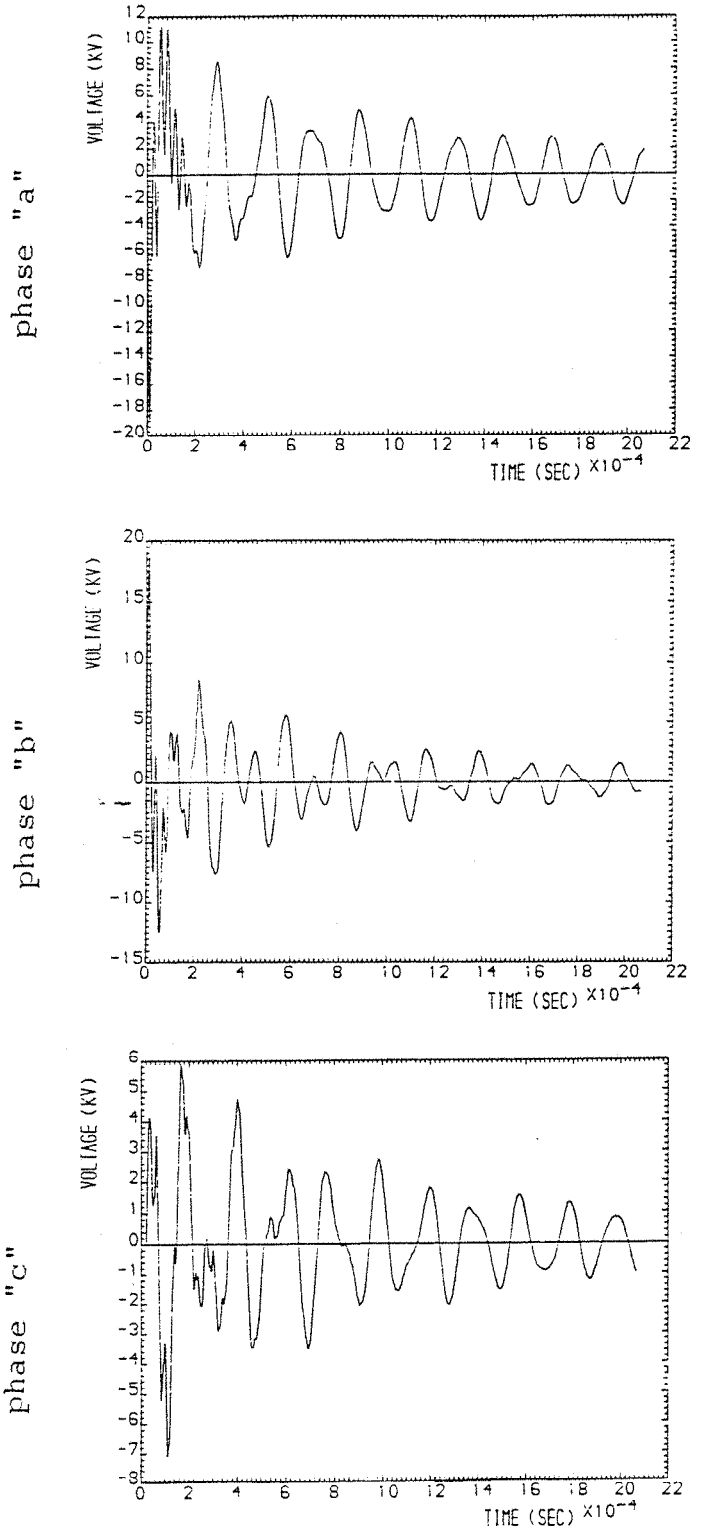

Fig.7.4 Sheath voltage transients at the first cross-bonding point limited by the devices.

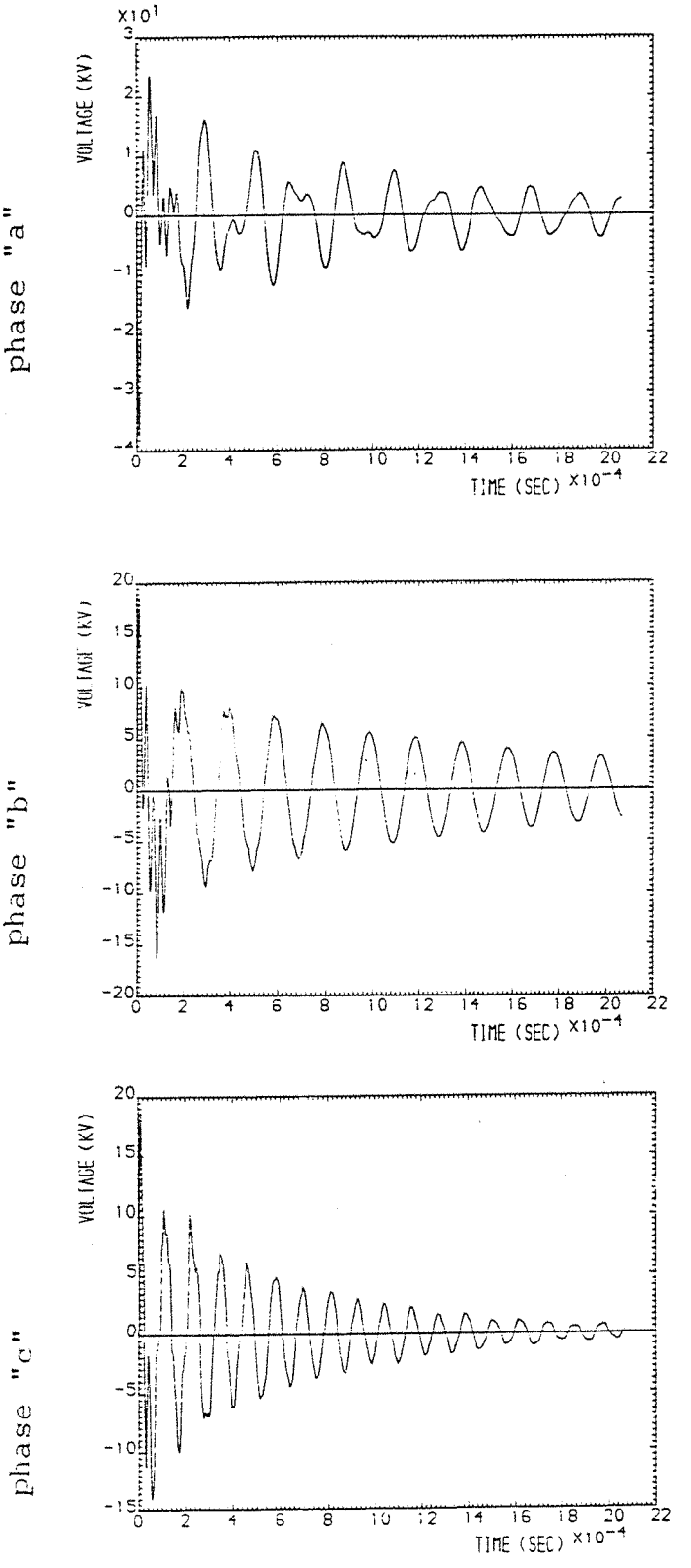

Fig.7.5 Voltages across the insulating joints at the first cros-bonding point, with the device in circuit.

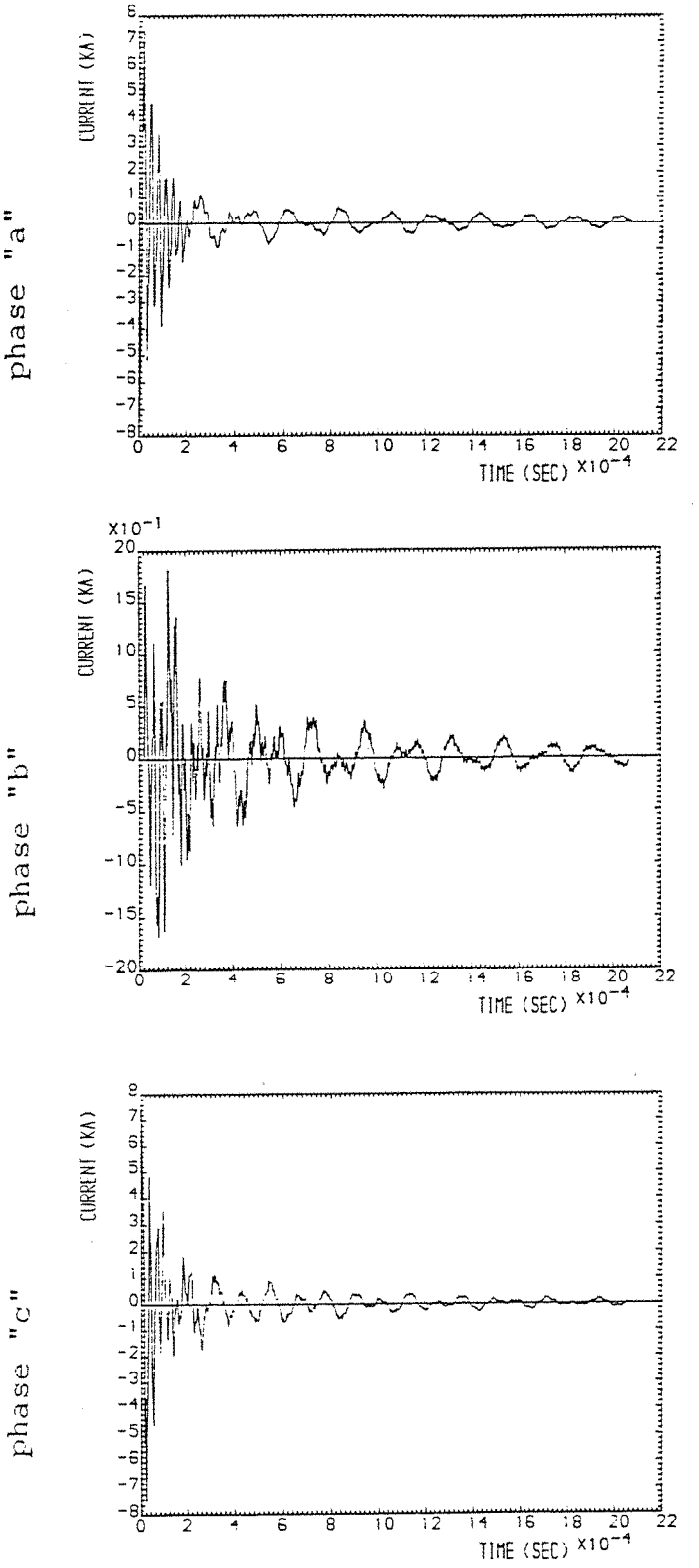

Fig.7.6 Current through the devices at the first cross-bonding point.

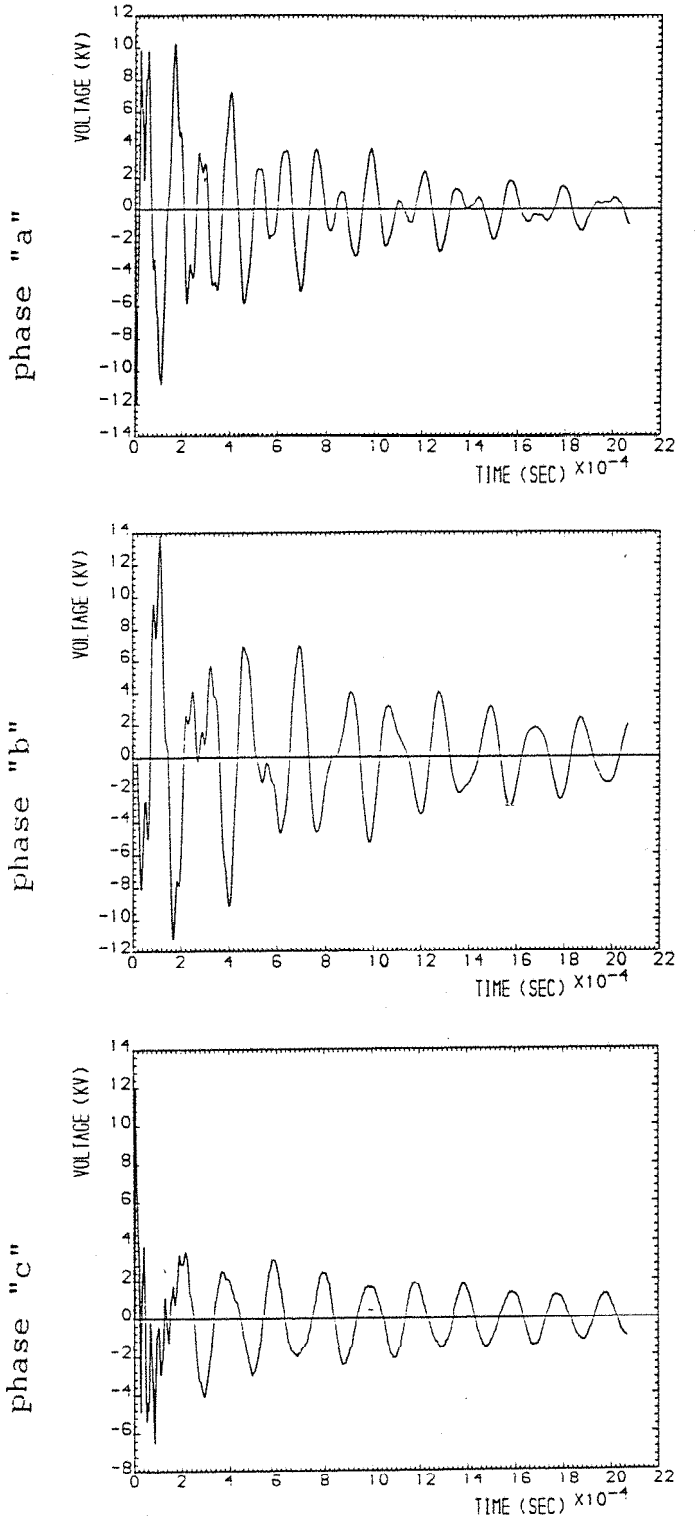

Fig.7.7 Sheath voltage transients at the second cross-bonding point limited by the device.

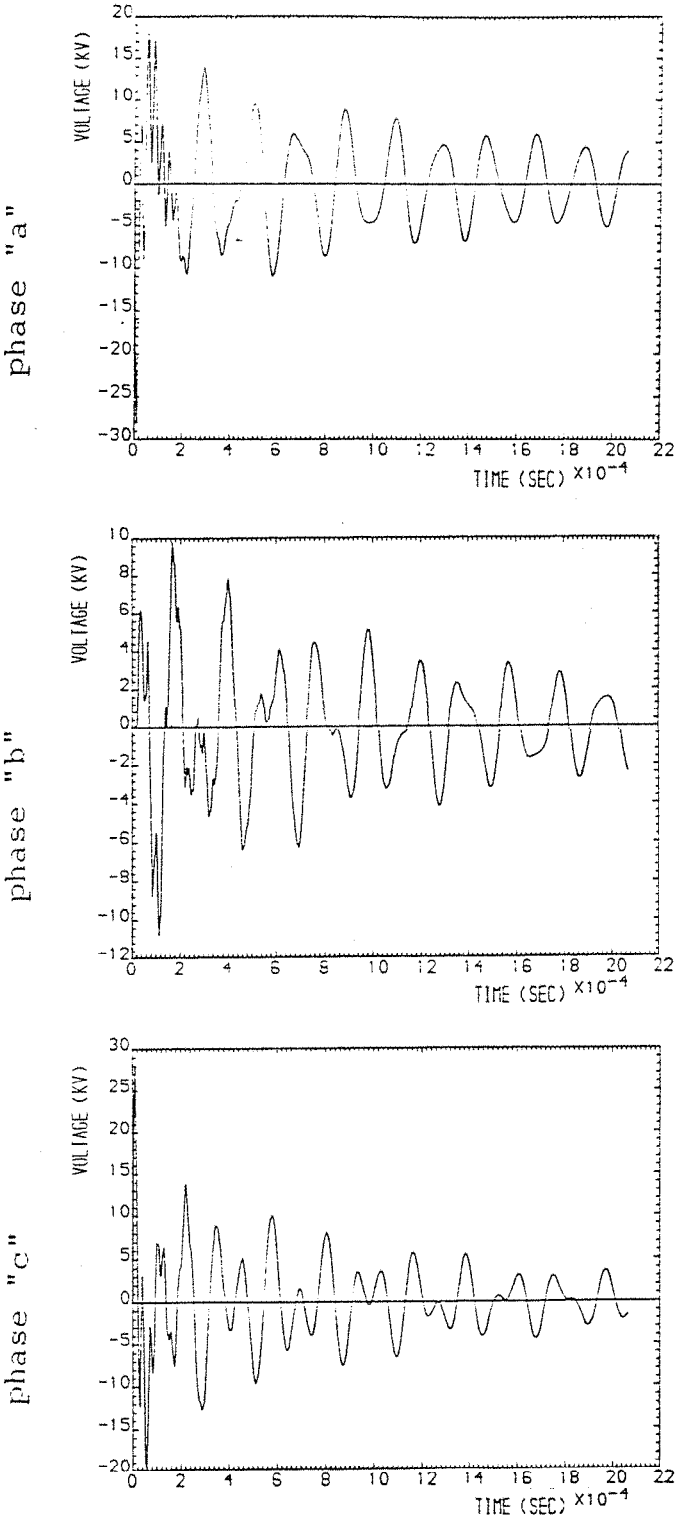

Fig.7.8 Sheath voltage transients at the first cross-bonding point, loaded system.

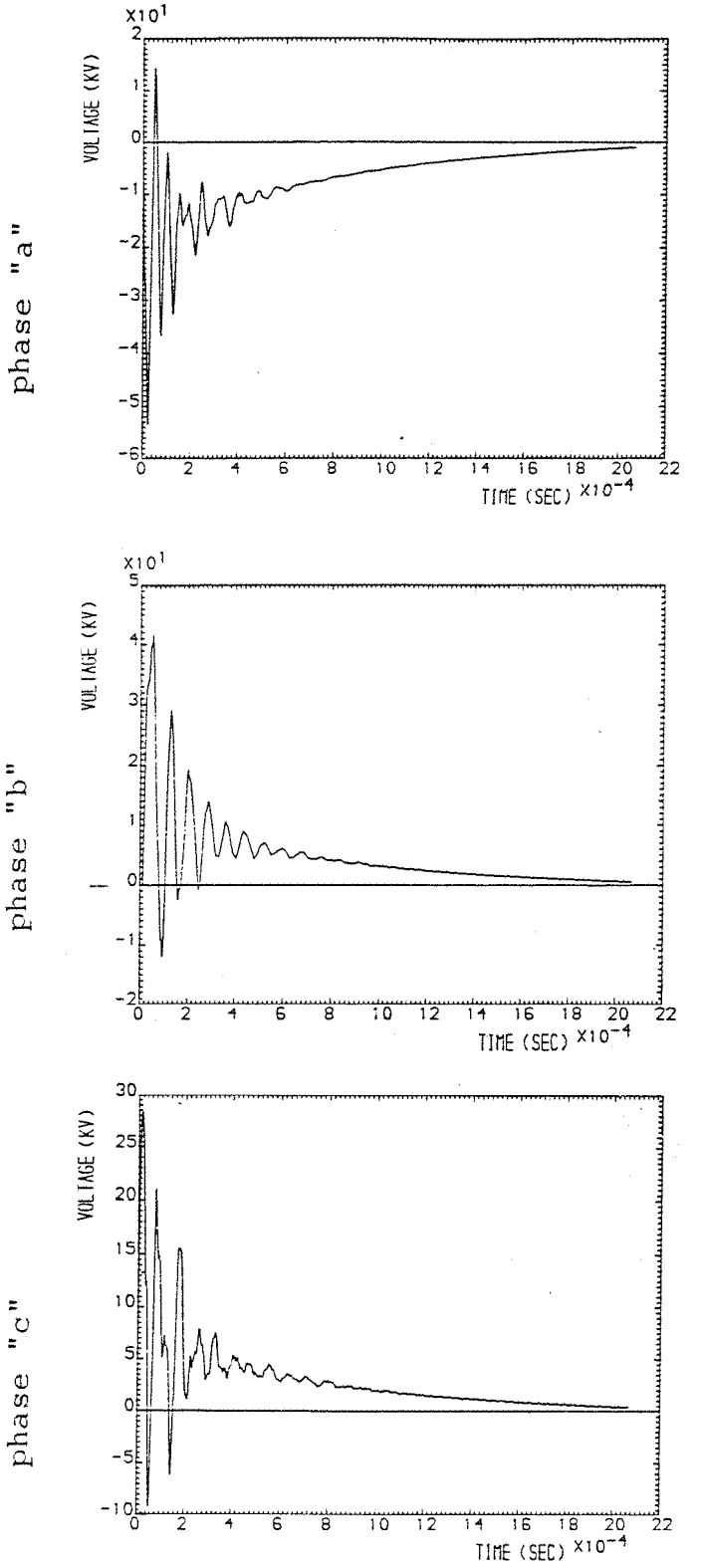

Fig.7.9 Sheath voltage transients at the first cross-bonding point, faulted system phase-to-phase fault.

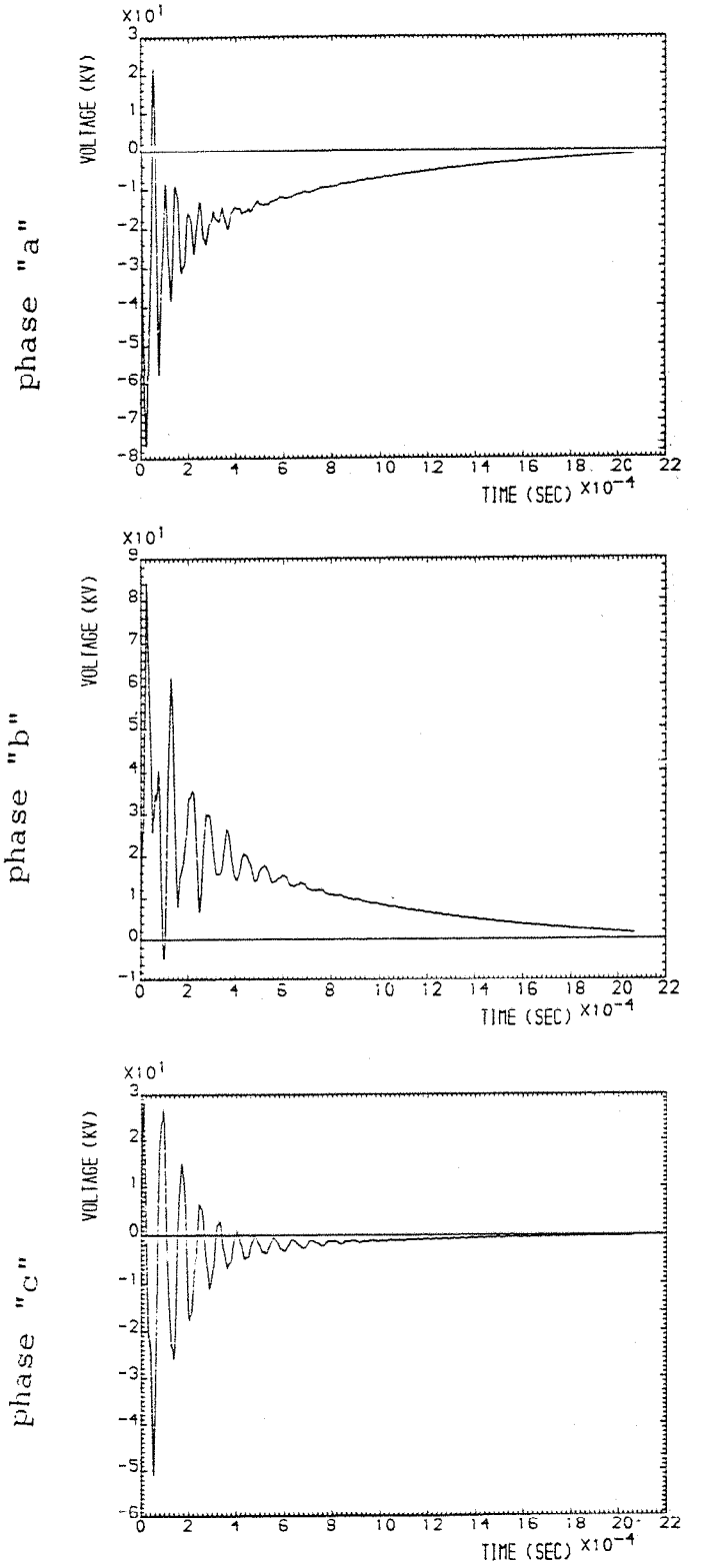

Fig.7.10 Voltages across the insulating joints at the first cros-bonding point, faulted system.

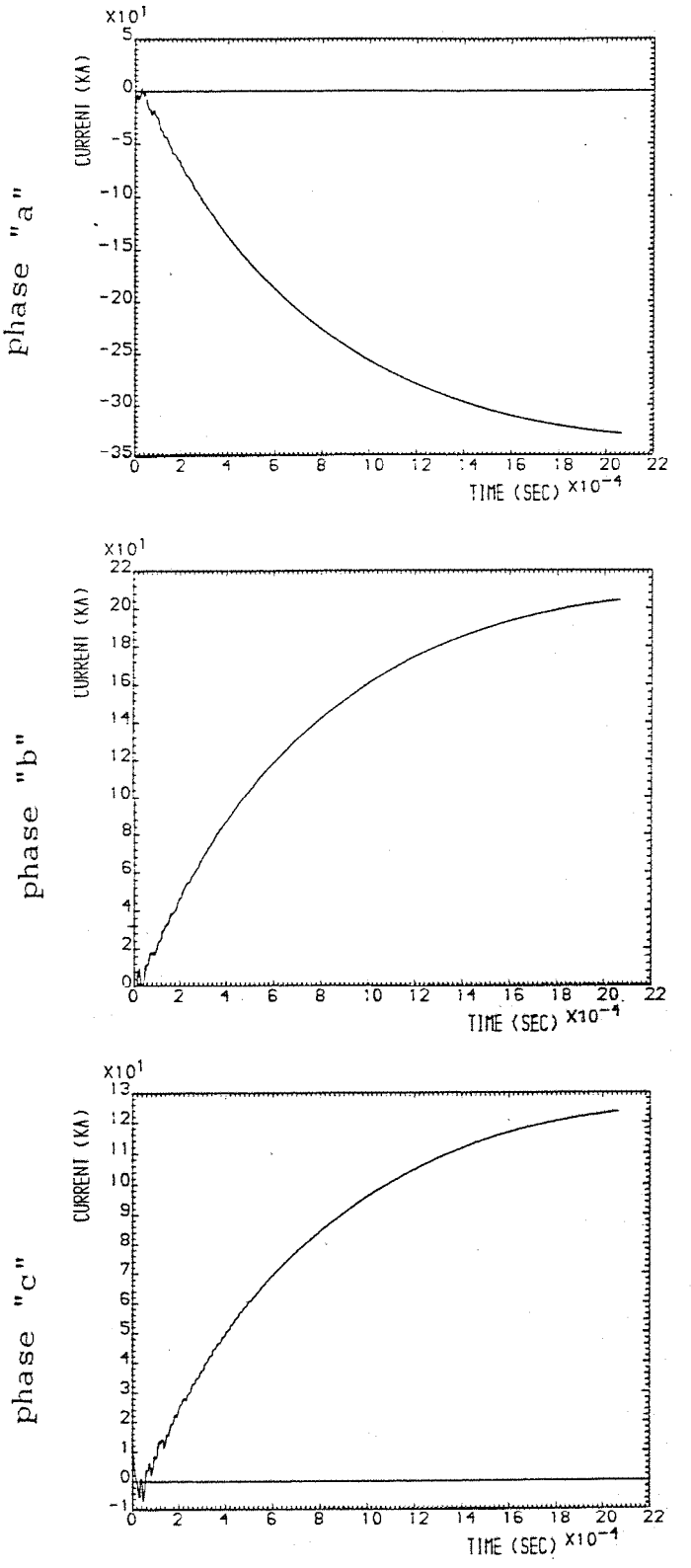

Fig.7.11 Current through the devices at the first cross-bonding point, faulted system.

CHAPTER EIGHT

DISCUSSION AND CONCLUSION

Overvoltages in transmission and distribution systems cannot be avoided. A detailed knowledge of this subject was necessary for economic design of equipment in the system and for safe operation. With the advent and introduction of EHV and UHV power systems it has became apparent that the construction costs of network and station material depend to a large degree on the overvoltages to be expected. Overvoltages are often symptoms of complex phenomena which occur in the system for various reasons.
Nobody will deny the necessity for providing power transmission network with protection against overvoltages. Starting from the simple spark gaps, we notice that over the years continuous improvements have been made in response to ever increasing demands. An intermediate stage is the surge arrester with plate gaps, still used today in medium-voltage network. The application of magnetic blast, which forms the basis of arresters in EHV networks, represents the most efficient solution at present.

The electrical utility companies and the electrical industry have been entrusted with the task of ensuring that networks and installations are as safe as possible. So far as overvoltages are concerned, this requirement was satisfied during the first half of the twentieth century. Up to the present the only device that has been able to perform the

rapid succession of switching operations is the arrester with spark gap and nonlinear resistors connected in series.

This investigation has been concerned with modelling the non-linear device connected to the sheath of a cable system, to determine its steady state and transient performances in the cable system under different load conditions. A mathematical model of the device and the cable system was formulated. The very simplified, but nevertheless effective, method of analysis presented in chapter two is based on the fact the conductor and sheath are considered as the primary and secondary of a transformer, and consequently can be represented by a simple equivalent circuit. This is valid for most cases of interest, and it shown that each cable system is approximated by an equivalent circuit. The method of analysis is relatively simple to compute.

The next stage of the work involves the representation of the non-linear device for simulation on the digital computer. Given the physical dimensions of the device and the B/H curve of the material, λ^{P}/i^{P} relationship was determined. Initially, the λ^{P}/i^{P} curve of the device was pesented by a piece-wise linear approximation but because of the nature of the curve, the equations ran into numerical instability at the change-over-point. To reduce this problem a curve fitting technique was used to obtain an analytical expression for the characteristic so that any derivation from the curve around the knee point resulting in numerical instability would be corrected.

Based on the mathematical model presented, a computer program was developed to calculate the voltage and current across and through the device. Numerical steady state analysis of the cable including the device show that the choice of an adequate step length was essential for stable numerical solution. Satisfactory steady state results were obtained using $\frac{1}{2}$°elect. step length. The implementation of the analysis on the digital computer have proved to be successful from a consideration of the results obtained.

The work done in chapter five an six is an extension of the rotation matrix method previously applied for analysing the transient performance of cross-bonded systems. A brief resume of the method reveals that the method of analysis involves a detailed representation of the cross-bonded system, and that the most accurate formulation of the system equations has been used. When analysing the cross-bonded system by the modal analysis and Z-transform technique, the a-priori requirement is to evaluate eigenvalues and eigenvectors over a range of frequencies. The cable system used in this investigation consists of one major cross-bonded section, the sheaths are earthed at both ends through a common resistor, the devices being installed at the cross-bonding points and each device is represented by a resistor, a capacitor and a non-linear inductance in parallel. The full representation of the system was accommodated in the computer program to investigate the performance of the non-linear device.

Three considerations enter into the device choice. First, it should in principle be chosen such that in the current range of the interest for the device applications, the nonlinearity of the characteristic should be maximum. Second, the diameter and length of the device determine the voltage protective level, finally there is a limit to the maximum diameter and length that can be used in practice. There, as for the determination of the field, a process of optimization was necessary. The results of this optimization depends of course on the exact application considered (system load current, length of the transmission system, etc...). This results in an equivalent circuit for device as shown in Fig.6.4. The capacitance of the device depends only on the gap between the iron tube and the bonding lead. The resistive part, represents losses in the iron tube. The non-linear inductance L is given by the volt/ampere characteristic of the device.

It can be concluded from the results obtained that the mathematical model of the device gives a reasonable representation. Some form of non-linear inductance would evidently form a satisfactory protective device. The requirements of such a non-linear inductance have not yet been completely defined. It is known that it must be capable of limiting the current in the sheath as a result of the fault. It must be capable of reducing the overvoltage on the sheath to a low value as possible. Protective non-linear inductances are less expensive than the protective devices

installed in the present day; also they would make for a much simpler installation. It might, for instance, be found practicable to bury a protective non-linear inductance alongside each joint. Their simplicity and stability imply very good performance in service and it is to be expected that they will come into wider use in future.

It is hoped that the results not only give an indication to the general behaviour of the device in a cable network, but also form a basis for comparison in future work. A detailed investigation on the material which the protective device is made up, can be done in the future to determine the best protection device.

REFERENCES

[1] BALL E.H., OCCHINI E. and LUONI G. : "Sheath overvoltages in high-voltage cables resulting from special sheath-bonding connections", IEEE TRANS.,VOL. PAS-84, No.10 1965 pp.974-989

[2] WOLLASTON F.O. and KIDD K.H. : "Cable sheath jacket requirements to withstand abnormal voltage stresses", AIEE, TRANS., VOL. PAS-80, 1961 pp.1116-29

[3] WATSON W. and ERVEN C.C. :"Surge potentials on underground cable sheath and joint insulation", IEEE TRANS., VOL. PAS-82, 1963 pp.239-249

[4] RHODES D.J. and WRIGHT A. :"Induced voltages in the sheaths of cross-bonded a.c. cables", PROC. IEE, VOL.113, No.1 1968 pp.99-110

[5] TANAKA I. :"Mathematical analysis of the surge performance of three-phase, single core cable system with crossbonded sheaths", Elect. Eng. in Japan, VOL.93, No.6, 1973 pp.79-87

[6] WILCOX D.J. and LAWLER K.J. :"Transient phenomena in crossbonded cable system: analytical results", PROC. IEE, VOL.125, No.10, 1978 pp.999-1005

[7] Prof. WEDEPOHL L.M. and INDULKAR C.S. :"Switching overvoltages in short crossbonded cable systems using the Fourier transform", PROC. IEE, VOL.122, No.11, 1975 pp.1217-1221

[8] BROOKES A.S. :"The design of specially bonded cable systems", Electra, No.28 1973 pp.55-81

[9]* SKIPPER D.J :"The design of specially bonded cable circuits", Electra, No.47 1976 pp.61-86

[10] Prof. WEDEPOHL L.M. and WILCOX D.J. :"Transient analysis of underground power-transmission systems: system model and wave-propagation characteristics", PROC. IEE, VOL.120, No.2, 1973 pp253-260

[11] NOUALY J.P and LE ROY G. :"Wave propagation modes on high-voltage cables", IEEE TRANS., VOL. PAS-96, No.1, 1977 pp.158-165

[12] WASLEY R.G. and SELVAVINAYAGAMOORTHY S. :"Computation of sheath transient response in a single-point bonded cable section", IEEE TRANS., VOL. PAS-96, No.1, 1977 pp.248-254

[13] KERSTEN W.F.J :"Surge arresters for sheath protection in crossbonded cable system", PROC. IEE, VOL.126 No.12, 1979 pp.1255-1262

[14] PARMIGIANI B., QUAGGIA D., ELLI E. and FRANCHINA S. : "Zinc oxide sheath voltage limiter for HV and EHV power cable", IEEE TRANS., VOL. PWRD-1, N0.1, 1986 pp.164-171

[15] WEDMORE E.B, MORGAN P.D and WHITEHEAD S. :"A critical study of a three-phase system of unarmoured single-conductor cables, from the standpoint of the power losses, line constants and interference with communication circuits", Journal IEE, VOL.67,1929 pp.359-434

[16] HALPERIN H. and MILLER K.W. :"Reduction of sheath losses in single-conductor cables", AIEE TRANS., VOL.48, 1929 pp.399-416

[17] HALPERIN H., CLEM J.E and MILLER K.M :"Transient voltages on bonded cable sheaths", TRANS. AIEE, VOL.54, 1935 pp.73-82

[18] AMETANI A. :"A general formulation of impedance and admittance of cables", IEEE TRANS., VOL. PAS-99 No.3, 1980 pp.902-910

[19] HUMPAGE W.D :"Z-transform electromagnetic transient analysis in high-voltage networks", Book, Peter Peregrinus Ltd., london, UK, 1982

[20] GRANEAU P. :"Underground power transmission", Book, John Wiley & sons 1979

[21] HEATON A.G and ISSA A.M.H :"Transient response of crossbonded cable system", PROC. IEE, VOL.117, No.3 1970 pp.578-586

APPENDIX No.1

INTEGRATION METHODS

To solve the non-linear differential equations in our study, a number of integration methods were studied. Some of them are more accurate than others.

Central difference.

Using the differential equation:

$$V(t) = L \frac{di(t)}{dt} \qquad \text{A.1.1}$$

integrating equation A.1.1 from t- t to t.

$$\int_{t-\Delta t}^{t} V(t)dt = L \int_{t-\Delta t}^{t} di(t) \qquad \text{A.1.2}$$

By applying the central difference method to equation A.1.2 gives:

$$i(t) = \frac{\Delta t}{2.L} V(t) + \frac{\Delta t}{2.L} V(t-\Delta t) + i(t-\Delta t) \qquad \text{A.1.3}$$

Fig.A.1.1 shows the method graphically:

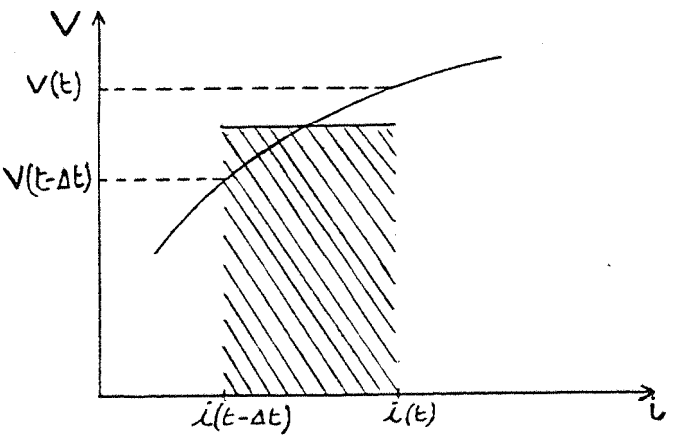

Fig.A.1.1 Central difference method.

The central difference method was found that is not numerical stable.

Forward difference method.

Applying the forward difference method to equation A.1.2 obtains:

$$i(t) = \frac{\Delta t}{L} V(t-\Delta t) + i(t-\Delta t) \qquad A.1.4$$

this method is reffered to in Fig.A.1.2.

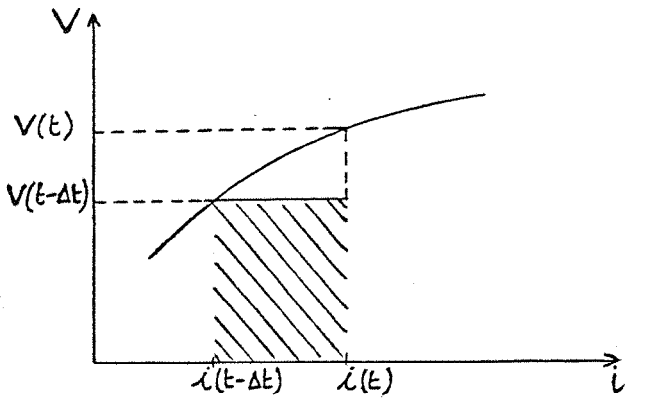

Fig.A.1.2 Forward difference method.

Backward difference method

Applying the backward difference method to equation A.1.2 gives:

$$i(t) = \frac{\Delta t}{L} V(t) + i(t-\Delta t) \qquad A.1.5$$

Fig.A.1.3 shows the method graphically.

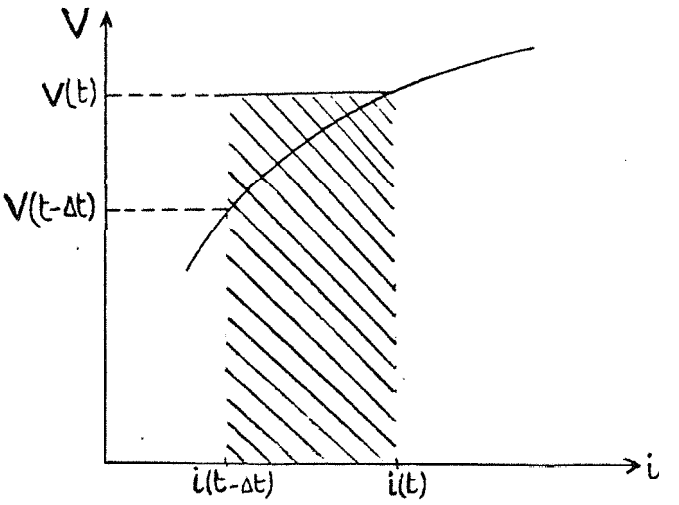

Fig.A.1.3 Backward difference method.

Runge Kutta.

From equation A.1.1, the following equation can be written:

$$\frac{d}{dt} i(t) = \frac{V(t)}{L} \qquad \text{A.1.6}$$

this method consists of computing:

$$K_1 = \frac{\Delta t.\ V(t)}{L}$$

$$K_2 = \Delta t.\left(\frac{V(t) + \frac{1}{2}.K_1}{L}\right)$$

$$K_3 = \Delta t.\left(\frac{V(t) + \frac{1}{2}.K_2}{L}\right)$$

$$K_4 = \Delta t.\left(\frac{V(t) + K_3}{L}\right)$$

then the runge Kutta's formula is:

$$i(t+\Delta t) = \frac{1}{6}.(K_1 + 2.K_2 + 2.K_3 + K_4) + i(t)$$

It was found that central, forward and backward difference have the advantage of being represented by a simple equivalent circuit.

APPENDIX No.2

BASE pu. SYSTEM

MVA_b = 100 KVA

V_b = 100 V

I_b = 1000 A

$\lambda_b = V_b/w_b$ = 2. Wb-turn

T_b = 0.02 sec

$w_b = 1/T_b$ = 50 rad/sec

$F_b = w_b/2\pi$ = 7.95775 Hz

$L_b = V_b . T_b/I_b$ = 0.002 H

$Z_b = V_b/I_b$ = 0.1 Ω

APPENDIX No.3

```
C*************************************************************
C
C   THIS PROGRAM INVESTIGATE THE Z-TRANSFORM TRANSIENT
C  ANALYSIS IN HIGH-VOLTAGE CABLE INCLUDING THE NON-LINEAR
C  DEVICE USED AS SURGE ARRESTER AT THE CROSS-BONDING JOINTS
C
C*************************************************************
C
      PROGRAM ZTRANS
      INTEGER M,N,P,I,J,MI
      REAL I21,I32,I4,I21C,I12C,I23C,I23,I32C,I34C,I34,I1P,L1,L2,
     +  L3,L4,L5,L6,IS1,IS2,IS3,IS4,IS5,IS6,IGX,IGX2,LT,LT2,
     +  I4P,IC4P,IS4P,I12
      PARAMETER (IFREQ=50,PI=3.14159,DELT=3.14E-06)
      PARAMETER (X1=-0.3392,X2=-0.3968,X3=-0.4351,X4=-0.3557,
     +          X5=0.0004,X6=0.01234,Y1=0.0797,Y2=0.00966,
     +          Y3=-0.07,Y4=-2.1015,Y5=1.5352,Y6=-0.464,
     +          Y7=0.0497,Z0=80.4,Z1=15.50,Z2=10.85)
      DIMENSION        C1(6,),C11(6,6),C2(6,6),C22(6,6),ZL(6,6),
     + ZLP(6,6),T1(6,6),T11(6,6),T1ZLP(6,6),ZT(6,6),U(6,6),
     + H(6,6),HI(6,6),Q(6,6),C11Q(6,6),T1C1(6,6),X(6,6),
     + C11HI(6,6),Y(6,6),ZLI(6,6),V(6,1),VP(6,1),ZV(6,1),
     + C1ZL(6,6),ZLPI(6,6),ZTZLPI(6,6),I12(6,1)
     + VP21(6,1),VP23(6,1),XVP21(6,1),YVP23(6,1),V21(6,1),
     + ZV21(6,1),I21(6,1),VP32(6,1),VP34(6,1),XVP32(6,1),
     + YVP34(6,1),V32(6,1),ZV32(6,1),I32(6,1),VP4(6,1),
     + V4(6,1),ZV4(6,1),I4(6,1),WRSPCE(20),G1(6,6),
     + V21C(6,1),I12C(6,1),I23C(6,1),I23(6,1),V23C(6,1),
     + V34C(6,1),I34C(6,1),V23(6,1),V32C(6,1),I32C(6,1),V34(6,1),
     + I34(6,1),V4C(3,1),G2(6,6),I1P(4,1),ZVE(4,6),G(4,4),
     + CZLPI(4,6),CT(6,4),YPR(4,4),YPRG(4,4),YPGI(4,4),XX(4,6),
     + XXC1(4,6),V4C1(6,1),I21C(6,1),C(4,6)
      DIMENSION SU(6,6),W(6,6),BB(6,6),ZTW(6,6),LT(6,6),
     + ZTWL(6,6),ZTWLW(6,6),LT2(6,6),ZTWL2(6,6),ZZ(6,1),
     + ZTWW(6,6),VV2(6,1),ZZ2(6,1),ZTIG2(6,1),IGX2(6,1),VVV(6,1),
     + ZTIG(6,1),IGX(6,1),I4P(6,1),IC4P(3,1),RRI(3,3),RRY(3,3),
```

```
     + RRYI(3,3),Y11(3,3),Y12(3,1),Y21(1,3),YY12(3,1),YY121(3,3),
     + YY11(3,3),SI4P(3,1),P4I(3,1),CNT(6,6),CNT2(6,6),
     + V21CX(6,1),V32CX(6,1),CVX(6,1),CVX2(6,1),VIX(6,1),
     + VIX2(6,1),RR(3,3),R1(3,3),RR1(3,3)
      REAL V1AC(0:59),V1BC(0:59),V1CC(0:59),VE1(0:59),IL1(-1:59),
     +   V11(-1:59),V12(-6:59),V13(-1:59),IL2(-1:59),IL3(-1:59),
     +     V14(-6:59),V15(-1:59),V16(-18:59),IL4(-1:59),
     +     V1(-1:59),V2(-1:59),V3(-1:59),IL5(-1:59),IL6(-1:59),
     +     V1P(-14:45),V21P(-14:45),V23P(-14:45),V32P(-14:45),
     +     V34P(-14:45),V4P(-14:45),B1(-5:58),B21(-5:58),
     +   B23(-5:58),B32(-5:58),B34(-5:58),B4(-5:58),V121(-1:59),
     +  V221(-6:59),V321(-1:59),V421(-6:59),V521(-1:59),
     +  V621(-18:59),I112(-1:59),
     +  I212(-6:59),I312(-1:59),I412(-6:59),I512(-1:59),
     +  I612(-16:59),FR1(-1:58),FR2(-6:53),FR3(-1:58),FR4(-6:53),
     +     FR5(-1:58),FR0(-18:45),FS1(-1:58),FS2(-6:53),
     +     FS3(-1:58),FS4(-6:53),FS5(-1:58),FS0(-18:45),
     +     I121(-1:59),I221(-6:59),I321(-1:59),I421(-6:59),
     +     I521(-1:59),I621(-16:59)
      REAL V123(-1:59),V223(-6:59),V323(-1:59),V423(-6:59),
     +     V523(-1:59),V623(-18:59),I123(-1:59),I223(-6:59),
     +     I323(-1:59),I423(-6:59),I523(-1:59),I623(-16:59),
     +     V132(-1:59),V232(-6:59),V332(-1:59),V432(-6:59),
     +     V532(-1:59),V632(-18:59),I132(-1:59),I232(-6:59),
     +     I332(-1:59),I432(-6:59),I532(-1:59),I632(-16:59),
     +     V134(-1:59),V234(-6:59),V334(-1:59),V434(-6:59),
     +     V534(-1:59),V634(-18:59),I134(-1:59),I234(-6:59),
     +     I334(-1:59),I434(-6:59),I534(-1:59),I634(-16:59),
     +     V41(-1:59),V42(-6:59),V43(-1:59),V44(-6:59),V45(-1:59)
      REAL I41(-1:59),I42(-6:59),I43(-1:59),I44(-6:59),
     +     I45(-1:59),I46(-16:59),V4AC(0:59),V4AS(0:59),
     +     V4BC(0:59),V4CC(0:59),V46(-18:59),
     +    KS1(-1:58),KS2(-6:53),KS3(-1:58),KS4(-6:53),KS5(-1:58),
     +   KS0(-18:45),KR1(-1:58),KR2(-6:53),KR3(-1:58),KR4(-6:53),
     +    KR5(-1:58),KR0(-18:45),VE4(0:59),TS1(-1:58),TS2(-6:53),
     +   TS3(-1:58),TS4(-6:53),TS5(-1:58),TS0(-18:45),TR1(-1:58),
     +    TR2(-6:53),TR3(-1:58),TR4(-6:53),TR5(-1:58),TR0(-18:45)
C     INITIALIZATION
```

```
 DATA FS0/64*0.0/,FR0/64*0.0/,FR1/60*0.0/,FR2/60*0.0/,
+      FR3/60*0.0/,FR4/60*0.0/,FR5/60*0.0/,FS1/60*0.0/,
+      FS2/60*0.0/,FS3/60*0.0/,FS4/60*0.0/,FS5/60*0.0/,
+      V1AC/60*0.0/,V1BC/60*0.0/,V1CC/60*0.0/,VE1/60*0.0/,
+      V11/61*0.0/,V12/66*0.0/,
+      V13/61*0.0/,V14/66*0.0/,V15/61*0.0/,V16/78*0.0/,
+      V121/61*0.0/,V221/66*0.0/,V321/61*0.0/,V421/66*0.0/,
+      V521/61*0.0/,V621/78*0.0/,
+      I112/61*0.0/,I212/66*0.0/,I312/61*0.0/,
+      I412/66*0.0/,I512/61*0.0/,I612/76*0.0/,
+      I121/61*0.0/,I221/66*0.0/,I321/61*0.0/,
+      I421/66*0.0/,I521/61*0.0/,I621/76*0.0/
 DATA V123/61*0.0/,V223/66*0.0/,V323/61*0.0/,V423/66*0.0/,
+      V523/61*0.0/,V623/78*0.0/,I123/61*0.0/,I223/66*0.0/,
+      I323/61*0.0/,I423/66*0.0/,I523/61*0.0/,I623/76*0.0/,
+      V132/61*0.0/,V232/66*0.0/,V332/61*0.0/,V432/66*0.0/,
+      V532/61*0.0/,V632/78*0.0/,I132/61*0.0/,I232/66*0.0/,
+      I332/61*0.0/,I432/66*0.0/,I532/61*0.0/,I632/76*0.0/,
+      V134/61*0.0/,V234/66*0.0/,V334/61*0.0/,V434/66*0.0/,
+      V534/61*0.0/,V634/78*0.0/,I134/61*0.0/,I234/66*0.0/,
+      I334/61*0.0/,I434/66*0.0/,I534/61*0.0/,I634/76*0.0/
 DATA V42/66*0.0/,V43/61*0.0/,V44/66*0.0/,V45/61*0.0/,
+      V46/78*0.0/,I41/61*0.0/,I42/66*0.0/,I43/61*0.0/,
+      I44/66*0.0/,I45/61*0.0/,I46/76*0.0/,VE4/60*0.0/,
+      V4AC/60*0.0/,V4AS/60*0.0/,V4BC/60*0.0/,V41/61*0.0/,
+      V4CC/60*0.0/,V1P/60*0.0/,V21P/60*0.0/,V23P/60*0.0/,
+      V34P/60*0.0/,V4P/60*0.0/,B1/64*0.0/,B21/64*0.0/,
+      B23/64*0.0/,B32/64*0.0/,B34/64*0.0/,B4/64*0.0/,
+      KS1/60*0.0/,KS2/60*0.0/,KS3/60*0.0/,KS4/60*0.0/,
+      KS0/64*0.0/,KR1/60*0.0/,KR2/60*0.0/,KR3/60*0.0/,
+      KR4/60*0.0/,KR0/64*0.0/,TR1/60*0.0/,TR2/60*0.0/,
+      TR3/60*0.0/,TR4/60*0.0/,TR5/60*0.0/,TR0/64*0.0/,
+      TS1/60*0.0/,TS2/60*0.0/,TS3/60*0.0/,TS4/60*0.0/,
+     TS5/60*0.0/,KR5/60*0.0/,V32P/60*0.0/,KS5/60*0.0/,
+      TS0/64*0.0/,V1/61*0.0/,V2/61*0.0/,V3/61*0.0/
 K=0
 ICON=0
 N=6
```

```
      IA=6
      IUNIT=6
      IFAIL=1
      P=1
      M=6
      MI=4
C-----------------------------------------------------------
C     READ THE PARAMETERS OF CABLE AND DO ALL THE  MATRICES
C     OPERATIONS
C-----------------------------------------------------------
      READ(5,*)((C2(I,J),J=1,N),I=1,N)
      READ(5,*)((C1(I,J),J=1,N),I=1,N)
      READ(5,*)((ZL(I,J),J=1,M),I=1,M)
      DO 110 I=1,N
      DO 110 J=1,N
      G1(I,J)=C1(I,J)
      G2(I,J)=C2(I,J)
110   CONTINUE
C
      CALL MAT(M,M,M,C1,ZL,C1ZL)
      CALL F01AAF(C2,IA,N,C22,IUNIT,WRSPCE,IFAIL)
      CALL MAT(M,M,M,C1ZL,C22,ZLP)
      READ(3,*)((T1(I,J),J=1,M),I=1,M)
      READ(3,*)((T11(I,J),J=1,M),I=1,M)
      CALL MAT(M,M,M,T1,ZLP,T1ZLP)
      CALL MAT(M,M,M,T1ZLP,T11,ZT)
      DO 1 I=1,N
      DO 1 J=1,N
1     BB(I,J)=ZT(I,J)
      CALL F01AAF(ZLP,IA,N,ZLPI,IUNIT,WRSPCE,IFAIL)
      CALL MAT(M,M,M,ZT,ZLPI,ZTZLPI)
      READ(5,*)((U(I,J),J=1,M),I=1,M)
      CALL ADD(M,M,U,ZTZLPI,SU)
      READ(5,*)((W(I,J),J=1,M),I=1,M)
      CALL MAT(M,M,M,BB,W,ZTW)
      CALL F01AAF(C1,IA,N,C11,IUNIT,WRSPCE,IFAIL)
      CALL MAT(M,M,M,T1,G1,T1C1)
      CALL F01AAF(ZL,IA,N,ZLI,IUNIT,WRSPCE,IFAIL)
```

```
C
C-------- SHEATHS EARTHING ----------------
C
      READ(2,*)((C(I,J),J=1,M),I=1,MI)
      READ(2,*)((CT(I,J),J=1,MI),I=1,M)
      READ(2,*)((G(I,J),J=1,MI),I=1,MI)
      CALL MAT(MI,M,M,C,ZLPI,CZLPI)
      CALL MAT(MI,M,MI,CZLPI,CT,YPR)
      CALL ADD(MI,MI,YPR,G,YPRG)
      CALL F01AAF(YPRG,4,4,YPGI,4,WRSPCE,IFAIL)
      CALL MAT(MI,MI,M,YPGI,CZLPI,XX)
      CALL MAT(4,6,6,XX,G1,XXC1)
      CALL MAT(4,6,6,CZLPI,G1,ZVE)
      Y211=YPRG(4,1)
      Y212=YPRG(4,2)
      Y213=YPRG(4,3)
      Y44=YPRG(4,4)
      DO 777 I=1,3
      Y12(I,1)=YPRG(I,4)
      Y21(1,I)=YPRG(4,I)
      YY12(I,1)=Y12(I,1)/Y44
      DO 777 J=1,3
777   Y11(I,J)=YPRG(I,J)
      CALL MAT(3,1,3,YY12,Y21,YY121)
      CALL SUB(3,3,Y11,YY121,YY11)
C
C------ THE LOAD RESISTORS -------------
C
      READ(5,*)((RR(I,J),J=1,3),I=1,3)
      READ(5,*)((R1(I,J),J=1,3),I=1,3)
      CALL ADD(3,3,RR,R1,RR1)
      CALL F01AAF(RR1,3,3,RRI,3,WRSPCE,IFAIL)
      CALL SUB(3,3,RRI,YY11,RRY)
      CALL F01AAF(RRY,3,3,RRYI,3,WRSPCE,IFAIL)
C
C------ NONLINEAR INDUCTANCE -----------
C
      READ(2,*) R,CAP,L1,L2,L3,L4,L5,L6
```

```
      DO 71 I=1,6
      V21CX(I,1)=0.0
71    V32CX(I,1)=0.0
      SAT=0.250
C
C------ DEFINE THE INPUT -------------------------------------
C
10000 CONTINUE
      DO 1000 N=ICON,59
      T=(N+60*K)*DELT
      RAD=2*PI*IFREQ*(N+60*K)*DELT
      A=RAD+PI/2
      B=RAD-5*PI/6
      D=RAD-PI/6
      V1(N)=150*SIN(A)
      V2(N)=150*SIN(B)
      V3(N)=150*SIN(D)
C------FIND THE VARIABLES ------------------
      FS1(N-1)=V11(N-1)+Z1*I112(N-1)
      FS2(N-6)=V12(N-6)+Z2*(2*I212(N-6)+I412(N-6))
      FS3(N-1)=V13(N-1)+Z1*I312(N-1)
      FS4(N-6)=V14(N-6)+Z2*(2*I412(N-6)+I212(N-6))
      FS5(N-1)=V15(N-1)+Z1*I512(N-1)
      FS0(N-14)=V16(N-14)+X3*V16(N-15)+X4*V16(N-16)+X5*V16(N-17)
     +          +X6*V16(N-18)+Z0*I612(N-14)+Z0*X1*I612(N-15)
     +          +Z0*X2*I612(N-16)-X3*FS0(N-15)-X4*FS0(N-16)
     +          -X5*FS0(N-17)-X6*FS0(N-18)
      FR1(N-1)=V121(N-1)+Z1*I121(N-1)
      FR2(N-6)=V221(N-6)+Z2*(2*I221(N-6)+I421(N-6))
      FR3(N-1)=V321(N-1)+Z1*I321(N-1)
      FR4(N-6)=V421(N-6)+Z2*(2*I421(N-6)+I221(N-6))
      FR5(N-1)=V521(N-1)+Z1*I521(N-1)
      FR0(N-14)=V621(N-14)+X3*V621(N-15)+X4*V621(N-16)
     +          +X5*V621(N-17)+X6*V621(N-18)+Z0*I621(N-14)
     +          +Z0*X1*I621(N-15)+Z0*X2*I621(N-16)-X3*FR0(N-15)
     +          -X4*FR0(N-16)-X5*FR0(N-17)-X6*FR0(N-18)
      KS1(N-1)=V123(N-1)+Z1*I123(N-1)
      KS2(N-6)=V223(N-6)+Z2*(2*I223(N-6)+I423(N-6))
```

```
      KS3(N-1)=V323(N-1)+Z1*I323(N-1)
      KS4(N-6)=V423(N-6)+Z2*(2*I423(N-6)+I223(N-6))
      KS5(N-1)=V523(N-1)+Z1*I523(N-1)
      KS0(N-14)=V623(N-14)+X3*V623(N-15)+X4*V623(N-16)
     +          +X6*V623(N-18)+Z0*I623(N-14)+Z0*X1*I623(N-15)
     +          +Z0*X2*I623(N-16)-X3*KS0(N-15)-X4*KS0(N-16)
     +          -X5*KS0(N-17)-X6*KS0(N-18)+X5*V623(N-17)
      KR1(N-1)=V132(N-1)+Z1*I132(N-1)
      KR2(N-6)=V232(N-6)+Z2*(2*I232(N-6)+I432(N-6))
      KR3(N-1)=V332(N-1)+Z1*I332(N-1)
      KR4(N-6)=V432(N-6)+Z2*(2*I432(N-6)+I232(N-6))
      KR5(N-1)=V532(N-1)+Z1*I532(N-1)
      KR0(N-14)=V632(N-14)+X3*V632(N-15)+X4*V632(N-16)
     +          +X6*V632(N-18)+Z0*I632(N-14)+Z0*X1*I632(N-15)
     +          +Z0*X2*I632(N-16)-X3*KR0(N-15)-X4*KR0(N-16)
     +          -X5*KR0(N-17)-X6*KR0(N-18)+X5*V632(N-17)
      TS1(N-1)=V134(N-1)+Z1*I134(N-1)
      TS2(N-6)=V234(N-6)+Z2*(2*I234(N-6)+I434(N-6))
      TS3(N-1)=V334(N-1)+Z1*I334(N-1)
      TS4(N-6)=V434(N-6)+Z2*(2*I434(N-6)+I234(N-6))
      TS5(N-1)=V534(N-1)+Z1*I534(N-1)
      TS0(N-14)=V634(N-14)+X3*V634(N-15)+X4*V634(N-16)
     +          +X5*V634(N-17)+X6*V634(N-18)+Z0*I634(N-14)
     +          +Z0*X1*I634(N-15)+Z0*X2*I634(N-16)-X3*TS0(N-15)
     +          -X4*TS0(N-16)-X5*TS0(N-17)-X6*TS0(N-18)
C
      TR1(N-1)=V41(N-1)+Z1*I41(N-1)
      TR2(N-6)=V42(N-6)+Z2*(2*I42(N-6)+I44(N-6))
      TR3(N-1)=V43(N-1)+Z1*I43(N-1)
      TR4(N-6)=V44(N-6)+Z2*(2*I44(N-6)+I42(N-6))
      TR5(N-1)=V45(N-1)+Z1*I45(N-1)
      TR0(N-14)=V46(N-14)+X3*V46(N-15)+X4*V46(N-16)+X5*V46(N-17)
     +          +X6*V46(N-18)+Z0*I46(N-14)+Z0*X1*I46(N-15)
     +          +Z0*X2*I46(N-16)-X3*TR0(N-15)-X4*TR0(N-16)
     +          -X5*TR0(N-17)-X6*TR0(N-18)
C
      B1(N-1)=V16(N-1)+X3*V16(N-2)+X4*V16(N-3)+X5*V16(N-4)
     +  +X6*V16(N-5)-Z0*I612(N-1)-Z0*X1*I612(N-2)-Z0*X2*I612(N-3)
```

```
+      -X3*B1(N-2)-X4*B1(N-3)-X5*B1(N-4)-X6*B1(N-5)
 B21(N-1)=V621(N-1)+X3*V621(N-2)+X4*V621(N-3)+X5*V621(N-4)
+ +X6*V621(N-5)-Z0*I621(N-1)-Z0*X1*I621(N-2)-Z0*X2*I621(N-3)
+       -X3*B21(N-2)-X4*B21(N-3)-X5*B21(N-4)-X6*B21(N-5)
 B23(N-1)=V623(N-1)+X3*V623(N-2)+X4*V623(N-3)+X5*V623(N-4)
+ +X6*V623(N-5)-Z0*I623(N-1)-Z0*X1*I623(N-2)-Z0*X2*I623(N-3)
+       -X3*B23(N-2)-X4*B23(N-3)-X5*B23(N-4)-X6*B23(N-5)
 B32(N-1)=V632(N-1)+X3*V632(N-2)+X4*V632(N-3)+X5*V632(N-4)
+ +X6*V632(N-5)-Z0*I632(N-1)-Z0*X1*I632(N-2)-Z0*X2*I632(N-3)
+       -X3*B32(N-2)-X4*B32(N-3)-X5*B32(N-4)-X6*B32(N-5)
 B34(N-1)=V634(N-1)+X3*V634(N-2)+X4*V634(N-3)+X5*V634(N-4)
+ +X6*V634(N-5)-Z0*I634(N-1)-Z0*X1*I634(N-2)-Z0*X2*I634(N-3)
+      -X3*B34(N-2)-X4*B34(N-3)-X5*B34(N-4)-X6*B34(N-5)
 B4(N-1)=V46(N-1)+X3*V46(N-2)+X4*V46(N-3)+X5*V46(N-4)
+      +X6*V46(N-5)-Z0*I46(N-1)-Z0*X1*I46(N-2)-Z0*X2*I46(N-3)
+      -X3*B4(N-2)-X4*B4(N-3)-X5*B4(N-4)-X6*B4(N-5)
C
 V1P(N-14)=-X3*V16(N-1)-X4*V16(N-2)-X5*V16(N-3)
-          -X6*V16(N-4)+Z0*X1*I612(N-1)+Z0*X2*I612(N-2)
+          +(X3-Y4)*B1(N-1)+(X4-Y5)*B1(N-2)+(X5-Y6)*B1(N-3)
-     +(X6-Y7)*B1(N-4)+Y1*FR0(N-14)+Y2*FR0(N-15)+Y3*FR0(N-16)
 V21P(N-14)=-X3*V621(N-1)-X4*V621(N-2)-X5*V621(N-3)
+          -X6*V621(N-4)+Z0*X1*I621(N-1)+Z0*X2*I621(N-2)
+        +(X3-Y4)*B21(N-1)+(X4-Y5)*B21(N-2)+(X5-Y6)*B21(N-3)
+          +(X6-Y7)*B21(N-4)+Y1*FS0(N-14)+Y2*FS0(N-15)
+          +Y3*FS0(N-16)
 V23P(N-14)=-X3*V623(N-1)-X4*V623(N-2)-X5*V623(N-3)
+           -X6*V623(N-4)+Z0*X1*I623(N-1)+Z0*X2*I623(N-2)
+         +(X3-Y4)*B23(N-1)+(X4-Y5)*B23(N-2)+(X5-Y6)*B23(N-3)
+           +(X6-Y7)*B23(N-4)+Y1*KR0(N-14)+Y2*KR0(N-15)
+           +Y3*KR0(N-16)
 V32P(N-14)=-X3*V632(N-1)-X4*V632(N-2)-X5*V632(N-3)
+           -X6*V632(N-4)+Z0*X1*I632(N-1)+Z0*X2*I632(N-2)
+         +(X3-Y4)*B32(N-1)+(X4-Y5)*B32(N-2)+(X5-Y6)*B32(N-3)
+           +(X6-Y7)*B32(N-4)+Y1*KS0(N-14)+Y2*KS0(N-15)
+           +Y3*KS0(N-16)
 V34P(N-14)=-X3*V634(N-1)-X4*V634(N-2)-X5*V634(N-3)
+           -X6*V634(N-4)+Z0*X1*I634(N-1)+Z0*X2*I634(N-2)
```

```
     +          +(X3-Y4)*B34(N-1)+(X4-Y5)*B34(N-2)+(X5-Y6)*B34(N-3)
     +            +(X6-Y7)*B34(N-4)+Y1*TR0(N-14)+Y2*TR0(N-15)
     +            +Y3*TR0(N-16)
      V4P(N-14)=-X3*V46(N-1)-X4*V46(N-2)-X5*V46(N-3)
     +           -X6*V46(N-4)+Z0*X1*I46(N-1)+Z0*X2*I46(N-2)
     +         +(X3-Y4)*B4(N-1)+(X4-Y5)*B4(N-2)+(X5-Y6)*B4(N-3)
     +     +(X6-Y7)*B4(N-4)+Y1*TS0(N-14)+Y2*TS0(N-15)+Y3*TS0(N-16)
C-----------------------------------------------------------------
C       START THE CALCULATION OF VOLTAGES AND CURRENTS
C          FOR EACH SECTION OF THE CABLE
C-----------------------------------------------------------------
C
C--------FIRST SECTION -------------------
C
       V1AC(N)=V1(N)
       V1BC(N)=0
       V1CC(N)=0
       VP(1,1)=FR1(N-1)
       VP(2,1)=FR2(N-6)
       VP(3,1)=FR3(N-1)
       VP(4,1)=FR4(N-6)
       VP(5,1)=FR5(N-1)
       VP(6,1)=V1P(N-14)
       CALL MAT(4,6,1,ZVE,VP,I1P)
       VE1(N)=(-Y211*V1AC(N)-Y212*V1BC(N)-Y213*V1CC(N)
     +    +I1P(4,1))/Y44
      C      WRITE(6,*) VE1(N)
       V11(N)=V1AC(N)-VE1(N)
       V12(N)=0.0
       V13(N)=V1BC(N)-VE1(N)
       V14(N)=0.0
       V15(N)=V1CC(N)-VE1(N)
       V16(N)=3*VE1(N)
C
       V(1,1)=V11(N)
       V(2,1)=V12(N)
       V(3,1)=V13(N)
       V(4,1)=V14(N)
```

```
      V(5,1)=V15(N)
      V(6,1)=V16(N)
      CALL SUB(M,P,V,VP,ZV)
      CALL MAT(M,M,P,ZLI,ZV,I12)
      I112(N)=I12(1,1)
      I212(N)=I12(2,1)
      I312(N)=I12(3,1)
      I412(N)=I12(4,1)
      I512(N)=I12(5,1)
      I612(N)=I12(6,1)
      CALL MAT(M,M,P,G2,I12,I12C)
C
      VP21(1,1)=FS1(N-1)
      VP21(2,1)=FS2(N-6)
      VP21(3,1)=FS3(N-1)
      VP21(4,1)=FS4(N-6)
      VP21(5,1)=FS5(N-1)
      VP21(6,1)=V21P(N-14)
      VP23(1,1)=KR1(N-1)
      VP23(2,1)=KR2(N-6)
      VP23(3,1)=KR3(N-1)
      VP23(4,1)=KR4(N-6)
      VP23(5,1)=KR5(N-1)
      VP23(6,1)=V23P(N-14)
      IGX(1,1)=0
      IGX(2,1)=IL1(N-1)
      IGX(3,1)=0
      IGX(4,1)=IL2(N-1)
      IGX(5,1)=0
      IGX(6,1)=IL3(N-1)
      DO 2 I=1,6
      DO 2 J=1,6
      LT(I,J)=0
2     CNT(I,J)=0.0
      LT(2,2)=DELT/L1+CAP/DELT+1.0/R
      LT(4,4)=DELT/L2+CAP/DELT+1.0/R
      LT(6,6)=DELT/L3+CAP/DELT+1.0/R
      CNT(2,2)=CAP/DELT
```

```
      CNT(4,4)=CAP/DELT
      CNT(6,6)=CAP/DELT
      CALL MAT(6,6,6,ZTW,LT,ZTWL)
      CALL MAT(6,6,6,ZTWL,W,ZTWLW)
      CALL ADD(6,6,SU,ZTWLW,H)
      CALL F01AAF(H,6,6,HI,6,WRSPCE,IFAIL)
      CALL MAT(6,6,6,HI,ZTZLPI,Q)
      CALL MAT(6,6,6,C11,Q,C11Q)
      CALL MAT(6,6,6,C11Q,G1,X)
      CALL MAT(6,6,6,C11,HI,C11HI)
      CALL MAT(6,6,6,C11HI,T1C1,Y)
      CALL MAT(6,6,1,CNT,V21CX,CVX)
      CALL SUB(6,1,IGX,CVX,VIX)
      CALL MAT(6,6,1,ZTW,VIX,ZTIG)
      CALL MAT(6,6,1,C11HI,ZTIG,ZZ)
      CALL MAT(M,M,P,X,VP21,XVP21)
      CALL MAT(M,M,P,Y,VP23,YVP23)
      CALL ADD(M,P,XVP21,YVP23,VVV)
      CALL SUB(6,1,VVV,ZZ,V21)
      V121(N)=V21(1,1)
      V221(N)=V21(2,1)
      V321(N)=V21(3,1)
      V421(N)=V21(4,1)
      V521(N)=V21(5,1)
      V621(N)=V21(6,1)
C
      CALL MAT(M,M,P,G1,V21,V21C)
C
      IL1(N)=(DELT/L1)*V21C(2,1)+IL1(N-1)
      IL2(N)=(DELT/L2)*V21C(4,1)+IL2(N-1)
      IL3(N)=(DELT/L3)*V21C(6,1)+IL3(N-1)
      IR1(N)=V21C(2,1)/R
      IR2(N)=V21C(4,1)/R
      IR3(N)=V21V(6,1)/R
      IC1(N)=(CAP/DELT)*(V21C(2,1)-V21CX(2,1))
      IC2(N)=(CAP/DELT)*(V21C(4,1)-V21CX(4,1))
      IC3(N)=(CAP/DELT)*(V21C(6,1)-V21CX(6,1))
      IA1(N)=IL1(N)+IR1(N)+IC1(N)
```

```
      IA2(N)=IL2(N)+IR2(N)+IC2(N)
      IA3(N)=IL3(N)+IR3(N)+IC3(N)
      DET1=IL1(N)-IL1(N-1)
      IS1=ABS(IL1(N)+0.5*DET1)
      IF(IS1.GE.SAT) GO TO 21
      L1=4.0E-5+0.01395*EXP(0.02144*IS1)/(EXP(0.02144*IS1)+1)**2
      GO TO 31
21    L1=4.0E-5
31    DET2=IL2(N)-IL2(N-1)
      IS2=ABS(IL2(N)+0.5*DET2)
      IF(IS2.GE.SAT) GO TO 22
      L2=4.0E-5+0.01395*EXP(0.02144*IS2)/(EXP(0.02144*IS2)+1)**2
      GO TO 32
22    L2=4.0E-5
32    DET3=IL3(N)-IL3(N-1)
      IS3=ABS(IL3(N)+0.5*DET3)
      IF(IS3.GE.SAT) GO TO 23
      L3=4.0E-5+0.01395*EXP(0.02144*IS3)/(EXP(0.02144*IS3)+1)**2
      GO TO 998
23    L3=4.0E-5
C
998   CALL SUB(M,P,V21,VP21,ZV21)
      CALL MAT(M,M,P,ZLI,ZV21,I21)
      I121(N)=I21(1,1)
      I221(N)=I21(2,1)
      I321(N)=I21(3,1)
      I421(N)=I21(4,1)
      I521(N)=I21(5,1)
      I621(N)=I21(6,1)
      CALL MAT(M,M,P,G2,I21,I21C)
      DO 51 I=1,6
51    V21CX(I,1)=V21C(I,1)
```

```
C------------------ SECTION TWO ----------------------
C
      V23C(1,1)=V21C(1,1)
      V23C(2,1)=V21C(6,1)
      V23C(3,1)=V21C(3,1)
      V23C(4,1)=V21C(2,1)
      V23C(5,1)=V21C(5,1)
      V23C(6,1)=V21C(4,1)
C
      I23C(1,1)=-I21C(1,1)
      I23C(2,1)=-I21C(6,1)-IL3(N)
      I23C(3,1)=-I21C(3,1)
      I23C(4,1)=-I21C(2,1)-IL1(N)
      I23C(5,1)=-I21C(5,1)
      I23C(6,1)=-I21C(4,1)-IL2(N)
      CALL MAT(M,M,P,C22,I23C,I23)
      I123(N)=I23(1,1)
      I223(N)=I23(2,1)
      I323(N)=I23(3,1)
      I423(N)=I23(4,1)
      I523(N)=I23(5,1)
      I623(N)=I23(6,1)
      CALL MAT(M,M,P,C11,V23C,V23)
      V123(N)=V23(1,1)
      V223(N)=V23(2,1)
      V323(N)=V23(3,1)
      V423(N)=V23(4,1)
      V523(N)=V23(5,1)
      V623(N)=V23(6,1)
C
      VP32(1,1)=KS1(N-1)
      VP32(2,1)=KS2(N-6)
      VP32(3,1)=KS3(N-1)
      VP32(4,1)=KS4(N-6)
      VP32(5,1)=KS5(N-1)
      VP32(6,1)=V32P(N-14)
      VP34(1,1)=TR1(N-1)
```

```
      VP34(2,1)=TR2(N-6)
      VP34(3,1)=TR3(N-1)
      VP34(4,1)=TR4(N-6)
      VP34(5,1)=TR5(N-1)
      VP34(6,1)=V34P(N-14)
      IGX2(1,1)=0
      IGX2(2,1)=IL4(N-1)
      IGX2(3,1)=0
      IGX2(4,1)=IL5(N-1)
      IGX2(5,1)=0
      IGX2(6,1)=IL6(N-1)
      DO 61 I=1,6
      DO 61 J=1,6
      LT2(I,J)=0
61    CNT2(I,J)=0.0
      LT2(2,2)=DELT/L4+CAP/DELT+1.0/R
      LT2(4,4)=DELT/L5+CAP/DELT+1.0/R
      LT2(6,6)=DELT/L6+CAP/DELT+1.0/R
      CNT2(2,2)=CAP/DELT
      CNT2(4,4)=CAP/DELT
      CNT2(6,6)=CAP/DELT
      CALL MAT(6,6,6,ZTW,LT2,ZTWL2)
      CALL MAT(6,6,6,ZTWL2,W,ZTWW)
      CALL ADD(6,6,SU,ZTWW,H)
      CALL F01AAF(H,6,6,HI,6,WRSPCE,IFAIL)
      CALL MAT(6,6,6,HI,ZTZLPI,Q)
      CALL MAT(6,6,6,C11,Q,C11Q)
      CALL MAT(6,6,6,C11Q,G1,X)
      CALL MAT(6,6,6,C11,HI,C11HI)
      CALL MAT(6,6,6,C11HI,T1C1,Y)
      CALL MAT(6,6,1,CNT2,V32CX,CVX2)
      CALL SUB(6,1,IGX2,CVX2,VIX2)
      CALL MAT(6,6,1,ZTW,VIX2,ZTIG2)
      CALL MAT(6,6,1,C11HI,ZTIG2,ZZ2)
      CALL MAT(M,M,P,X,VP32,XVP32)
      CALL MAT(M,M,P,Y,VP34,YVP34)
      CALL ADD(M,P,XVP32,YVP34,VV2)
      CALL SUB(6,1,VV2,ZZ2,V32)
```

```
      V132(N)=V32(1,1)
      V232(N)=V32(2,1)
      V332(N)=V32(3,1)
      V432(N)=V32(4,1)
      V532(N)=V32(5,1)
      V632(N)=V32(6,1)
      CALL MAT(M,M,P,G1,V32,V32C)
C
      IL4(N)=(DELT/L4)*V32C(2,1)+IL4(N-1)
      IL5(N)=(DELT/L5)*V32C(4,1)+IL5(N-1)
      IL6(N)=(DELT/L6)*V32C(6,1)+IL6(N-1)
      IR4(N)=V32C(2,1)/R
      IR5(N)=V32C(4,1)/R
      IR6(N)=V32C(6,1)/R
      IC4(N)=(CAP/DELT)*(V32C(2,1)-V32CX(2,1))
      IC5(N)=(CAP/DELT)*(V32C(4,1)-V32CX(4,1))
      IC6(N)=(CAP/DELT)*(V32C(6,1)-V32CX(6,1))
      IA4(N)=IL4(N)+IR4(N)+IC4(N)
      IA5(N)=IL5(N)+IR5(N)+IC5(N)
      IA6(N)=IL6(N)+IR6(N)+IC6(N)
      DET4=IL4(N)-IL4(N-1)
      IS4=ABS(IL4(N)+0.5*DET4)
      IF(IS4.GE.SAT) GOTO 25
      L4=4.0E-5+0.01395*EXP(0.02144*IS4)/(EXP(0.02144*IS4)+1)**2
      GOTO 35
25    L4=4.0E-5
35    DET5=IL5(N)-IL5(N-1)
      IS5=ABS(IL5(N)+0.5*DET5)
      IF(IS5.GE.SAT) GOTO 26
      L5=4.0E-5+0.01395*EXP(0.02144*IS5)/(EXP(0.02144*IS5)+1)**2
      GOTO 36
26    L5=4.0E-5
36    DET6=IL6(N)-IL6(N-1)
      IS6=ABS(IL6(N)+0.5*DET6)
      IF(IS6.GE.SAT) GOTO 27
      L6=4.0E-5+0.01395*EXP(0.02144*IS6)/(EXP(0.02144*IS6)+1)**2
      GOTO 102
27    L6=4.0E-5
```

```
C
102   CONTINUE
      CALL SUB(M,P,V32,VP32,ZV32)
      CALL MAT(M,M,P,ZLI,ZV32,I32)
      I132(N)=I32(1,1)
      I232(N)=I32(2,1)
      I332(N)=I32(3,1)
      I432(N)=I32(4,1)
      I532(N)=I32(5,1)
      I632(N)=I32(6,1)
      CALL MAT(M,M,P,G2,I32,I32C)
      DO 81 I=1,6
81    V32CX(I,1)=V32C(I,1)
C
C ---------------- SECTION THREE ----------------------------
C
      V34C(1,1)=V32C(1,1)
      V34C(2,1)=V32C(6,1)
      V34C(3,1)=V32C(3,1)
      V34C(4,1)=V32C(2,1)
      V34C(5,1)=V32C(5,1)
      V34C(6,1)=V32C(4,1)
C
      I34C(1,1)=-I32C(1,1)
      I34C(2,1)=-I32C(6,1)-IL6(N)
      I34C(3,1)=-I32C(3,1)
      I34C(4,1)=-I32C(2,1)-IL4(N)
      I34C(5,1)=-I32C(5,1)
      I34C(6,1)=-I32C(4,1)-IL5(N)
C
      CALL MAT(M,M,P,C11,V34C,V34)
      V134(N)=V34(1,1)
      V234(N)=V34(2,1)
      V334(N)=V34(3,1)
      V434(N)=V34(4,1)
      V534(N)=V34(5,1)
      V634(N)=V34(6,1)
      CALL MAT(M,M,P,C22,I34C,I34)
```

```
      I134(N)=I34(1,1)
      I234(N)=I34(2,1)
      I334(N)=I34(3,1)
      I434(N)=I34(4,1)
      I534(N)=I34(5,1)
      I634(N)=I34(6,1)
C
      VP4(1,1)=TS1(N-1)
      VP4(2,1)=TS2(N-6)
      VP4(3,1)=TS3(N-1)
      VP4(4,1)=TS4(N-6)
      VP4(5,1)=TS5(N-1)
      VP4(6,1)=V4P(N-14)
      CALL MAT(4,6,1,ZVE,VP4,I4P)
      IS4P=I4P(4,1)
      DO 235 I=1,3
      IC4P(I,1)=I4P(I,1)
235   SI4P(I,1)=IS4P*YY12(I,1)
      CALL SUB(3,1,SI4P,IC4P,P4I)
      CALL MAT(3,3,1,RRYI,P4I,V4C)
      V4C1(1,1)=V4C(1,1)
      V4C1(2,1)=0
      V4C1(3,1)=V4C(2,1)
      V4C1(4,1)=0
      V4C1(5,1)=V4C(3,1)
      V4C1(6,1)=0
      CALL MAT(M,M,P,C11,V4C1,V4)
      V41(N)=V4(1,1)
      V42(N)=V4(2,1)
      V43(N)=V4(3,1)
      V44(N)=V4(4,1)
      V45(N)=V4(5,1)
      V46(N)=V4(6,1)
      CALL SUB(M,P,V4,VP4,ZV4)
      CALL MAT(M,M,P,ZLI,ZV4,I4)
      I41(N)=I4(1,1)
      I42(N)=I4(2,1)
      I43(N)=I4(3,1)
```

```
      I44(N)=I4(4,1)
      I45(N)=I4(5,1)
      I46(N)=I4(6,1)
      V4AC(N)=V4C(1,1)
      V4BC(N)=V4C(2,1)
      V4CC(N)=V4C(3,1)
      V4AS(N)=0
      VE4(N)=V4AS(N)
      WRITE(6,100) T,V21C(2,1)
100   FORMAT(E11.4,2X,E11.4)
1000  CONTINUE
C
C -------------**SHIFT THE STATES**------------------------
C
      V11(-1)=V11(59)
      V13(-1)=V13(59)
      V15(-1)=V15(59)
      V121(-1)=V121(59)
      V321(-1)=V321(59)
      V521(-1)=V521(59)
      V123(-1)=V123(59)
      V323(-1)=V323(59)
      V523(-1)=V523(59)
      V132(-1)=V132(59)
      V332(-1)=V332(59)
      V532(-1)=V532(59)
      V134(-1)=V134(59)
      V334(-1)=V334(59)
      V534(-1)=V534(59)
      V41(-1)=V41(59)
      V43(-1)=V43(59)
      V45(-1)=V45(59)
      I112(-1)=I112(59)
      I312(-1)=I312(59)
      I512(-1)=I512(59)
      I121(-1)=I121(59)
      I321(-1)=I321(59)
      I521(-1)=I521(59)
```

```
I123(-1)=I123(59)
I323(-1)=I323(59)
I523(-1)=I523(59)
I132(-1)=I132(59)
I332(-1)=I332(59)
I532(-1)=I532(59)
I134(-1)=I134(59)
I334(-1)=I334(59)
I534(-1)=I534(59)
I41(-1)=I41(59)
I43(-1)=I43(59)
I45(-1)=I45(59)
IL1(-1)=IL1(59)
IL2(-1)=IL2(59)
IL3(-1)=IL3(59)
IL4(-1)=IL4(59)
IL5(-1)=IL5(59)
IL6(-1)=IL6(59)
DO 200 I=0,5
V12(I-6)=V12(I+54)
V14(I-6)=V14(I+54)
V221(I-6)=V221(I+54)
V421(I-6)=V421(I+54)
V223(I-6)=V223(I+54)
V423(I-6)=V423(I+54)
V232(I-6)=V232(I+54)
V432(I-6)=V432(I+54)
V234(I-6)=V234(I+54)
V434(I-6)=V434(I+54)
V42(I-6)=V42(I+54)
V44(I-6)=V44(I+54)
I212(I-6)=I212(I+54)
I412(I-6)=I412(I+54)
I221(I-6)=I221(I+54)
I421(I-6)=I421(I+54)
I223(I-6)=I223(I+54)
I423(I-6)=I423(I+54)
I232(I-6)=I232(I+54)
```

```
      I432(I-6)=I432(I+54)
      I234(I-6)=I234(I+54)
      I434(I-6)=I434(I+54)
      I42(I-6)=I42(I+54)
      I44(I-6)=I44(I+54)
200   CONTINUE
      DO 300 I=0,17
      V16(I-18)=V16(I+42)
      V621(I-18)=V621(I+42)
      V623(I-18)=V623(I+42)
      V632(I-18)=V632(I+42)
      V634(I-18)=V634(I+42)
      V46(I-18)=V46(I+42)
300   CONTINUE
      DO 400 I=0,15
      I612(I-16)=I612(I+44)
      I621(I-16)=I621(I+44)
      I623(I-16)=I623(I+44)
      I632(I-16)=I632(I+44)
      I634(I-16)=I634(I+44)
      I46(I-16)=I46(I+44)
400   CONTINUE
      DO 500 I=0,3
      FS0(I-18)=FS0(I+42)
      FR0(I-18)=FR0(I+42)
      KS0(I-18)=KS0(I+42)
      KR0(I-18)=KR0(I+42)
      TS0(I-18)=TS0(I+42)
      TR0(I-18)=TR0(I+42)
500   CONTINUE
      DO 600 I=0,3
      B1(I-5)=B1(I+55)
      B21(I-5)=B21(I+55)
      B23(I-5)=B23(I+55)
      B32(I-5)=B32(I+55)
      B34(I-5)=B34(I+55)
      B4(I-5)=B4(I+55)
600   CONTINUE
```

```
C
      IF(K.EQ.10) THEN
      GOTO 2000
      ELSE
      K=K+1
      GOTO 10000
      ENDIF
2000  CONTINUE
      STOP
      END
C
C ------------------**SUBROUTINES**-------------------------
C
C-----------------------------------------------
C   THIS SUBROUTINE DOES THE PRODUCT [A]*[B]
C-----------------------------------------------
C
      SUBROUTINE MAT(M,N,P,A,B,SUM)
      INTEGER M,N,P
      DIMENSION A(M,N),B(N,P),SUM(M,P)
      DO 97 J=1,P
      DO 99 I=1,M
      S=0.0
      DO 98 IJ=1,N
      S=S+A(I,IJ)*B(IJ,J)
98    CONTINUE
      SUM(I,J)=S
99    CONTINUE
97    CONTINUE
      RETURN
      END
C
C-----------------------------------------------
C   THIS SUBROUTINE DOES THE SUM [A]+[B]
C-----------------------------------------------
C
      SUBROUTINE ADD(M,P,A,B,CUM)
      INTEGER I,J,M,P
```

```
      DIMENSION A(M,P),B(M,P),CUM(M,P)
      DO 90 I=1,M
      DO 92 J=1,P
      C=A(I,J)+B(I,J)
      CUM(I,J)=C
92    CONTINUE
90    CONTINUE
      RETURN
      END
C
C-----------------------------------------------------
C   THIS SUBROUTINE DOES THE SUBTRACTION [A]-[B]
C-----------------------------------------------------
C
      SUBROUTINE SUB(M,P,A,B,CUM)
      INTEGER M,P,I,J
      DIMENSION A(M,P),B(M,P),CUM(M,P)
      DO 93 J=1,P
      DO 94 I=1,M
      C=A(I,J)-B(I,J)
      CUM(I,J)=C
94    CONTINUE
93    CONTINUE
      RETURN
      END
```